

ISBN 0-315-61823-X

THE STRATIGRAPHY AND STRUCTURAL
GEOLOGY OF THE TWILLINGATE REGION

CENTRE FOR NEWFOUNDLAND STUDIES

**TOTAL OF 10 PAGES ONLY
MAY BE XEROXED**

(Without Author's Permission)

EDWARD STANDER



National Library
of Canada

Bibliothèque nationale
du Canada

Canadian Theses Service

Service des thèses canadiennes

Ottawa, Canada
K1A 0N4

NOTICE

The quality of this microform is heavily dependent upon the quality of the original thesis submitted for microfilming. Every effort has been made to ensure the highest quality of reproduction possible.

If pages are missing, contact the university which granted the degree.

Some pages may have indistinct print especially if the original pages were typed with a poor typewriter ribbon or if the university sent us an inferior photocopy.

Reproduction in full or in part of this microform is governed by the Canadian Copyright Act, R.S.C. 1970, c. C-30, and subsequent amendments.

AVIS

La qualité de cette microforme dépend grandement de la qualité de la thèse soumise au microfilmage. Nous avons tout fait pour assurer une qualité supérieure de reproduction.

S'il manque des pages, veuillez communiquer avec l'université qui a conféré le grade.

La qualité d'impression de certaines pages peut laisser à désirer, surtout si les pages originales ont été dactylographiées à l'aide d'un ruban usé ou si l'université nous a fait parvenir une photocopie de qualité inférieure.

La reproduction, même partielle, de cette microforme est soumise à la Loi canadienne sur le droit d'auteur, SRC 1970, c. C-30, et ses amendements subséquents.



National Library
of Canada

Bibliothèque nationale
du Canada

Canadian Theses Service

Service des thèses canadiennes

Ottawa, Canada
K1A 0N4

The author has granted an irrevocable non-exclusive licence allowing the National Library of Canada to reproduce, loan, distribute or sell copies of his/her thesis by any means and in any form or format, making this thesis available to interested persons.

The author retains ownership of the copyright in his/her thesis. Neither the thesis nor substantial extracts from it may be printed or otherwise reproduced without his/her permission.

L'auteur a accordé une licence irrévocable et non exclusive permettant à la Bibliothèque nationale du Canada de reproduire, prêter, distribuer ou vendre des copies de sa thèse de quelque manière et sous quelque forme que ce soit pour mettre des exemplaires de cette thèse à la disposition des personnes intéressées.

L'auteur conserve la propriété du droit d'auteur qui protège sa thèse. Ni la thèse ni des extraits substantiels de celle-ci ne doivent être imprimés ou autrement reproduits sans son autorisation.

ISBN 0-315-61823-X

Canada

THE STRATIGRAPHY AND STRUCTURAL GEOLOGY
OF THE TWILLINGATE REGION

BY

© EDWARD STANDER B.Sc.

A Thesis submitted in partial fulfillment
of the requirements for the degree of
Master of Science

Department of Earth Sciences
Memorial University of Newfoundland
January, 1984

St John's

Newfoundland

ABSTRACT

The Twillingate region is underlain by three lithologic units. The oldest of these is the Sleepy Cove Group, a one to two kilometer thick volcanic pile which exhibits ophiolitic affinities. To the west, and in thrust contact with this group is the Moretons Harbour Group, a massive, 8 to 9 kilometer thick volcanic pile which most likely developed in an island arc environment. The Twillingate Granite is intrusive into both units and is thus the youngest unit in the region.

The Twillingate Granite and its basaltic hosts were affected by four deformational episodes. The earliest of these events (D_1) produced two high temperature shear zones. Of these, the SHTI zone parallels the southern boundary of the study area and is characterized by recrystallized quartz grains enclosed in a recrystallized sodic plagioclase matrix. The BBB zone forms the contact between the Moretons Harbour Group and the Sleepy Cove Group, and is characterized by sheared and elongate pillow basalts and dykes.

The D_2 deformation resulted in the development of open to tight upright folds in the basalt and a strong, localized L-S fabric in the granite body. Quartz microstructures and petrofabrics in the granite suggest that this deformation occurred at much lower temperatures than D_1 .

D_3 was also a low temperature deformation episode and was mainly responsible for developing broad, upright folds in the

basalts of North and South Twillingate Island. This event does not appear to have affected the granite terrain to any great extent.

The last event to affect the region (D_4), produced local kinks and faults in both the Twillingate Granite and the surrounding volcanic groups.

ACKNOWLEDGEMENTS

The techniques and conclusions presented in this thesis have developed as a result of discussions held at Memorial University during the period 1978-1980. Most of these discussions were initiated by Dr. T.J. Calon, advisor and supervisor, who suggested the present thesis topic and provided time for numerous discussions with the author in and out of the field. Other individuals who have added to the general discussion include Drs. P.F. Williams, A.R. Berger, D.F. Strong, and H. Williams, as well as graduate students D. Knapp, M. Snow, and B. Petronov. The author wishes to extend his appreciation to each of these individuals for their assistance.

Several members of the Memorial University technical staff were also extremely helpful in completing this thesis in the time provided. Messrs. L. Warford and F. Thornhill prepared thin sections for the study, while W. Marsh generously proffered his time and darkroom to produce the numerous plates which accompany the text. Similarly, the author would like to thank cartographer M. MacIntyre, P.N.G., for consultation time, and H. Trudel for helping type the final draft.

Furthermore, it is unlikely that this study would have been possible without the timely assistance provided by the Hamlyns and Smiths of North Twillingate and Tizzards Harbour respectively. Both families extended offers of food and

lodging when the author was in greatest need of both. In particular, I would like to thank Elsie and Frank Hamlyn for introducing me to the time worn art of squid jigging, cleaning, and drying.

Finally, the author would like to thank Ms. H Trudel and Mssrs. Y.A. Martineau and C.M.T. Lynas for providing much needed support during the final stages of thesis writing.

The Twillingate Study was sponsored by Memorial University and N.R.C. research grant 6044 awarded to Dr. T. Calon during the years 1978-1979.

TABLE OF CONTENTS

CHAPTER I

INTRODUCTION

	PAGE
I.A. Location.....	1
I.B. Access and Exposure.....	1
I.C. Previous Work.....	4
C.1. Early Work.....	4
C.2. Later Work.....	5
I.D. Purpose and Scope of the Present Thesis.....	9

CHAPTER II

PETROGRAPHY AND FIELD RELATIONSHIPS

II.A. Introduction.....	11
II.B. Mafic Extrusive and Intrusive Rocks.....	14
B.1. Basaltic Pillow Lavas and Massive Flows.....	14
1a. Aphyric Pillow Lavas and Flows.....	14
1b. Webber Bight Pillows (after Strong and Payne ,1973).....	21
B.2. Mafic Dykes	21
2a. Pre- and Syn-Tectonic Mafic Dykes.....	22
2b. Layered Basalt Dykes.....	23
2c. Hornblend-Plagioclase Porphyritic Dykes....	26
2d. Diabase Dykes.....	29
2e. Lamprophyre Dykes.....	31
2f. Other Dyke Types.....	32
B.3. Volcaniclastic Sediments.....	32
II.C. The Twillingate Granite.....	35
C.1. Field Characteristics.....	35
C.2. Quartz Porphyry Dykes.....	41

II.D. Diatremes.....	41
II.E. Metamorphism.....	44
E.1. M ₁ Metamorphic Zonation in the Sleepy Cove and Moretons Harbour Groups.....	44
E.2. M ₁ Metamorphic Zonation in the Twillingate Granite	47
E.3. The M ₂ Metamorphic Episode.....	48

CHAPTER III

STRUCTURAL GEOLOGY - INTRODUCTION AND MACROSCOPIC ANALYSIS

III.A. Introduction.....	49
III.B. Deformation Characteristics of the Twillingate region.....	50
III.C. Macroscopic Structures of the Twillingate Region.	
C.1. Introduction.....	53
C.2. The D ₁ Deformation - General Characteristics....	54
2a. Deformational style.....	58
2b. Orientation of Structural Elements.....	60
C.3. The D ₂ Deformation - General Characteristics..	63
3a. Structural Elements.....	63
3b. The Spatial Extent of D ₂ Structural Elements.....	72
C.4. The D ₃ Deformation - General Characteristics...	74
4a. Structural Elements.....	74
C.5. The D ₄ Deformation.....	77
5a. Kinking.....	77
5b. Faults - General Characteristics.....	77
b.1. Orientation, Distribution, and Fault Movement.....	78

CHAPTER IV

STRUCTURAL GEOLOGY-MICROSTRUCTURAL ANALYSIS

IV.A. General Aspects of Microstructural Development...	81
IV.B. Microstructures in the Twillingate Granite.....	86
B.1. The Type 0 (Initial) Microstructure.....	87
B.2. The Type 1 Microstructure.....	88
2a. Introduction.....	88
2b. Morphology of the Type 1 Microstructures....	88
B.3. The Type 2 Microstructure.....	92
3a. Introduction.....	92
3b. Morphology of the Type 2 Microstructure.....	92
B.4. The Type 3 Microstructures.....	100

CHAPTER V

STRUCTURAL GEOLOGY-PETROFABRIC ANALYSIS

V.A. Petrofabrics in the Twillingate Granite.	103
A.1. Introduction.....	103
A.2. Methods.....	103
A.3. Fabric Classification.....	105
3a. Group 0 Fabrics.....	107
3b. Group 1 Fabrics.....	107
3c. Group 2 Fabrics.....	109
3d. Group 3 Fabrics.....	110
A.4. Fabric Summary.....	112

CHAPTER VI

ANALYSIS AND SYNTHESIS

VI.A. Stratigraphic Analysis.....	113
VI.B. Structural Analysis.....	118
B.1. Structural Summary.....	118
B.2. Structural Models.....	122
2a. The D ₁ Deformation.....	122
2b. The D ₂ Deformation.....	123
2c. The D ₃ Deformation.....	127
2d. The D ₄ Deformation.....	129

CHAPTER VII

TECTONIC SYNTHESIS AND CONCLUSIONS

VII.A. Tectonic Synthesis.....	130
VII.B. Conclusions.....	133
Bibliography.....	135

LIST OF FIGURES

	PAGE
FIGURE 1 Location map for the Twillingate region.....	3
FIGURE 2 Generalized geologic map of the Twillingate region.....	13
FIGURE 3 Sleepy Cove pillow lava from Back Harbour. Twillingate.....	17
FIGURE 4 Moretons Harbour Group pillow lava from Sam Jeans Cove.....	17
FIGURE 5 Aeromagnetic map of the Twillingate region..	19
FIGURE 6 Rare earth element abundances in the Twillingate study area.....	20
FIGURE 7 Dyke orientations on the Moretons Harbour Peninsula.....	24
FIGURE 8 Layered Basalt dykes intruding pillow lavas just south of Beachy Cove on the Moretons Harbour Peninsula.....	25
FIGURE 9 Close-up of the chilled margins in a dyke at Beachy Cove.....	25
FIGURE 10 Undeformed Hornblende-Plagioclase porphyritic dyke from Wild Bight.....	28
FIGURE 11 Deformed Hornblende-Plagioclase porphyritic dyke from Sam Jeans Cove.....	28
FIGURE 12 Diabase dyke from Wild Bight.....	30
FIGURE 13 Diabase dyke from the southeastern corner of Salt Harbour Island.....	30
FIGURE 14 Slightly sheared basalt/granite breccia at Gallows Cove, North Twillingate Island.....	34
FIGURE 15 Strongly deformed "siliciclastic" sediments (Payne. 1974) at Bread and Butter Point...	34

FIGURE 16	Mildly deformed Twillingate Granite from Durrels Arm.....	38
FIGURE 17	Strongly foliated Twillingate Granite from Gunning Head.....	38
FIGURE 18	Deformed granite from Gunning Head.....	39
FIGURE 19	Mildly deformed granite from the tip of Gunning Head.....	39
FIGURE 20	Granite/basalt contact at Jenkins Cove.....	40
FIGURE 21	Close-up of the granite/basalt contact at Jenkins Cove.....	40
FIGURE 22	Quartz porphyry dykes at South Trump Island.....	43
FIGURE 23	Hand specimen of diatreme material from the tip of Long Point, Twillingate.....	43
FIGURE 24	Metamorphic map of the Twillingate region...	45
FIGURE 25	Form surface map of foliations in the Twillingate region.....	51
FIGURE 26	Intensity of L-S fabric development in the Twillingate region.....	52
FIGURE 27	A refolded fold from Grassy Point, Twillingate.....	55
FIGURE 28	Sketch of sample 57, showing the orientation of S_1 and the axial planes of the F_2 and F_3 folds.....	55
FIGURE 29	Orientation data for the D_1 deformation.....	56
FIGURE 30	L_1 as observed in the amphibolites of South Trump Island.....	57
FIGURE 31	L_1 observed in the granite of South Trump Island.....	57
FIGURE 32	Approximate areal extent of the BBB and The SHTI zones.....	59

FIGURE 33	The presence of small scale shear zones in the granite terrain of Salt harbour Island may suggest that S_1 in this region developed as a result of simple shear.....	62
FIGURE 34	Possible F_1 folds in the siliciclastic sediments of South Trump Island.....	62
FIGURE 35	Orientation data for the D_2 deformation....	66
FIGURE 36	F_2 folds on North Trump Island.....	67
FIGURE 37	F_2 folds on Salt Harbour Island.....	67
FIGURE 38	Sketch map of the F_2 (?) fold at Jenkins Cove, Twillingate.....	68
FIGURE 39	Sketch map of the F_2 folds on the west shore of North Trump Island.....	69
FIGURE 40	Development of the tectonic pillow breccia on North Trump Island.....	70
FIGURE 41	Hand specimen of the tectonic breccia on North Trump Island.....	70
FIGURE 42	S_2 on Salt Harbour Island.....	71
FIGURE 43	S_2 on North Trump Island.....	71
FIGURE 44	The spatial extent of D_2 structural elements.....	73
FIGURE 45.a	Poles to S_0/S_2 on North Twillingate island.....	76
FIGURE 45.b	Poles to S_1 in the BBB shear zone region..	76
FIGURE 45.c	Poles to S_0/S_2 on South Twillingate island.....	76
FIGURE 45.d	Composite diagram for the D_3 deformation..	76
FIGURE 46	87 poles to fault planes in the Twillingate region.....	80
FIGURE 47	Deformation mechanism maps for quartz of 1 mm. and 10 μ m.....	84

FIGURE 48	Development of dislocations in a stressed crystal.....	85
FIGURE 49	Recrystallized quartz grain from the southernmost tip of SouthTwillingate Island.....	90
FIGURE 50	Recrystallized feldspar grains developing from a host plagioclase phenocryst.....	90
FIGURE 51	AVA diagram of one recrystallized quartz grain.....	91
FIGURE 52	Undulose extinction, subgrain boundaries, and basal slip lamellae in a quartz grain from Durrels Arm.....	96
FIGURE 53	Camera Lucida drawing of the quartz grain in figure 52.....	96
FIGURE 54	Bulge nucleation in quartz grains as noted in a sample collected at Durrels Arm.....	97
FIGURE 55	Development of new grains in protrusions....	98
FIGURE 56	Serrated grain boundary developed as a result of bulge nucleation.....	98
FIGURE 57	Microcracks (?) in quartz grains at Merritts Harbour.....	99
FIGURE 58	"Kinks" in a quartz grain from Merritts Harbour.....	102
FIGURE 59	Kinked grain in which one limb has recrystallized	102
FIGURE 60	Quartz petrofabrics in the Twillingate region.....	106
FIGURE 61	The orientation of basal planes in the kinked quartz grains before (61a) and after (61b) kinking.....	121
FIGURE 62	The magnitude of σ_1 as measured around a circular rigid object.....	125

FIGURE 63 Theoretical orientation of σ_1 as defined
by the Moretons Harbour "Strain Shadow".....128

I. INTRODUCTION

I.A. Location

The Twillingate study area is located along the east coast of Notre Dame Bay, North-central Newfoundland (fig. 1). It consists of four major islands and several smaller ones, including the Twillingate Islands, Black Island, the Trump Islands, New World Island, Matthews Island and Mouse Island. In all, the study area encompasses a total area of about 150 square miles, the centre of which lies at 49°40' west longitude and 54°45' north latitude.

I.B. Access and Exposure

Access to the Twillingate Islands is by good paved roads from Lewisporte or Gander. Unpaved secondary roads connect these highways to much of the study area, and afford access into many of the more distant parts of the region. Of the major land masses, only the Trump Islands and Black Island are inaccessible by car.

Access into the interior of the islands is made possible by numerous foot paths and moose runs. However, inland exposures are often lichen-covered and extremely difficult to interpret. This is especially true of the Moretons Harbour Peninsula, where even cliff faces are often without workable exposure.

In comparison, the shoreline of all islands offer extremely good exposure and are easily accessible by foot,

with the exception of the northernmost extremities of the Moretons Harbour Peninsula and North Twillingate Island. Boat work is feasible during the summer, although high cliffs and frequent gales make landing difficult on the windward shores.

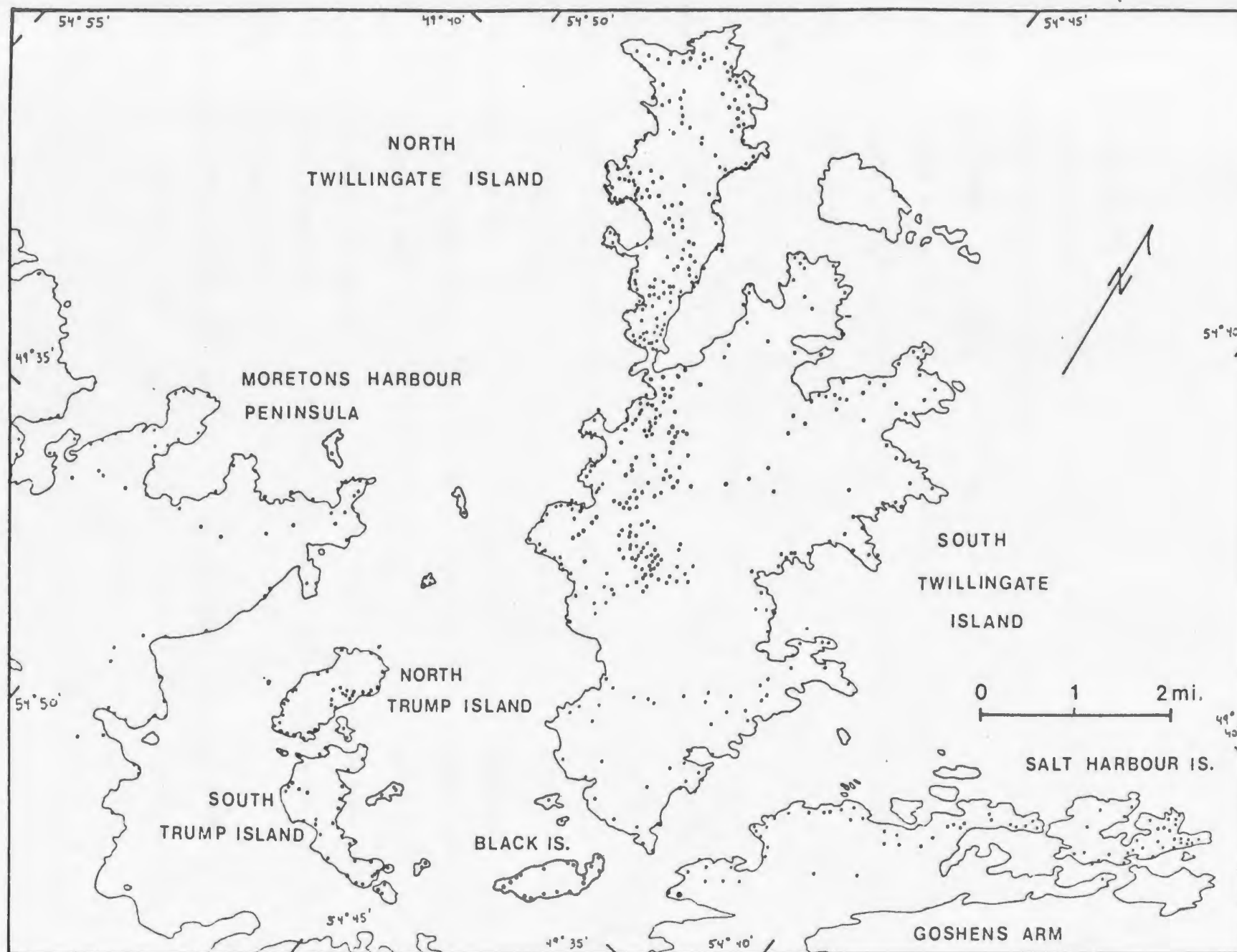


Figure 1. Location map for the Twillingate region. Dots indicate the location of outcrops visited during this study.

I.C. Previous Work

I.C.1. Early Work

The earliest geological description of the Twillingate region is that of Jukes (1842), who visited the Twillingate Islands in 1840. He described the two principal lithologies in the region as a 'rather fine grained white granite' and a 'coarse slate rock' which he assigned to the 'Lower Slate Unit' of the Avalon Peninsula.

Following this investigation, several groups of geologists visited the Twillingate region, although most concentrated on the sediments of the New World Island and Exploits region. First among these were Murray and Howley (1881), who described the Ordovician-Silurian sediments of New World Island and recognized their 'angular discordancy' at Goshens Arm. They hypothesized that the Silurian lay unconformably on top of the Ordovician, yet recognised the possibility that faulting may have also modified the contact. Heyl (1936) later showed that this contact was indeed structural, and named the tectonic lineament the 'Lukes Arm Fault'.

Heyl (1936) also attempted a structural analysis of Notre Dame Bay, and defined one major phase of deformation. F_1 folds were described as being noticeably asymmetric and locally isoclinal, with axial planes trending northeast-southwest and axes which 'change pitch both in degrees and

direction' (sic). Based on the attitudes and asymmetry of these folds, he suggested that the region was deformed 'under compressive stresses' acting from the southeast. Faults were thought to have developed concurrently with folds as a result of overtightening within the fold cores.

In 1953, D.M. Baird mapped the Twillingate region in reconnaissance fashion and described relationships between the 'Twillingate Granite' and its surrounding lava flows and greenstones. He suggested that the the granite mass was intruded in the Acadian Stage as it 'cuts the Ordovician volcanic rocks and includes many fragments and remnants of them' (Baird, 1954). The Twillingate Granite was also described by Williams (1963), who suggested that contrasts in structural style across the Lukes Arm Fault were related to the 'modifying effects' of the granite pluton to the north.

I.C.2. Later Work

Up to the late 1960's, interest was only cursorily extended to the present study area. However, with the advent of modern plate tectonic theory, the Twillingate region became the focus of debate, with controversy centering about two distinctly different models for the region. The earlier model, first proposed by Dewey (1969), and later modified by Bird and Dewey (1970) and Dewey and Bird (1971), suggested that granitic plutons, such as the Twillingate body, intruded

ophiolitic terrains during the early Ordovician. They argued that these plutons developed as a result of plate subduction, and were therefore intimately associated with regions of island arc volcanism. Alternatively, Williams et.al. (1972) argued that the Twillingate Granite represented an older crustal remnant enclosed in a matrix of younger mafic volcanic rocks. This hypothesis stems from relationships defined in the Little Port Complex (western Newfoundland), where a deformed granite pluton similar to the Twillingate Body was found to be surrounded by younger, undeformed volcanic rocks. (Comeau, 1972).

In order to determine the relative merits of each model, detailed field and geochemical studies were conducted in the study area under the leadership of Drs. D. Strong and H. Williams of Memorial University.

In 1972, Coish (1973) mapped the two Trump Islands and described the volcanic stratigraphy of the region. He supported Dewey and Bird's 1971 model by showing that the Twillingate Granite intruded and was deformed with the surrounding volcanic pile. He also suggested that variations in deformational intensity throughout the region occurred as a result of competency differences between the Twillingate Granite and its country rocks. In particular, he suggested that the granite pluton acted as a 'buttress' to deformation, and was therefore more competent than the surrounding basalts.

Following the publication of Coish's thesis, Strong and Payne (1973) formally described the stratigraphy of the Moretons Harbour-Twillingate region, and assigned all units to the 'Moretons Harbour Group'. They suggested that this group represented an Ordovician 'Island Arc', and pointed to its eight kilometer thickness and volcanic stratigraphy for supporting evidence. Payne (1974) and Payne and Strong (1979) further supported the Island Arc model by showing that the Twillingate Granite was trondhjemitic in composition, and probably developed in an oceanic (subduction zone?) environment.

Payne also conducted a detailed structural analysis on the region and was able to discern three deformational events. The first of these (D_1), was only noted in xenoliths at Little Harbour, and was therefore thought to have occurred prior to the intrusion of the Twillingate pluton. The main foliation in the region was assigned to D_2 , while late faults and kinks were collectively assigned to D_3 .

Although Payne (1974), and Strong and Payne (1973) both described the Moretons Harbour Group as a continuous sequence exhibiting a gradational but very definite eastward increase in intensity of strain and metamorphism, Williams and Payne (1975) suggested that a 'strong structural contrast' existed in the group at Tizzards Harbour and Sam Jeans Cove. They subdivided the volcanics into two groups on the basis of this contrast, and assigned the highly deformed volcanics east of Sam Jeans Cove and Tizzards Harbour to the Sleepy Cove Group.

The contact between the Sleepy Cove and Moretons Harbour Groups was defined as a major fault, which was thought to extend from Berry Island to the Chanceport Fault at Bridgeport. In order to explain this structural unconformity, they suggested that the Sleepy Cove Group represented an early island arc terrain which was intruded by the Twillingate Granite, deformed, and then overlain by the Moretons Harbour Group. Their hypothesis was based on the remnant arc model developed by Karig (1972), and explains the absence of granitic dykes and foliations on the Moretons Harbour Peninsula.

In 1978, Dean presented a third hypothesis which argued that the Sleepy Cove Group represents the upper unit of an ophiolite complex which was conformably overlain by the Moretons Harbour Group while being intruded by the Twillingate Granite. He saw no evidence for a structural unconformity at Tizzards Harbour, and preferred to include all rocks north of the Chanceport Fault in the Moretons Harbour Group.

The origin and displacement histories of the Lukes Arm and Chanceport Faults have also been the subject of numerous papers, with authors suggesting that fault displacement was either sinistral strike slip, dextral strike slip, or reverse. Evidence for each is presented by Dean and Strong (1977), and will be further discussed in chapter III.

I.D. Purpose and Scope of the Present Thesis

The field study described in this thesis was conducted during the fall of 1978 and the summer of 1979. Its main goals lay in answering some of the questions posed by earlier workers. In particular, effort was directed towards defining the geologic relationship of the Sleepy Cove Group to the Moretons Harbour Group. Can these volcanic units be separated on the basis of field and petrologic data?

In order to answer this question, a detailed petrologic and metamorphic analysis of the volcanic terrain was undertaken to see if any major lithologic breaks could be discerned. A detailed structural analysis was then conducted across all observed lithologic breaks to see whether variations in deformational history were present. If found, such variations would lend support to Williams and Payne's (1975) two stage model for the Twillingate region.

The question of deformational style in the Twillingate region was also considered during the present study. This problem was discussed by several authors (notably Coish (1973), Payne (1974) and Williams and Payne (1975)), all of whom commented on the heterogeneity of deformation in the region. In order to provide a reasonable explanation for this heterogeneity, a comprehensive study was undertaken of the macrostructures, microstructures, and petrofabrics present throughout the region. These data were then used to define the age of deformation, the strains associated with deformation, and the environmental conditions under which

deformation occurred.

In the chapters which follow, each of these questions are considered in turn. Chapter II deals with the stratigraphic questions outlined in this chapter, while chapters III through V consider the problem of structural history. Conclusions reached in each chapter are then discussed together in chapter VI.

II. PETROGRAPHY AND FIELD RELATIONSHIPS

II.A. Introduction

The lithologies exposed in the Twillingate study area may be broadly separated into two lithic types (fig. 2). Of these, the predominant rock type is the Twillingate Granite and its apophyses. This intrusive unit occupies over 60% of the exposed terrain and is the predominant rock type on South Twillingate Island, Black Island, South Trump Island, and the northeastern part of New World Island. Elsewhere in the region, mafic lithologies predominate, with the most common rock types being volcanoclastic sediments, basaltic pillow lavas, massive flows, and mafic dykes.

The contact between the Twillingate Granite and its basaltic host is usually fault modified. However, in the few observed cases where the boundary is apparently undeformed (for example, at Jenkins Cove), it consists of an intrusive breccia in which the mafic volcanics are incorporated and partially assimilated into the granite body (see figs. 20 and 21, page 40).

In the following sections, the petrology and field morphology of these two lithologic units are described. Previously defined stratigraphic names are retained, although the spatial relationship between groups has been redefined. Thus, the names 'Sleepy Cove Group' and 'Moretons Harbour Group' are used throughout the text, even though the contact

between the two groups has been relocated on the basis of petrologic, geochemical, and geophysical data.

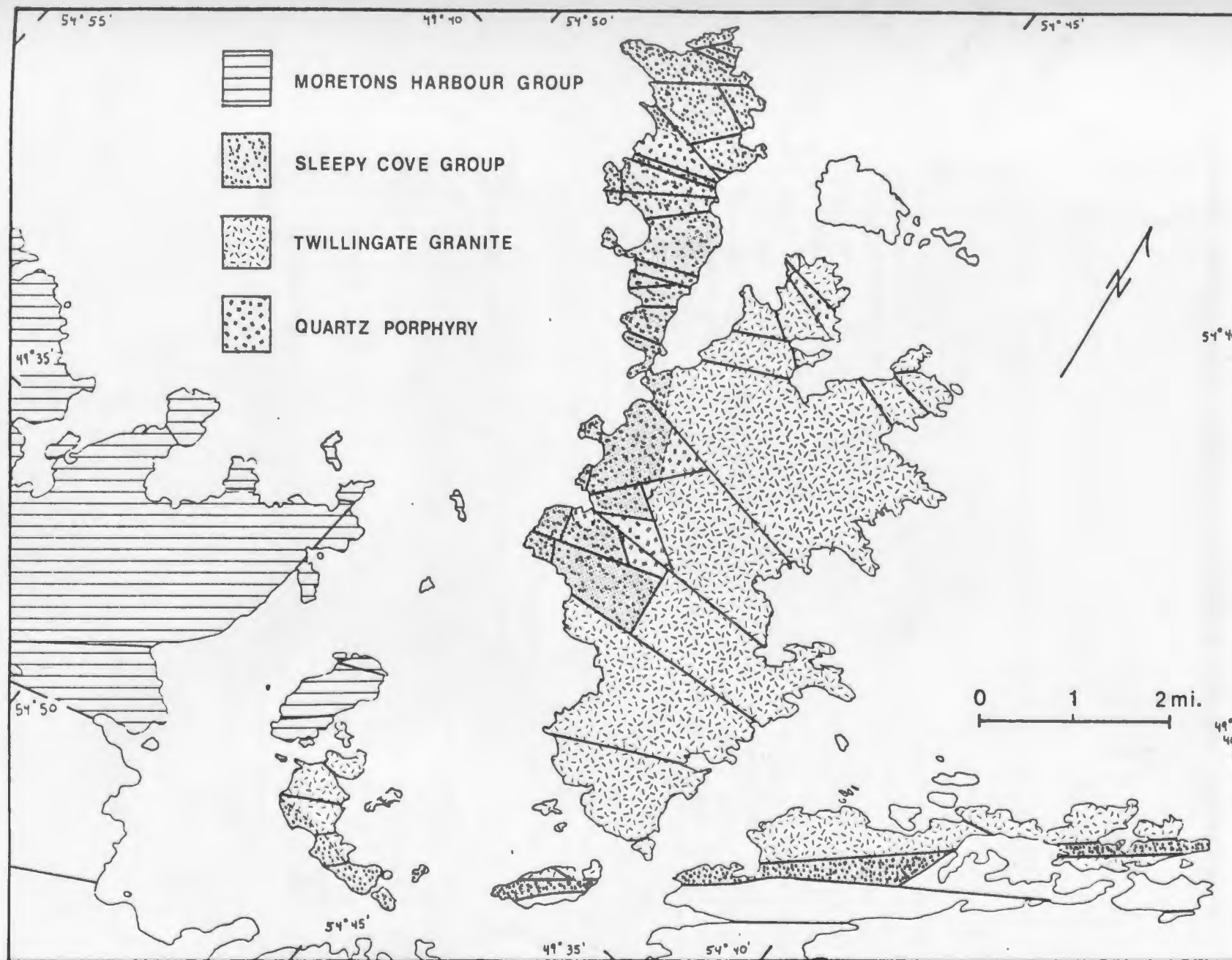


Figure 2. Generalized geologic map of the Twillingate region. Thick solid lines denote the trace of major faults.

II.B. Mafic Extrusive and Intrusive Rocks

Pillow lavas and massive basalt flows are by far the most common mafic rock types and underlie nearly 25% of the study area. Following these in order of abundance are basaltic and diabasic dykes (10%) and volcanoclastic sediments (5%), both of which are locally abundant on the Moretons Harbour Peninsula and are rare elsewhere.

II.B.1. Basaltic Pillow Lavas and Massive Flows

Well rounded to ellipsoidal pillow lavas are present throughout much of the study area and may be separated into two types on the basis of phenocryst abundance. Aphyric pillow lavas are the more common extrusive lithology and make up nearly 80% of the mafic exposures on North Trump Island and the Twillingate Islands. They are less common on the Moretons Harbour Peninsula, due to the intrusion of later dyke swarms, and form screens between these dykes (see fig. 8, page 25). In comparison, feldspar porphyritic pillow lavas (the Webber Bight Pillows of Strong and Payne (1973)) are only exposed on the Moretons Harbour Peninsula, where they lie in close association with a suite of porphyritic feeder dykes.

II.B.1.a. Aphyric Pillow Lavas and Flows

Aphyric pillow lavas are commonly grey-green to black and

Vary from 20 centimeters to over two meters in diameter. Although locally deformed, pillow lavas in the vicinity of Moretons Harbour and the Main Tickle of North Twillingate Island exhibit well defined 'V' shaped bottoms and vesicular tops which indicate that the units young to the northwest. The pillow lavas are often tightly packed without interstitial sediment.

Massive aphyric flows and feeder dykes are well developed at Moretons Harbour and North Twillingate Island, and have not been observed elsewhere. Basalt flows average 5 to 7 meters in thickness and often contain abundant epidote-filled amygdules. These amygdules attain diameters of over 5 centimeters and vary in abundance between adjacent flows. Feeder dykes are thin (<1 meter), non-vesicular basaltic intrusives which, when present in quantity, exhibit a sheeted character. They are best exposed in the cliffs of Long Point and north of the stage at Crow Head, where individual dykes may be seen feeding and cross-cutting the surrounding pillow lavas (see Payne (1974), fig. 6).

The petrography of the aphyric pillow lavas has been previously described by Payne (1974), who showed that they consist of small porphyroblasts of actinolite or hornblende enclosed in a fine-grained oligoclase-chlorite groundmass. Calcite, apatite, zoisite, and quartz occur as common accessory minerals and rarely exceed abundances of over 10%. Indeed, of all the phases present, only the abundance of opaque minerals appears to vary in a systematic manner.

In the present study, variations in the abundance of opaque minerals has been used to separate the Moretons Harbour Group from the Sleepy Cove Group. Volcanics located on the Moretons Harbour Peninsula and North Trump Island were found to be rich in sulphides and oxides and locally contained up to 30% opaque minerals. Since these rocks all lay within an area previously mapped as the Moretons Harbour Group by Strong and Payne (1973), they are formally assigned to that group here. Volcanics east of this region are noticeably deficient in sulphides and oxides and are formally assigned here to the Sleepy Cove Group (see figs 3 and 4).

Although the contact between these two units lies underwater over most of its length, its location is well marked by a strong magnetic lineament (see the Twillingate Magnetic Anomaly Sheet, G.S.C. map 4452g, and fig. 5). For the most part, this lineament follows the shoreline of North Trump Island and South Twillingate Island, and turns abruptly northwestward near Batrix Island. This relatively abrupt change in orientation may be a fault-related phenomenon, and will be discussed further in chapter III.

A preliminary study of rare earth element abundances in the aphyric pillow lavas of both groups tends to support the above lithologic subdivision (fig. 6). While the Sleepy Cove Group lavas were all found to exhibit chondrite-normative rare earth element patterns similar to oceanic tholeiites, all of the Moretons Harbour Group pillow lavas were found to be enriched in light rare earth elements, a feature

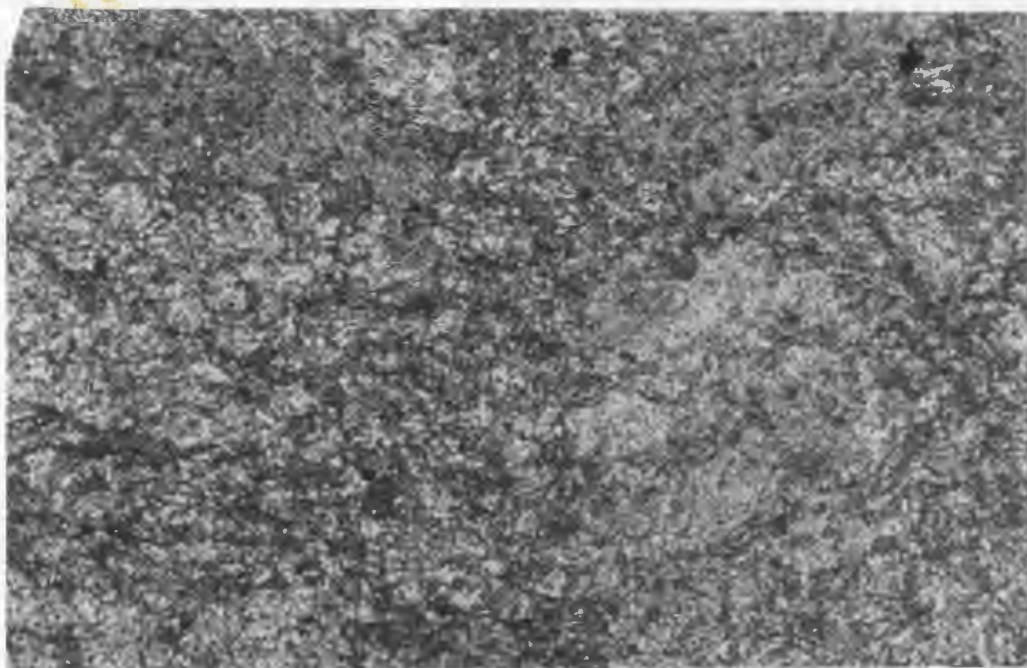


Figure 3: Sleepy Cove pillow lava from Back Harbour, Twillingate. Plane light. Note the absence of opaque minerals in the matrix. Scale: 1cm.= .25mm.

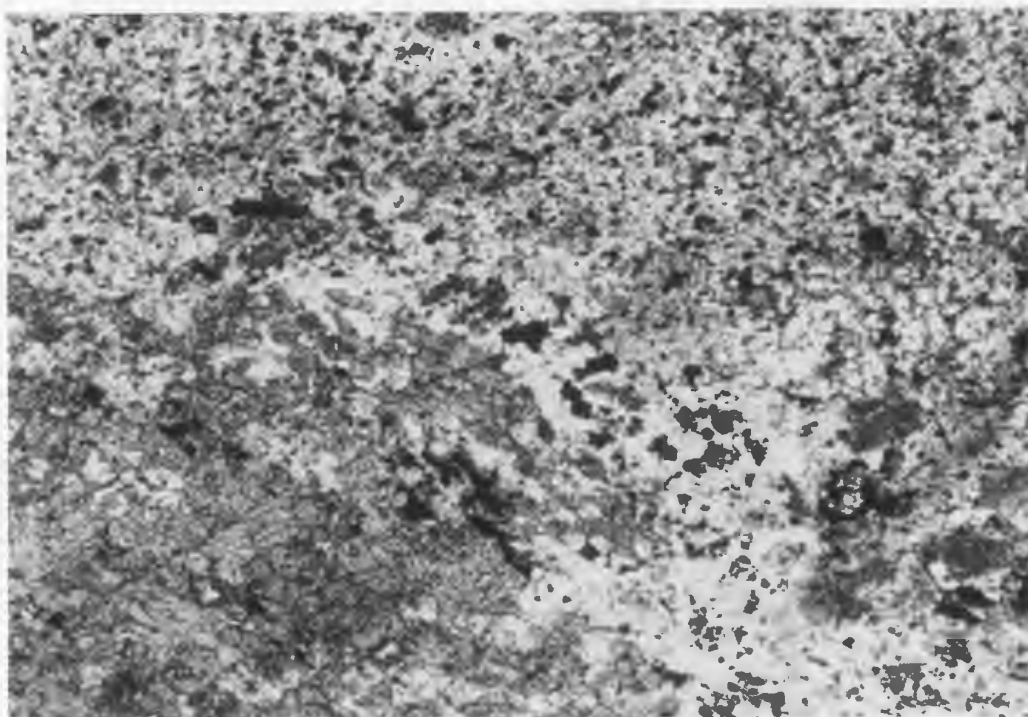


Figure 4: Moretons Harbour Group pillow lava from Sam Jeans Cove. Plane light. The opaque content of this pillow is 15-20%. Scale: 1cm.=.25mm.

characteristic of alkali basalts (Strong and Dostal, (1980)). Thus, based on these results, it appears that the Moretons Harbour/Sleepy Cove Group contact defined here has petrogenetic as well as lithologic significance, and may indeed mark the boundary between island arc and ophiolite, as was initially suggested by Dean (1978).

Figure 5. Aeromagnetic map of the Twillingate region. Each line=100 gammas. Dotted line lies at the inferred Moretons Harbour/ Sleepy Cove Group contact.

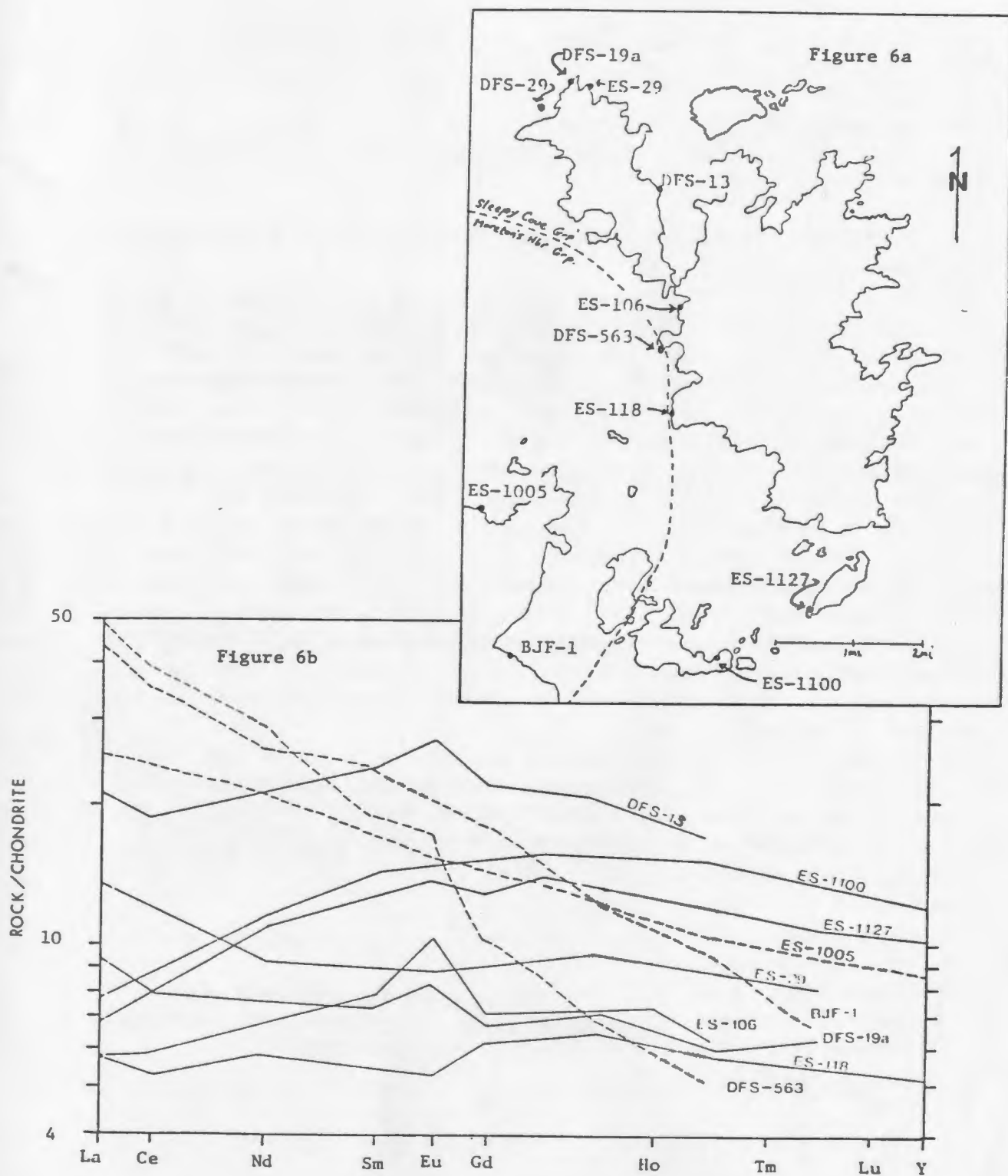


Figure 6: Rare earth element abundances in the Twillingate region. Figure 6a gives the location of samples used in this study as well as the location of the inferred Sleepy Cove Group-Moretons Harbour Group contact. Figure 6b gives the chondrite normative rare earth abundances found in the Sleepy Cove Group samples (dotted lines) and Moretons Harbour Group samples (solid lines). Sample numbers refer to samples stored in the Memorial University collection.

II.B.1.b. Webber Bight Pillows (after Strong and Payne, 1973)

Webber Bight Pillow lavas are locally exposed on the coast of Webber Bight, and have been described in detail by Strong and Payne (1973). These pillow lavas are 'spectacular feldspar-clinopyroxene porphyritic basalts' which contain large, poorly zoned plagioclase (50%) and augite (35%) crystals enclosed in a dark aphyric matrix. The pillows are often large (>2 meters), closely packed, and are intimately associated with hornblende-plagioclase porphyritic dykes. The dyke swarms are enclosed in a chocolate brown aphyric basalt matrix, suggesting that they may have been intruded into a pre-existing basaltic terrain.

II.B.2. Mafic Dykes

Mafic dykes of various compositions and ages occur throughout the Twillingate region. Most of these have been previously described by Coish (1973) and Payne (1974), who separated the dyke types into three groups on the basis of deformational style. Of these, the 'pre- or syn-tectonic dykes' were first to develop and are characterized by a strong foliation which usually parallels that found in the Twillingate Granite, but in some instances lies oblique to the granite foliation. The 'post-tectonic' dykes occur in the strongly deformed granite terrain, yet are themselves undeformed. They were considered to be co-genetic with the Herring Neck Group volcanic rocks which are found just south of the present study area.

Dykes emplaced in regions which escaped the effects of deformation and therefore could not be categorized were placed in a third group entitled 'dykes of uncertain age'.

In this section, these three dyke types, and others which have not been previously noted, will be described according to their order of intrusion.

II.B.2.a. Pre- and Syn-Tectonic Mafic Dykes

Pre- and syn-tectonic mafic dykes were first observed by Payne (1974), who described them as green to black weathering, fine grained intrusives locally found within the granite pluton. They are basaltic or amphibolitic in composition, and are extremely altered. The amphibolitic dykes were found to contain about 50% green pleochroic hornblende \pm chlorite enclosed in a quartz-feldspar matrix, while the diabasic dykes consisted of subhedral augite and chlorite crystals enclosed in a fine grained plagioclase groundmass.

These dykes are commonly ruptured and discontinuous, and usually contain a strong foliation trending parallel to the regional schistosity. In some regions, particularly in the granite body just east of the White Hills, they occur so pervasively that it is difficult to tell where the actual basalt/granite contact lies. This may explain why the granite boundary reported in this thesis differs from that previously reported by Payne (1974).

II.B.2.b. Layered Basalt Dykes

Layered basalt dykes are only found on the Moretons Harbour Peninsula, and are particularly well developed on the northeast shore of Moretons Harbour, where they locally occupy nearly 100% of the exposure. These dykes average 10 to 20 centimeters in width and radically vary in orientation along their length. A stereonet of layered basalt dyke orientations is given in Figure 7.

Layered basalt dykes are most easily distinguished in the field by their coarsely layered appearance. This morphology is produced by numerous thin (1-2cm wide) one-sided chilled margins which parallel the dyke walls and coarsen towards the dykes core. Always occurring in sets symmetrically distributed about the center of the dykes, most dykes contain from four to twelve parallel sets of chilled zones (Fig. 8 and 9).

In hand specimen, layered basalt dykes are composed of an aphyric grey-green vesicular basalt similar to that found in the pillow lavas they intrude. They are also petrologically similar to the pillow lavas and consist of small, euhedral plagioclase and chlorite crystals enclosed in a glassy matrix. Chilled margins are defined by the proportion and size of feldspar grains, with the chilled zones containing less plagioclase and more matrix than the intervening basalt.

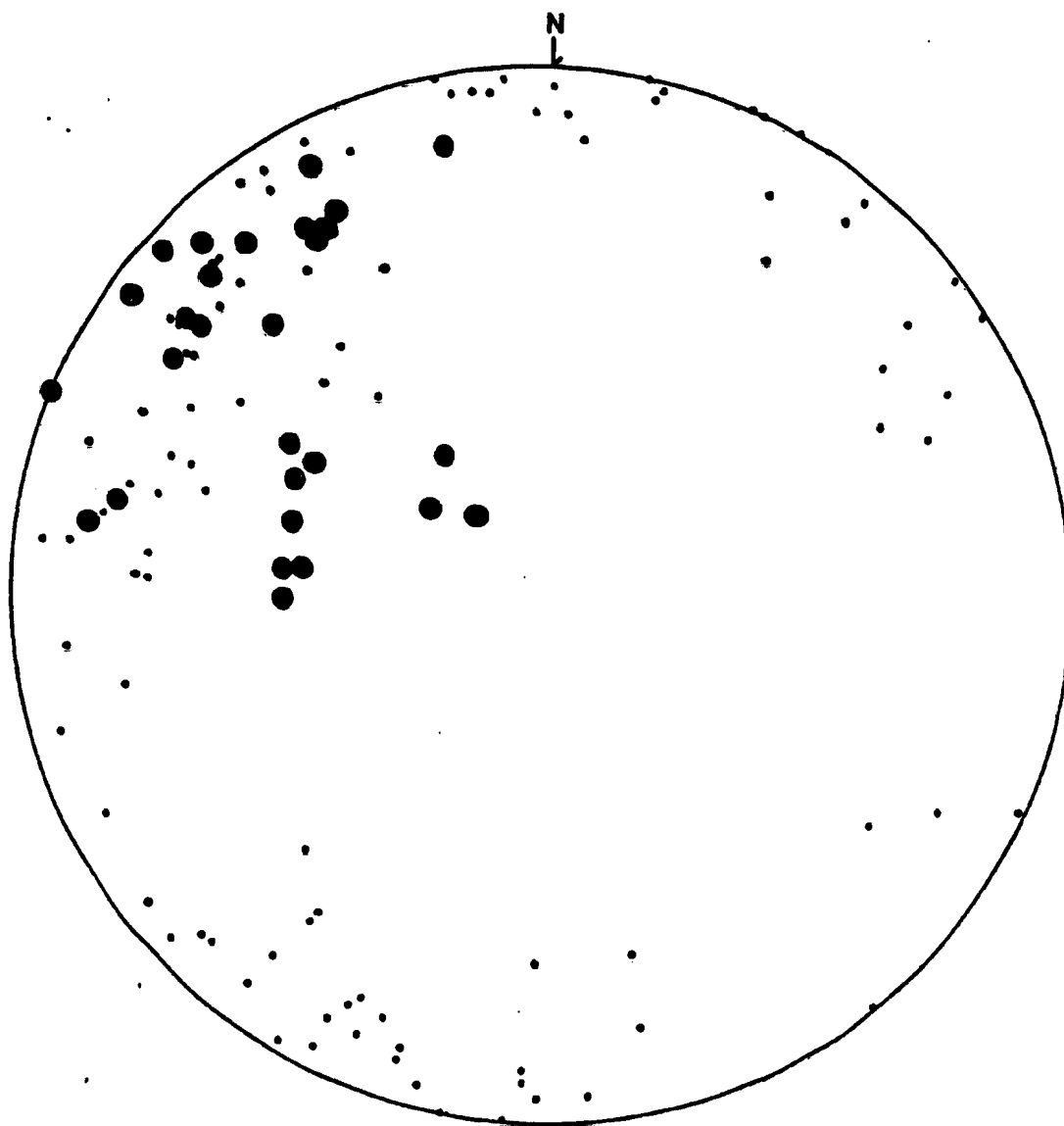


Figure 7: Dyke orientations on the Moretons Harbour Peninsula. Small dots indicate the orientation of layered basalt dykes, while the larger dots denote the orientation of the hornblende-plagioclase porphyritic dykes. Schmidt net, lower hemisphere projection.

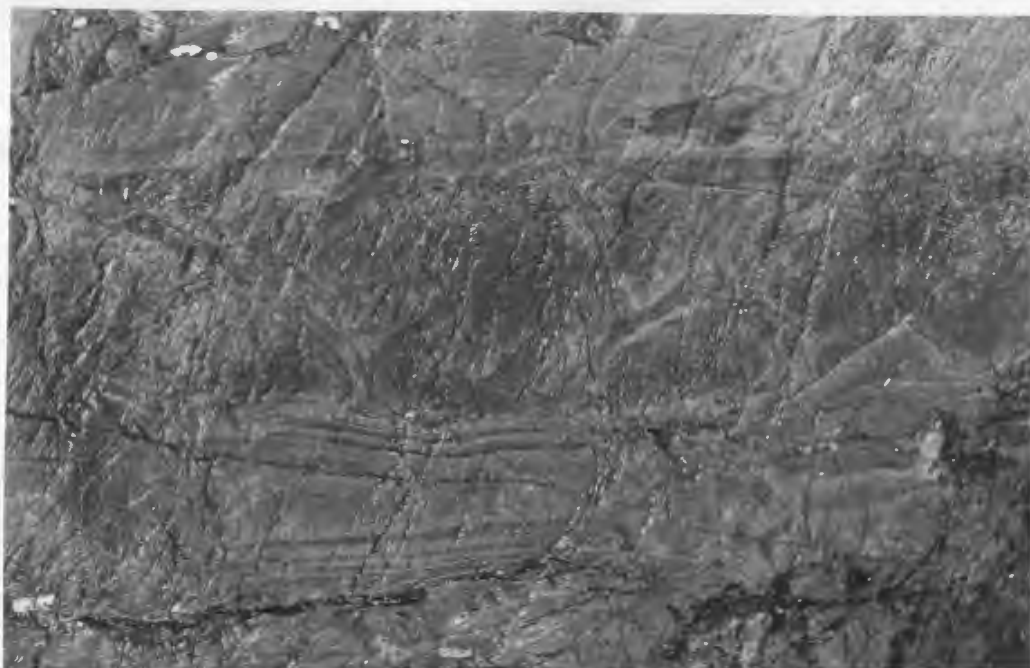


Figure 8: Layered Basalt dykes intruding pillow lavas just south of Beachy Cove on the Moretons Harbour Peninsula. Note the asymmetric chilled margins in the lowermost dyke. Width of lower dyke = 16 cm.



Figure 9: Closeup of the chilled margins in a dyke at Beachy Cove.

On the eastern shore of Moretons Harbour, layered basalt dykes intrude and feed an overlying pile of undeformed pillow lavas. In this region, variations in dyke orientation are extreme, with the result that a sinuous tangle of crosscutting dykes has developed.

The origin of these dykes is debatable, although it is likely that they developed in a manner similar to sheeted dykes; i.e. by the permissive and multiple injection of fresh magma into a pre-existing and partially cooled basalt dyke.

II.B.2.c.Hornblende-Plagioclase Porphyritic Dykes

Hornblende-plagioclase porphyritic dykes only occur on the Moretons Harbour Peninsula and are especially common east of Webber Bight. At this locality, the dykes feed and intrude Webber Bight Pillows. The dykes average 1 meter in width and are easily distinguished from all other intrusive rocks by the presence of large, euhedral phenocrysts of plagioclase and hornblende. The dykes always crosscut, and are therefore younger than, the layered basalt dykes.

In thin section, hornblende-plagioclase dykes consist of abundant phenocrysts of saussuritized plagioclase (40%) and green pleochroic hornblende (40%) enclosed in a groundmass of fine grained plagioclase, devitrified glass and minor opaques (20%) (Fig. 10). On the south shore of Sam Jeans Cove, dykes of similar composition are present, although here both the plagioclase and hornblende phenocrysts

display the effects of extensive deformation and recrystallization (Fig. 11). The hornblende prisms become aligned and define the main foliation and lineation in the area, while the plagioclase matrix recrystallizes into a polygonal groundmass of optically strain free new grains. Only the large plagioclase phenocrysts appear to have remained unaffected by the deformation episode.

The spatial orientation of 29 hornblende-plagioclase dykes is given in Figure 7, page 24.

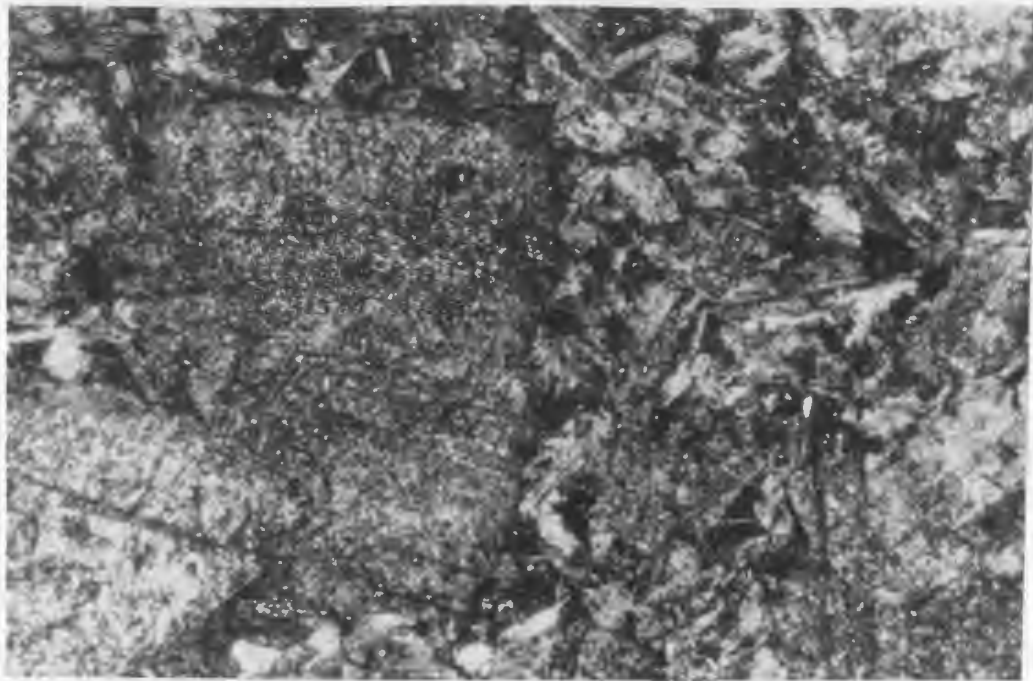


Figure 10: ES-3121. Undeformed Hornblende-Plagioclase porphyritic dyke from Wild Bight. X polars. This rock consists of large plagioclase phenocrysts enclosed in a plagioclase and hornblende matrix. Scale: 1cm=.25mm.

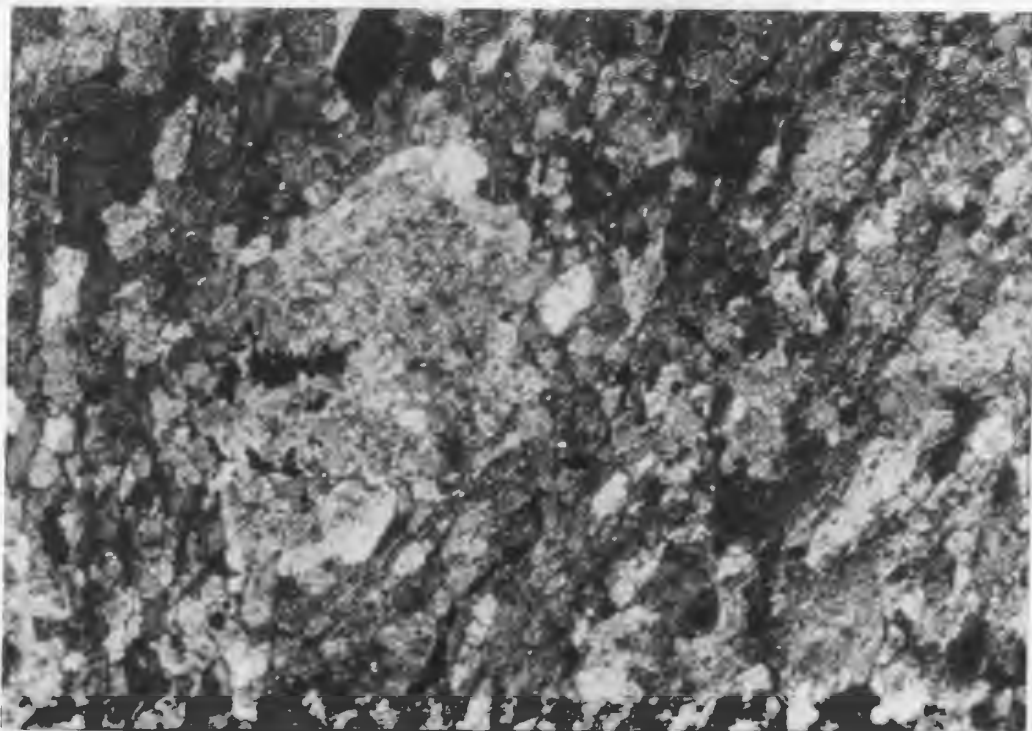


Figure 11: ES-1090. Deformed Hornblende-Plagioclase dyke from Sam Jeans Cove. X polars. In this rock, both the hornblende and plagioclase grains have been deformed and partially recrystallized during the D_1 deformation. Scale: 1cm=.25mm.

II.B.2.d. Diabase Dykes

Diabase dykes are by far the most common dyke type in the Twillingate region. They occur on Salt Harbour Island, South Twillingate Island, the Trump Islands, and the Moretons Harbour Peninsula. In the latter area, they are the prevailing rock type and are known to cut both layered basalt and hornblende-plagioclase porphyritic dykes. On Trump Island and Salt Harbour Island, they intrude a highly deformed terrain yet are themselves undeformed, suggesting that they were emplaced post-tectonically. This is important, since their isotopic age of 473 ± 9 ma. (Williams et al., 1976) sets constraints on the minimum age of deformation within the region.

Diabase dykes are recognized in the field by their felted texture, produced by the random distribution of small plagioclase laths (<1 mm) enclosed in a dark aphyric matrix. In thin section, these plagioclase laths (An_{30} - An_{40}) are mildly saussuritized and strongly zoned, while the groundmass consists of 35-40% augite (or hornblende), 10% chlorite, and minor amounts of calcite, apatite, and opaques (Fig. 12 and 13). A coarse grained gabbro body of similar composition has been described by Strong and Payne (1973) from the Moretons Harbour Peninsula, and may be genetically related to these dykes.

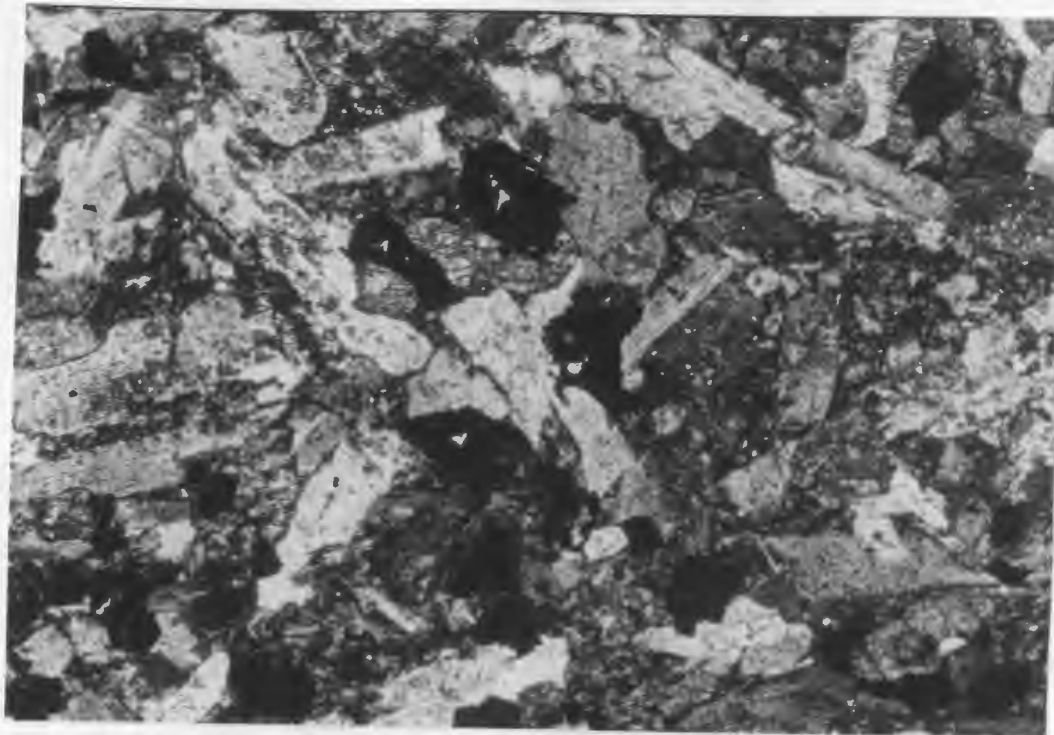


Figure 12: ES-1020. Diabase dyke from Wild Bight. X polars. This rock consists of large plagioclase laths and anhedral augite crystals surrounded by chlorite, calcite, and opaques. Scale: 1cm=.25mm.



Figure 13: ES-1052. Diabase Dyke from the southeastern corner of Salt Harbour Island. X polars. The mineralogy of this dyke is identical to ES-1020. This is the dyke which was dated at 473 ± 9 ma. by Williams *et. al.* (1976). Scale: 1cm=.25mm.

II.B.2.e. Lamprophyre Dykes

Lamprophyre dykes were first observed in the Twillingate region by Jukes (1842) who made note of an 'extensive brown dyke' on the east coast of Twillingate Harbour. Since then, Payne (1974) has conducted a petrographic study on these dykes, and Williams et. al. (1976) has assigned a late Jurassic age to their emplacement.

Lamprophyre dykes are dispersed throughout the region and, although most have been cut by late faults, some have preferentially intruded along the fault zones themselves. Thus fault development and dyke emplacement may have occurred simultaneously.

In hand specimen, lamprophyre dykes are brown, knobby weathering intrusives which are characterized by large, euhedral phenocrysts of augite, biotite, and hornblende. These phenocrysts are enclosed in a medium grained matrix of acicular augite surrounded by minor biotite and magnetite. None of these minerals exhibit any optical effects of deformation in thin section.

The isotopic age and crosscutting relationships noted in the field both suggest that lamprophyre dykes represent the youngest intrusive event to affect the Twillingate region.

II.B.2.f. Other Dyke Types

Several rare dyke types were described by Payne (1974), but were not observed during the present study. These include Alkaline-Olivine Basalt Dykes and Herring Neck dykes, both of which only occur in the rocks immediately south of the present study area. For a detailed discussion of these dyke types, the reader is referred to Payne (1974; pages 50-64.)

II.B.3. Volcaniclastic Sediments

The least common rock types found in the study area are the volcaniclastic sediments, which occupy less than 5% of the total regional exposure. Localized outcrops of this lithology occur at Jenkins Cove and Back Harbour (Twillingate), near Fools Harbour (South Trump Island), on Salt Harbour Island, and at Berry Island and Moretons Harbour on the Moretons Harbour Peninsula.

In all but the last two occurrences, fine grained crystal tuffs and agglomerates predominate. The tuffs are medium-bedded (<5 cm thick), extremely fine grained, and are multicolored, with shades of grey, green, and red being most common (see, for example, figure 34, page 62). In comparison, the agglomerates are massively bedded, and consist of coarsely graded sequences of pink rhyolite clasts enclosed in a dark green matrix. To date, these agglomerates have only been observed in a small outcrop east of Back Harbour Head (North Twillingate Island), although it has been suggested that elongate felsite clasts at Bread and

Butter Point and Salt Harbour Island may represent localized agglomerate horizons (Payne, 1974).

At this last locality, the agglomerate clasts are coarse grained and strongly resemble nearby dykes of the Twillingate Granite. This suggests that the clasts and dykes may be deformed equivalents of each other, although geochemical analysis would probably be necessary to substantiate such a proposal (Fig. 14 and 15).

Graded volcanoclastic agglomerates are locally abundant in the cliff exposures east of Moretons Harbour, and may represent turbidite deposits derived from a nearby volcanic source. Distinct graded beds in this region attain thicknesses of 5 to 10 meters and are frequently capped by thick tuffaceous horizons and pillow basalts, suggesting interludes of quiescence between episodes of rapid sedimentation. In all cases, these graded beds suggest that the sedimentary sequence youngs to the northwest.

In thin section, the tuffs are extremely fine grained and difficult to analyze. Quartz appears to be the major component, while chlorite, epidote, and an acicular amphibole (actinolite?) have been recognized as accessory phases. Localized domains of coarser grained quartz and chlorite may represent late veins or original detrital clasts.



Figure 14: Slightly sheared basalt/granite breccia at Gallows Cove, North Twillingate Island.

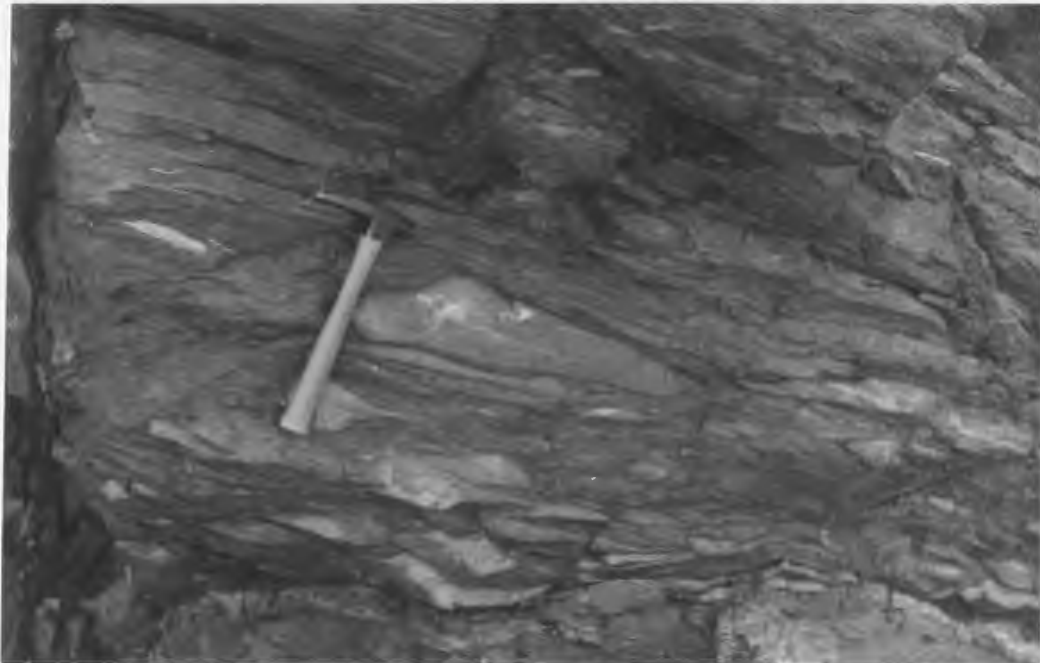


Figure 15: Strongly deformed 'siliciclastic' sediments (Payne, 1974) at Bread and Butter Point. The close spatial proximity of this outcrop with the one at Gallows Cove suggests that the former is a deformed equivalent of the latter.

II.C. The Twillingate Granite

The Twillingate Granite is an intrusive body of batholithic proportions (see Fig.2, page 13). It underlies an insular region of over 12 square miles on northeastern New World Island, South Twillingate Island, Black Island, and South Trump Island, and may extend beneath Notre Dame Bay to include a total area of about 70 square miles. It has been isotopically dated from specimens collected on Salt Harbour Island by Williams et al. (1976) and has yielded a U/Pb age of 510 ± 17 ma.

II.C.1. Field Characteristics

In general, the Twillingate Granite is a greyish- green equigranular rock consisting of 40% anhedral, clear to blue quartz, 40% sodic plagioclase, and up to 20% mafic minerals, including green pleochroic hornblende, chlorite, and pyrite. It is an extremely resistant rock, and usually forms steep-sided hills and cliffs of massively jointed stone. Talus slopes of granite are rare, and are only well developed near Spilers Cove, where a less resistant pink variety of granite is present. In most other regions the granite weathers to a chalky white or light grey colour.

The textures present in the Twillingate pluton depend on the degree of deformation it has undergone. In regions of little deformation, the granite exhibits a hypidiomorphic equigranular texture in which the crystal size ranges from .5 to 1 cm. (Fig. 16). With increasing strain, the quartz

grains become progressively more elongate and develop a strong L-S fabric (Fig. 17).

The Twillingate pluton is massive near its center and becomes strongly foliated as one approaches its eastern, northern and southern outcrop margins. This transition is well exposed at Clam Rock Head, where a progressive increase in foliation strength can be observed by walking seaward along the north shore of the peninsula (see Fig. 26).

A similar traverse may also be made from Codjack Cove towards Gunning Head, although here the region of highest strain has been intruded by a stock of nearly undeformed granite (Fig. 18 and 19). This late stock is similar in composition to the surrounding granite (Payne, 1974) and exhibits good intrusive relationships with the main granite pluton. Its presence suggests that localized stocks of the Twillingate Granite were emplaced after the cessation of the main deformation in the area.

Apart from apophyses and dykes, intrusive contacts of the Twillingate Granite with the Sleepy Cove Group are rare and only occur at Jenkins Cove and the west shore of Salt Harbour Island. At these localities, the Sleepy Cove Group basalts were intruded and metamorphosed by the granite (Fig. 20 and 21). A large xenolith of green massive basalt also occurs on the north shore of Martineau Pond (informal name) and shows the effects of partial assimilation into the pluton. In all three locations, the contact is marked by intense brecciation of the country rock with no evidence of

chilling between the two lithologies.

In contrast to these contacts, the basalt/granite interface on the west side of South Twillingate Island is marked by a narrow zone of fine grained quartz porphyritic granite which may represent a chilled margin to the pluton. This chilled zone is best exposed on the west end of the White Hills, where it dips shallowly to the east and is overlain by basalts of the Sleepy Cove Group. Although neither its upper or lower contacts were directly observed, this finer grained zone appears to grade transitionally into the main pluton and may attain a total thickness in excess of 8 meters.



Figure 16: Mildly deformed Twillingate Granite from Durrels Arm. X polars. Note the straight to curvilinear boundaries developed between the feldspar and quartz grains. Scale: 1cm=.25mm.

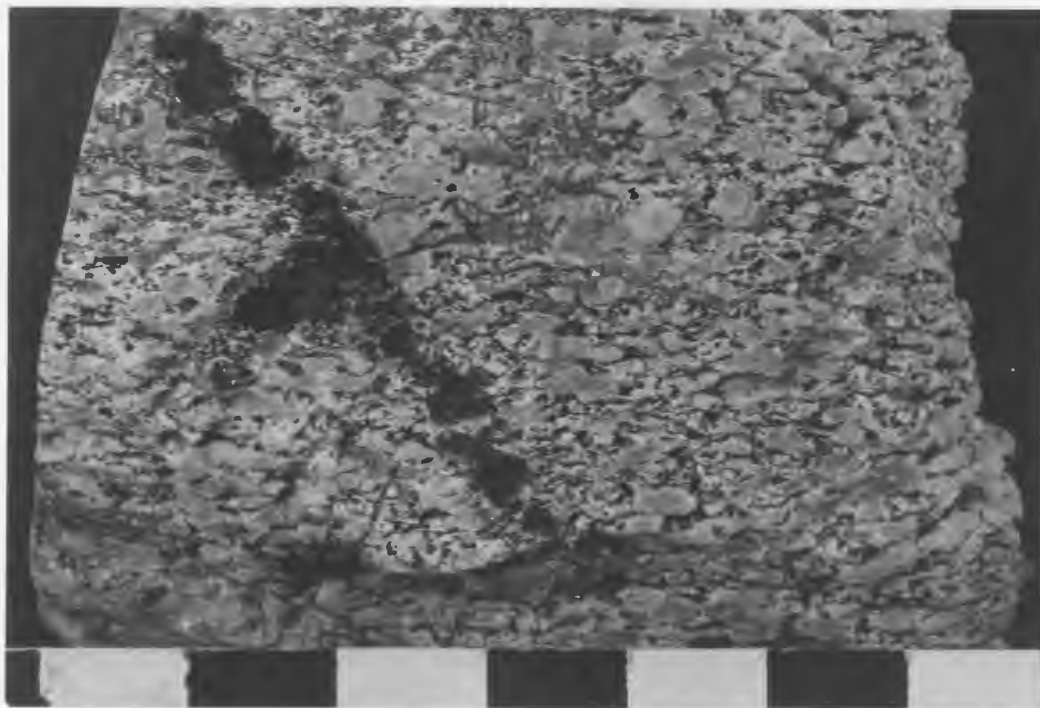


Figure 17: Strongly foliated Twillingate Granite from Gunning Head. Note the development of anhedral quartz blebs by the local intergrowth of adjacent grains. Scale: 1 block=1 cm.



Figure 18: ES-1001. Deformed Granite from Gunning Head. X polars. Note the presence of small new grains at the boundaries of the larger, elongate quartz grains. Scale: 1cm=.25mm.

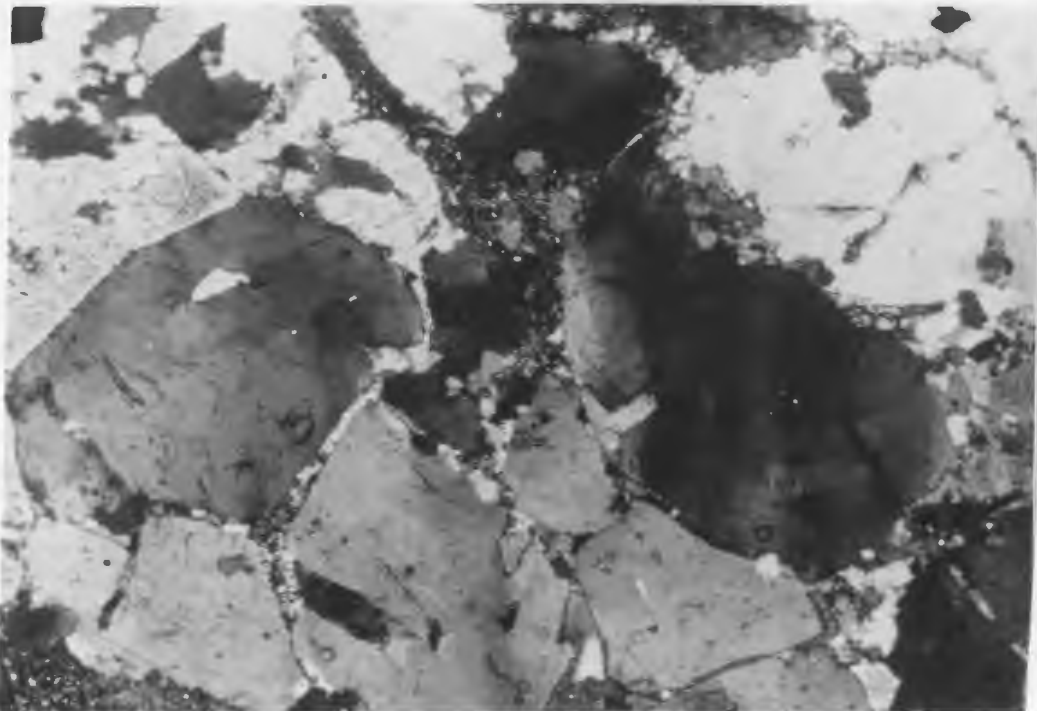


Figure 19: ES-1002. X polars. Mildly deformed granite from the tip of Gunning Head. This sample was collected 30 feet from sample ES-1001. Scale: 1cm=.25mm.



Figure 20: Granite/basalt contact at Jenkins Cove. This is by far the best exposed contact of the Twillingate Granite in the region.



Figure 21: Close-up of the granite/basalt contact at Jenkins Cove. Note the absence of a chilled margin at this location.

II.C.2. Quartz Porphyry Dykes

Quartz porphyry dykes commonly occur throughout the Sleepy Cove Group, and extend into the rocks of the Moretons Harbour Group on North Trump Island and Mouse Island. They exhibit a tectonic history similar to the rocks they intrude and were therefore emplaced prior to deformation. The dykes vary in width from 30 cm. to over 3 m. and exhibit a preferred regional orientation in areas of high strain (Fig. 22). They are mineralogically and chemically similar to the Twillingate granite (Coish, 1973), but differ texturally in consisting of large (~5 cm.) phenocrysts of quartz and sodic plagioclase enclosed in a fine grained quartzo-feldspathic groundmass. Accessory minerals, such as hornblende and chlorite, rarely exceed 5% in abundance and decrease in importance away from the pluton.

II.D. Diatremes

Diatremes are late features in the Twillingate area, and occur throughout much of the region. They are circular to elliptical structures in plan which probably extend as pipes vertically. They average 1 to 2 m. in diameter and contain a heterogeneous assortment of well rounded clasts enclosed in a fine grained matrix. The best examples of diatremes occur behind Ashbourne's store at Twillingate Harbour, and on the southwest shore of Webber Bight, where the breccia pipe is cut by a late diabase dyke.

The lithologies exposed in the brecciated zones are primarily those of the surrounding country rocks, although some exotic clasts have been noted. At Twillingate, the principal rock types are massive basalt and granite, with minor clasts of gabbro and ultramafic rocks (serpentinite?). At Webber Bight, the breccia pipe consists of basaltic and feldspar porphyritic clasts enclosed in a basaltic matrix (fig. 23). No granite or ultramafic blocks were noted in this occurrence.



Figure 22: Quartz porphyry dykes at South Trump Island. Note the parallism of these dykes with amphibolitized pillow lavas at this locality.



Figure 23: Hand specimen of diatrema material from the tip of Long Point, Twillingate. Scale: 1 block= 1cm.

II.E. Metamorphism

The metamorphic history of the Twillingate region consists of one major period of high-temperature dynamic metamorphism (M_1) followed by a period of lower-temperature metamorphism (M_2). Of these, M_1 in the basalts was previously recognised by Coish (1973), Payne (1974), and Williams & Payne (1975), while the effects of M_1 and M_2 in the granite are new observations.

II.E.1. M_1 Metamorphic Zonation in the Sleepy Cove and Moretons Harbour Groups

M_1 was the strongest metamorphic event to affect the Sleepy Cove and Moretons Harbour Groups, and led to the development of amphibolites to the south and epidote-amphibole (actinolite?) bearing rocks to the north. The surface trace of this metamorphic zonation parallels the Lukes Arm Fault at Sam Jeans Cove and northeastern New World Island, although this may be due, in part, to the truncation of the amphibolite facies zone by later faulting (fig. 24).

The amphibolite zone is best exposed on northeastern New World Island, at Sam Jeans Cove, and at the Trump Islands, where the typical metamorphic assemblage includes plagioclase (50%), hornblende (30%), clinopyroxene (1-10%), chlorite, epidote, apatite, and opaques (10%).

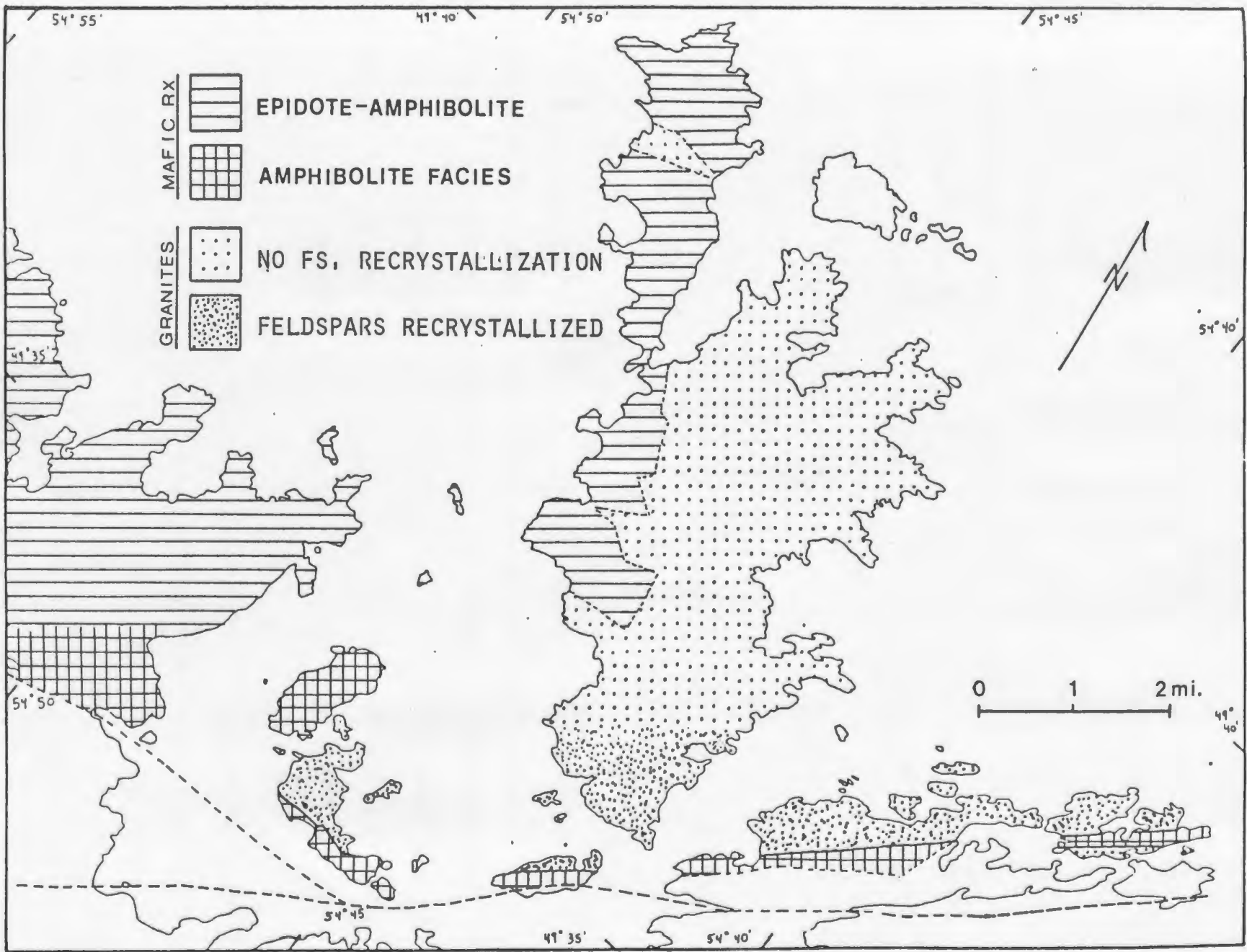


Figure 24. Metamorphic map of the Twillingate region.

Plagioclase in this zone is usually recrystallized and free from inclusions, although phenocrysts, where present, are frequently clouded. Recrystallized grains are optically strain-free and sometimes twinned, with compositions ranging from An₃₀ to An₄₅.

Hornblende is the characteristic mineral of this zone and is typically blue-green to brown pleochroic. It defines the dominant lineation and foliation in the southern extremities of the region and occurs as anhedral crystals within vesicles elsewhere.

Metamorphic clinopyroxene is also locally abundant at Sam Jeans Cove, where it forms equilibrium textures with plagioclase (see Payne and Strong, 1979). In this region, it is recognized by its high birefringence and relief, and its slight yellow pleochroism.

North and west of these occurrences, metamorphic grade gradually decreases, and phases characteristic of the Epidote-Amphibolite Facies become prevalent. The mineralogy of this zone consists of plagioclase (30-50%), actinolite (20-60%), chlorite (5-40%), epidote (15%) and calcite (5%). Minor opaques, apatite and sphene are also present in some areas.

Within this zone, plagioclase ranges in composition from An₅ to An₂₀ and is often saussuritized but not recrystallized. Fibrous actinolite occurs as vesicle fillings at Webber Bight and ranges from clear to light green pleochroic. Elsewhere, and especially on Mouse and Matthews

Islands, actinolite is the dominant mineral in thin section and forms small rosettes of acicular needles. Chlorite is a minor component in the southern part of the zone, but increases in abundance northwards, a feature which again suggests a gradual decrease in metamorphic grade in that direction.

No abrupt variations in metamorphic grade were noted within the study area. This is particularly true of the region north of Sam Jeans Cove, where an apparent metamorphic break led Williams and Payne (1975) to apply Karig's (1972) remnant arc model to the region. During the present study, it was found that this apparent break was caused by the intrusion, and possible fault juxtaposition of young, post M_1 diabase dykes against the older, metamorphosed sediments of the Moretons Harbour Group.

II.E.2. M_1 Metamorphic Zonation in the Twillingate Granite

Metamorphic grade in the Twillingate Granite appears to decrease towards the north. This is suggested on the basis of microstructural evidence, since the bulk composition of the granite body does not lend itself to the development of metamorphic index minerals.

In the southernmost parts of the study area, both the quartz and plagioclase fractions of the Twillingate Granite have undergone dynamic recrystallization. Since recrystallized feldspar grains of the type observed in the

study area (see page 89) are only known to occur in amphibolite/granulite facies terrains (Marshall and Wilson, 1976), the granite in this region must have been exposed to relatively high-grade metamorphic conditions.

As one progresses northwards, past an imaginary line connecting Purcells Harbour to the northern tip of South Trump Island, recrystallization in the quartz grains becomes virtually non-existent, and the plagioclase grains become saussuritized rather than recrystallized (see page 90). Thus, it appears that metamorphic grade in the granite decreases northwards in a manner consistent to that found in the surrounding volcanic terrain.

II.E.3. The M_2 Metamorphic Episode

Following the M_1 metamorphic period, retrogression of the high-temperature mineral assemblages occurred locally during M_2 . During this event, rims of chlorite and actinolite were developed around cores of hornblende and clinopyroxene at Sam Jeans Cove, while at Salt Harbour Island they developed at the expense of hornblende. In the granite terrain, evidence for this later metamorphic event is less convincing, and is restricted to the development of albite rims in the clouded feldspar phenocrysts.

III. STRUCTURAL GEOLOGY- INTRODUCTION AND MACROSCOPIC ANALYSIS

III.A. Introduction

In section I.C., reference was made to various tectonic models applied to the Twillingate region since Heyl (1936). All of these models have been based on the existence of large scale variations in structural style and deformational intensity within the Twillingate region. However, since none of these variations have been adequately documented to date, it has been impossible to discuss the relative merits of any tectonic model. In order to resolve this problem, it was decided to conduct a detailed structural study of the Twillingate region, placing particular emphasis on the spatial extent of structural elements. This analysis is presented in the following chapters.

Chapter three considers the structural geometry of the region on the macroscopic scale, while chapters four and five analyse deformation on the microscopic scale. Together, these three chapters provide the data base for developing the stratigraphic/structural models presented in chapter six.

III.B. Deformational Characteristics of the Twillingate Region

In order to facilitate the comparison of the Moretons Harbour Group to the Sleepy Cove Group and Twillingate Granite, the study area was initially separated into two subregions.

The western subregion was defined to include rocks of the Moretons Harbour Group. It is characterized by a broad, west facing homocline of sediments and basaltic extrusives which have been tectonized near the southern and eastern margins of the area and are nearly undeformed elsewhere. The contact between the deformed and undeformed regions is usually gradational, although abrupt changes in structural style occur locally across fault boundaries (see Fig. 25, 26 and plate 1).

The eastern subregion includes exposures of the Sleepy Cove Group and the Twillingate Granite and is more intensely deformed than the western region. Its most distinguishing characteristic is a strong east-west trending foliation which is best developed near the northern, eastern and southern margins of the region and decreases in strength westward. This foliation overprints an early high strain zone to the south and is itself intensely folded to the north. Furthermore, a late faulting episode is locally evident and has subdivided the region into east-west trending tectonic blocks, each of which has its own distinctive structural characteristics.

Figure 25: Form surface map of foliations in the Twillingate region. The short lines indicate the strike of $S_0/S_1/S_2$. The thick, continuous line denotes the eastern margin of the BBB Zone.

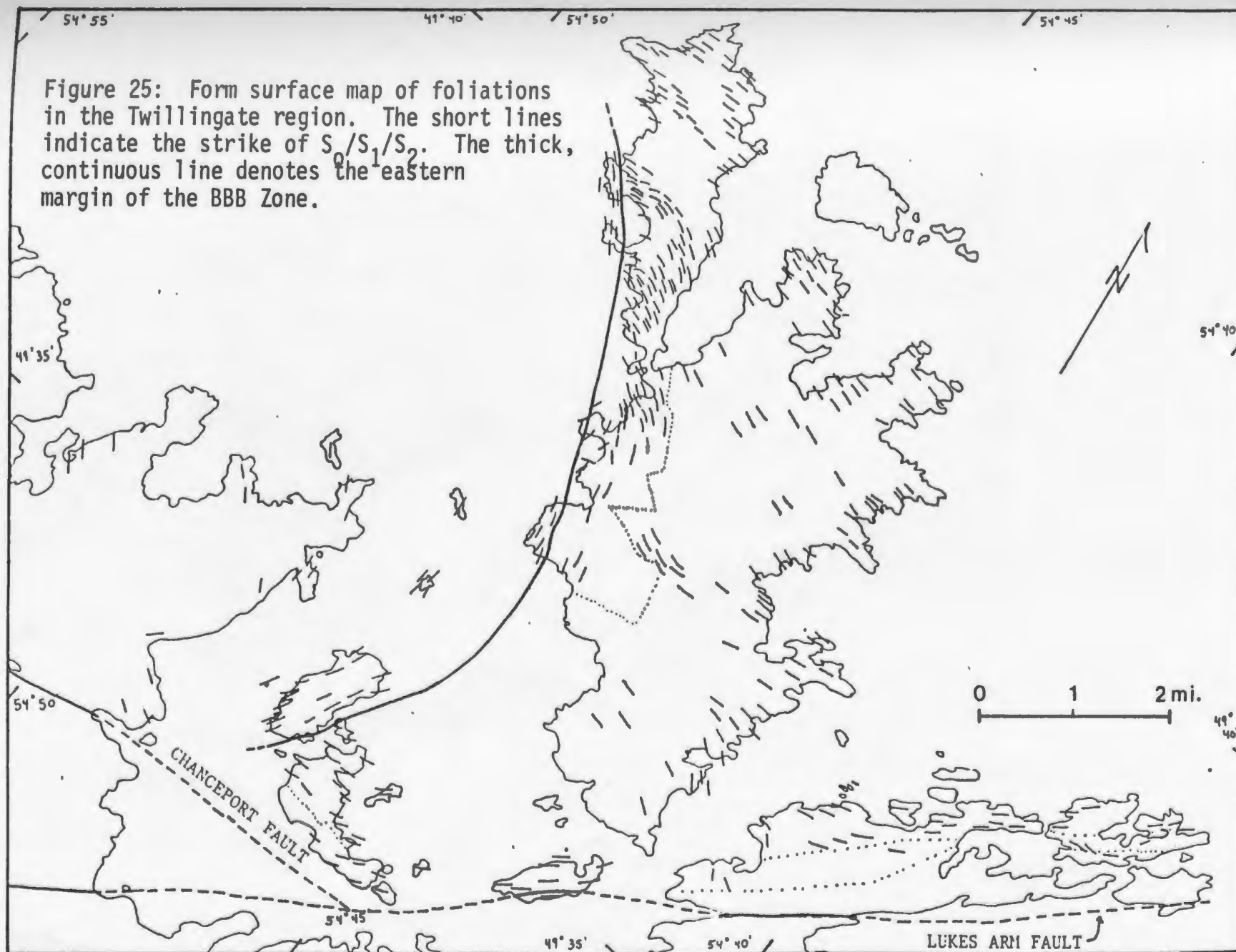
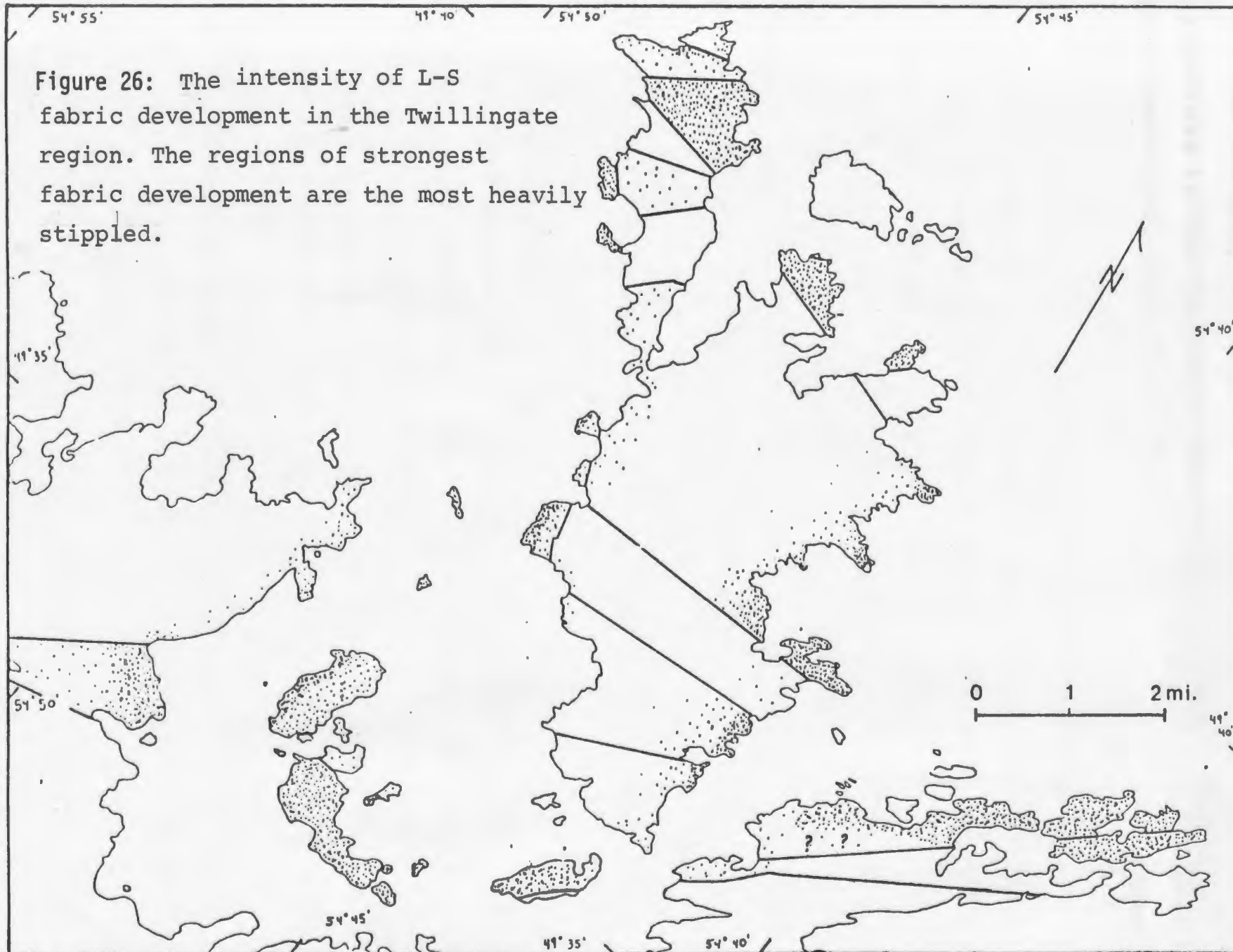


Figure 26: The intensity of L-S fabric development in the Twillingate region. The regions of strongest fabric development are the most heavily stippled.



The boundary between the western and eastern subregions is defined in the field by a narrow zone of highly foliated rock which extends from North Trump Island to Back Harbour Head and follows the west coast of the Twillingate Island (fig. 26). This zone, hereafter referred to as the BBB (or Bluff Head-Batrix Island-Back Harbour) zone, follows the Moretons Harbour/Sleepy Cove Group contact on the Trump Islands and South Twillingate Island, and deviates slightly on North Twillingate Island. Thus, it seems that the Moretons Harbour/Sleepy Cove boundary (as defined in this thesis) may have structural, as well as petrologic, geochemical, and geophysical significance.

III.C. Macroscopic Structures of the Twillingate Region

III.C.1. Introduction

Four phases of deformation have been defined in the present study area. Of these, D_1 and D_2 were the principal fabric-forming events, while D_3 was responsible for reorientating the earlier fabrics into local, open flexures. Late kinks and faults overprint F_3 folds and are therefore assigned to D_4 .

According to Payne (1974), an early (pre- D_1) event may have affected the study area prior to the emplacement of the Twillingate Granite. This event was hypothesized on the basis of folded layering observed in some of the amphibolite inclusions at Little Harbour, South Twillingate Island. How-

ever, since unambiguous evidence for internally folded xenoliths was not observed at this locality during the present study, this event can not be further discussed here.

Overprinting evidence for D_1 through D_4 occurs at Grassy Point, where a strong D_1 foliation has been folded by D_2 and D_3 , and subsequently kinked during D_4 (Figs. 27 and 28). Elsewhere in the study area, evidence for overprinting is rare, with the result that most determinations of structural age are based on structural style, orientation, and the metamorphic grade of mineral assemblages associated with the various fabric elements.

III.C.2. The D_1 Deformation-General Characteristics

D_1 was the first deformation event to affect the Twillingate region. It occurred during the M_1 metamorphic episode and is characterized by a strong metamorphic foliation (S_1) and stretching lineation (L_1) (Fig. 29). On the southern margin of the study area, both S_1 and L_1 are defined by aligned hornblende and quartz crystals, while actinolite, chlorite and quartz define the structural elements further to the north (Figs. 30 and 31). Both the Twillingate pluton and its apophyses were affected by D_1 and therefore must have been emplaced prior to or during this event.



Figure 27: A refolded fold from Grassy Point, Twillingate.
 Scale: each box = 1 cm.²

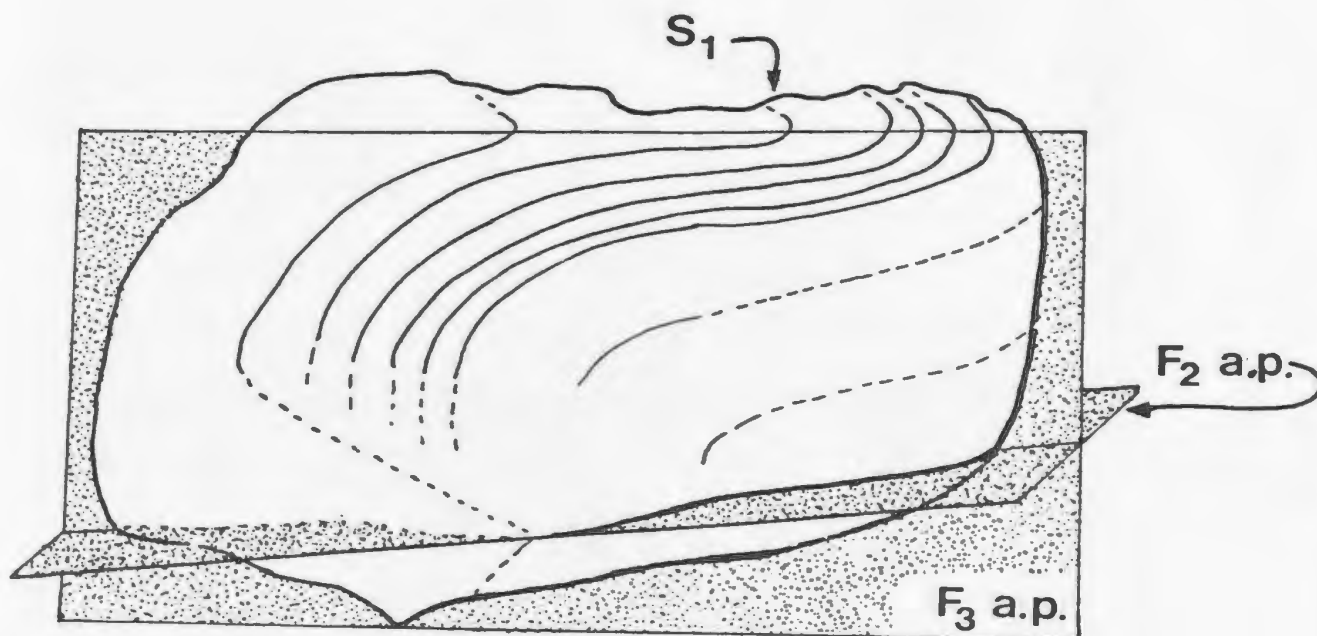


Figure 28: Sketch of sample 57, showing the orientation of S_1 and the axial planes of the F_2 and F_3 folds. Note the curvilinear nature of the F_3 fold axis.

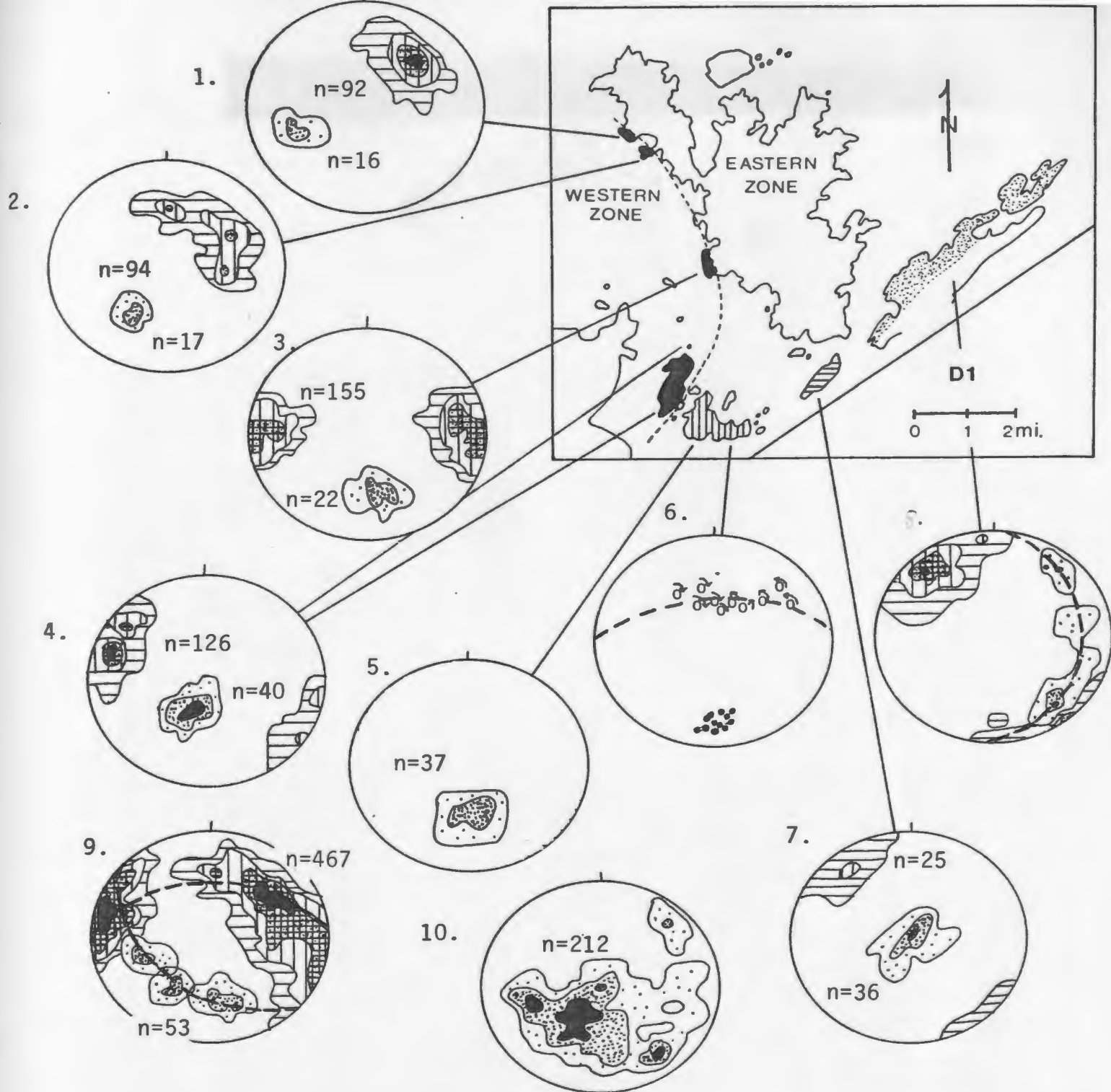


Figure 29: Orientation data for the D_1 deformation. Stippled regions denote the orientation of L_1 , lined regions enclose the poles to S_1 . Contour interval: $> 0, 5, 10$, and 20% per 1% area. 'n' = the number of recorded measurements in each subregion. These are equal area, lower hemisphere stereographs. Figure 29.6 gives the orientation of the axial planes (dots) and plunges (o's) of F_1 folds. The vergence of these folds is given by the arrows (clockwise = 'z' vergence, counterclockwise = 's' vergence). Fig. 29.9 shows the orientation of S_1 and L_1 in areas 1, 2, and 3. Figure 29.10 is a composite diagram of L_1 as it occurs in both subregions.

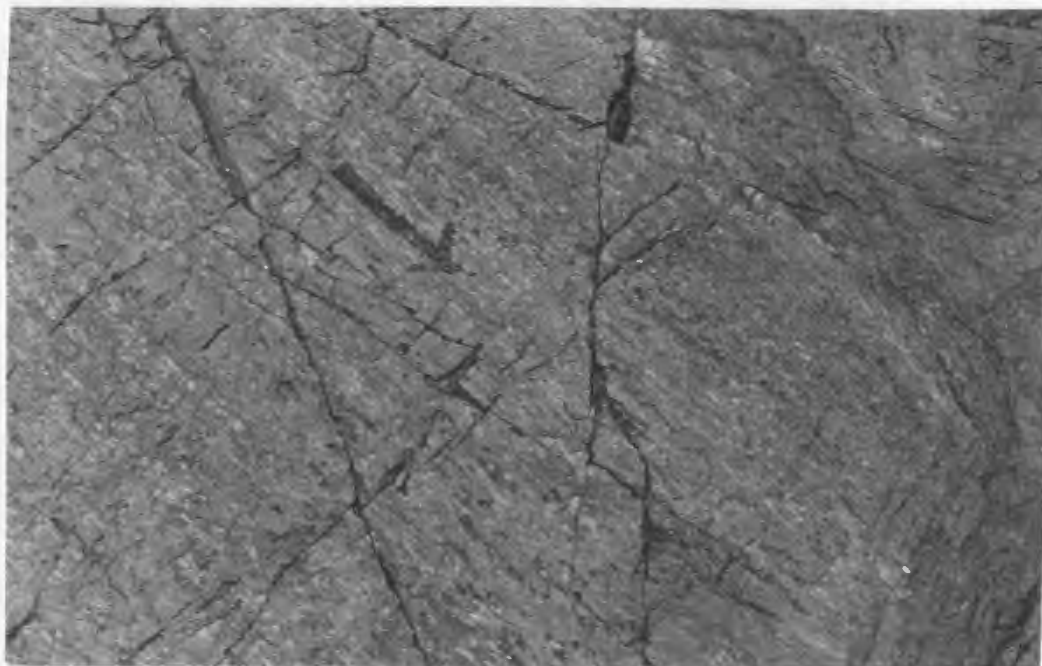


Figure 30: L₁ as observed in the amphibolites of South Trump Island. Here, L₁ is defined by elongate, calcite filled vesicles in pillow basalts.



Figure 31: L₁ observed in the granite of South Trump Island. Here, L₁ is oriented vertically. Scale: 1 block = 1 cm.

III.C.2.a. Deformational Style

Structures related to D_1 are localized in two zones of high strain (fig. 32). These zones lie at nearly right angles to each other and meet at Trump Island where, due to the absence of workable exposure, it is impossible to determine which zone developed first. The more southerly zone -the Salt Harbour/Trump Island (or SHTI) zone- extends from Salt Harbour Island to South Trump Island and approximately parallels the Lukes Arm Fault. L_1 and S_1 are strongest near the fault, and weaken to the north, suggesting that strain decreases northwards (see fig. 26, page 52). The BBB zone lies to the north of the SHTI zone and parallels the coast of North Trump Island and the Twillingate Islands. Both zones are structurally identical and differ mainly in the degree of metamorphism each has suffered (Fig. 24, page 45).

The most accessible cross section through one of these zones occurs on the north shore of Bluff Head, where it is possible to walk from the nearly undeformed eastern margin of the BBB zone into its highly deformed core. Variations in strain intensity along this section are gradational and extreme, with pillows extended to over ten times their initial length within a distance of about 100 meters. In the most deformed part of this zone, a stretching lineation defined by aligned clots of actinolite and chlorite, parallels the long axis of the elongated pillows, and defines the X-direction of the finite strain ellipsoid.

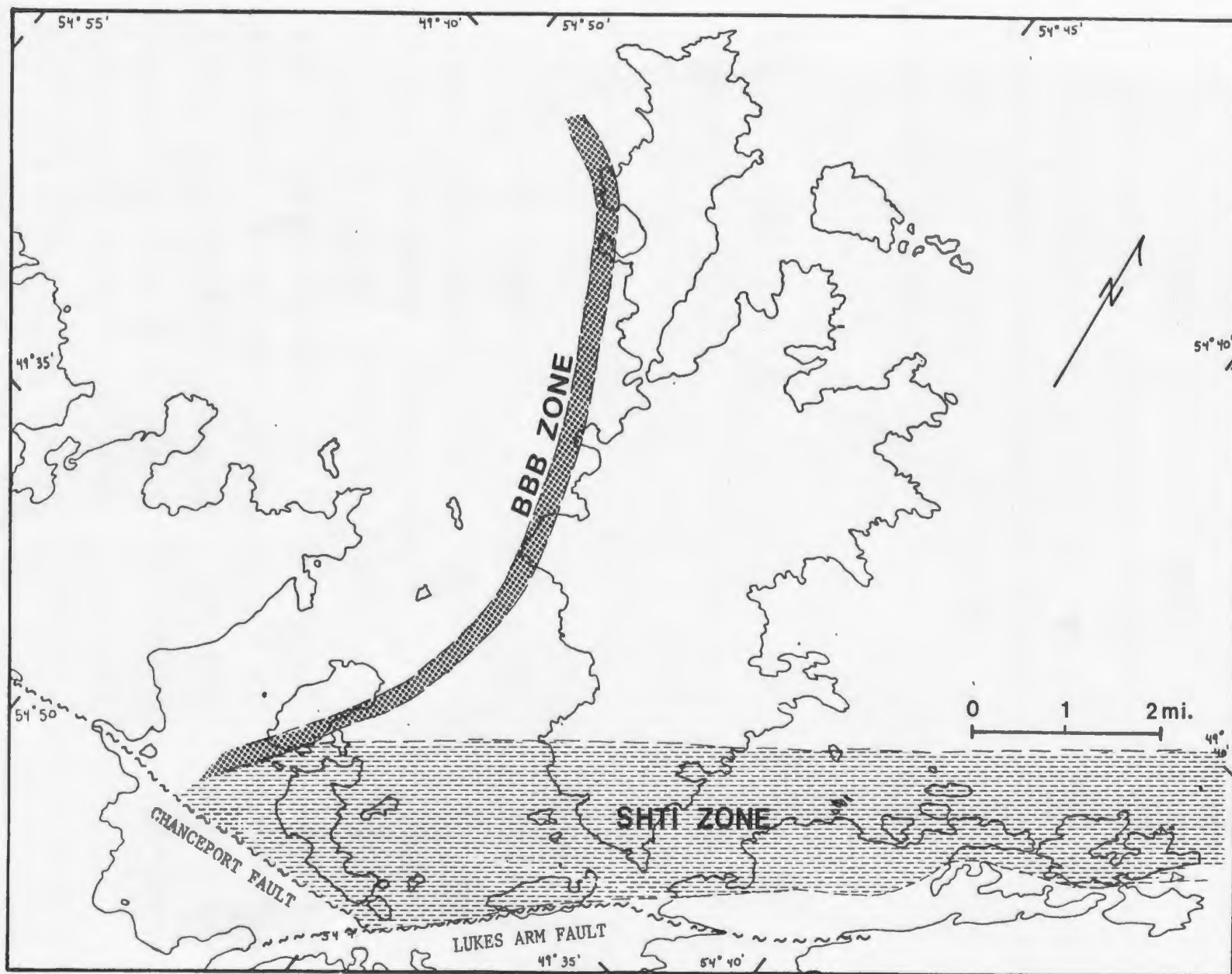


Figure 32. Approximate areal extent of the BBB and SHTI zones. See text for discussion.

The width of the two zones is impossible to determine due to structural segmentation and overprinting during D_4 . The highly deformed core of the BBB zone, for example, lies in fault contact with nearly undeformed volcanic rocks at Batrix Island and Back Harbour Head, while at North Trump Island, the deformed core has been faulted out altogether. Fault segmentation also occurred throughout the SHTI zone, although in this case the zone margins are mainly obscured by D_2 overprinting.

III.C.2.b. Orientation of Structural Elements

Throughout most of the region, S_1 parallels the inferred boundaries of the BBB and SHTI zones while L_1 plunges down the dip of the foliation (fig.29, page 56). Variations in the orientation of S_1 locally occur, however, and are related to either reorientation during D_2 and D_3 , or variations in the magnitude of finite strain imposed by D_1 . At Merritts Harbour, Salt Harbour Island, and Lobster Cove, for example, small scale variations in S_1 orientation are associated with abrupt changes in finite strain as defined by quartz grain elongation (fig. 33). These zones of variable strain parallel the inferred boundary of the SHTI zone and average three meters in width. They are laterally extensive, and usually continue until truncated by faults.

These high strain zones are structurally identical to those described from ductile simple shear regimes by Ramsay

and Graham (1970) and suggests that they developed in a similar environment.

Larger scale variations in the orientation of S_1 and L_1 occur locally as a result of reorientation during D_2 and D_3 . On Salt Harbour Island, for example, L_1 has been locally rotated into parallelism with F_2 fold axes, while S_1 has been folded to produce F_2 folds (fig 29.8, page 56, and fig 37, page 67). Later deformation has also affected the BBB zone to the point that S_1 and L_1 have been redistributed into great circle configurations (fig.29.9, page 56).

Folds related to D_1 are extremely rare, although one outcrop on the southeast tip of South Trump Island (the SHTI zone) may contain several examples (fig.34). At this locality, volcanoclastic sediments (S_0) have been deformed into asymmetric folds with variable plunges and axial planes which strike east-west and dip $52-68^\circ N$ (fig 29.6, page 56). Their sense of asymmetry, when viewed down plunge, varies from "S" to "Z" and suggests that movement in the zone was updip towards the north (Hansen, 1971). D_1 folds were not recognized in the BBB zone.

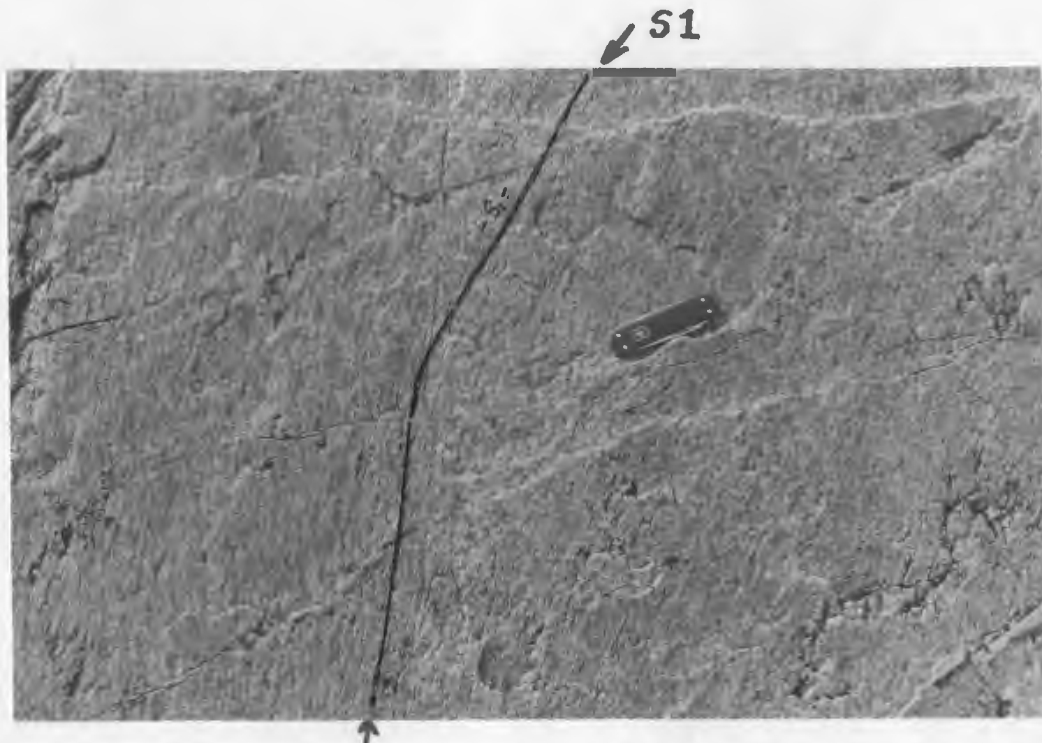


Figure 33: The presence of small scale shear zones in the granite terrain on Salt Harbour Island may suggest that S_1 in this region developed as a result of simple shear.



Figure 34: Possible F_1 folds in the siliciclastic sediments of South Trump Island.

III.C.3. The D₂ Deformation-General Characteristics

D₂ represents a low-temperature deformational event which affected all lithologies in the study area. (fig. 35). In the eastern subregion, D₂ resulted in the development of a strong foliation (S₂) and lineation (L₂), both of which are geometrically related to local F₂ folds. These three structural elements also occur in the western subregion, although their development is restricted to the west shore of North Trump Island and rocks immediately adjacent to Tizzards Harbour and Sam Jeans Cove.

III.C.3.a. Structural Elements

F₂ folds are the most distinctive structural feature associated with the D₂ deformation. They are especially well exposed at Salt Harbour Island, North Trump Island, and Grassy Point on South Twillingate Island, where they fold and crenulate S₁. (Figs 36 and 37). Geometrically comparable structures at Webber Bight, Jenkins Cove, and Wild Cove may also have developed during this event, but lack definitive overprinting criteria (see Fig. 38).

F₂ folds are tight to isoclinal class III structures (Ramsay, 1967), which do not exhibit a preferred asymmetry (Fig. 39). They have nearly vertical northwest/southeast trending axial planes and axes which typically plunge from 45 to 55 degrees towards the northeast (fig 35.2). At Grassy Point, however, D₃ resulted in the reorientation of F₂ folds such that their axial planes lie north-south and their axes

plunge at a high angle towards the east and west. Elsewhere in the region, the effect of D_3 on F_2 structures was less intense and resulted in the regional shifting of S_2 towards the north or east (Fig. 45, page 76).

In some localities, notably on the west coast of North Trump Island, F_2 fold hinges are locally preserved in an otherwise chaotic pillow breccia. The presence of these hinges suggests that the breccia developed by the folding and rupturing of pillows whose long axes (L_1) originally lay near the axis of maximum D_2 shortening (fig. 40 and 41).

S_2 lies axial planar to F_2 folds and is well developed in both the basalt and granite terrains (Figs. 42 and 43). It is delineated in the basalts by either a strong biotite or chlorite alignment, or a coarse crenulation cleavage produced by the small scale folding of S_1 .

S_2 is also well developed in the Twillingate granite, where it takes one of two forms depending on the grain size of the granitic rocks. In the coarser grained regions of the pluton, S_2 is defined by aligned quartz ribbons which locally give the granite a finely streaked appearance (see fig. 17, page 38). In the aphanitic or quartz porphyritic varieties of the granite, S_2 consists of a closely spaced fracture cleavage whose microlithons average three to five mm. in width. Both foliation types parallel S_2 in the basalts and are best developed along the southern, eastern, and northern margins of the exposed pluton.

L_2 , like S_2 , is an extensively developed fabric element which is geometrically related to F_2 . It parallels the axis of F_2 folds and is usually delineated by either rodded pillows, as on North Trump Island, or by a preferred mineral alignment of biotite, chlorite, and/or quartz aggregates. On the regional scale, L_2 is strongest in the southern and eastern parts of the region and is only locally observed to the north.

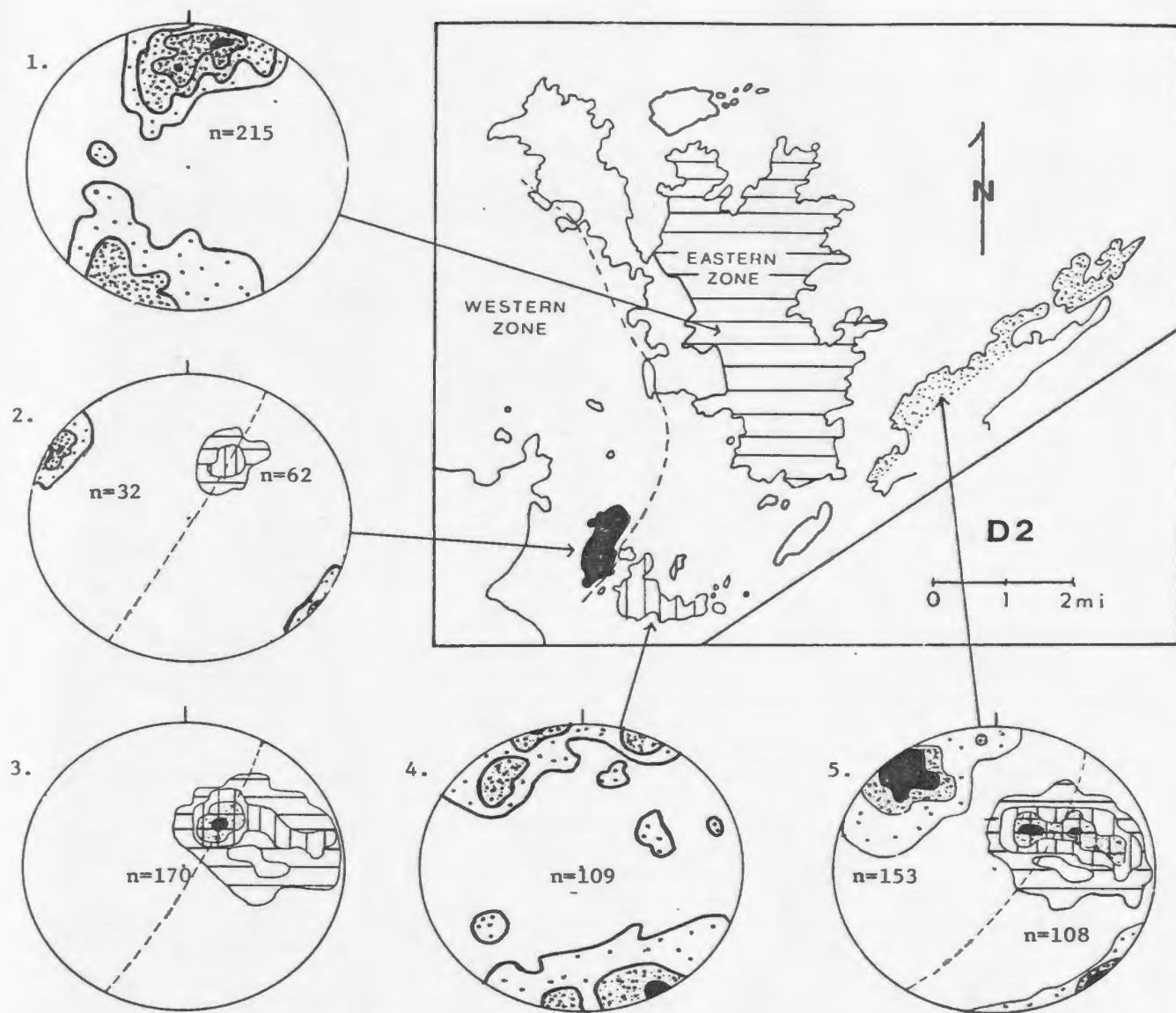


Figure 35: Orientation data for the D_2 deformation. Stippled regions denote the orientation of S_2 , lined regions L_2 . Contour interval \Rightarrow 0,5,10 and 15% per 1% area. The number of measurements made in each subregion is given in the stereonet itself. The dashed line in stereonets 2,3, and 5 give the average orientation of the F_2 axial plane, while the dots in diagram 3 give the actual orientations throughout the area. Diagram 3 is a composite diagram of L_2 as it occurs throughout the area.



Figure 36: F_2 folds on North Trump Island. In this location S_1 is folded.



Figure 37: F_2 folds on Salt Harbour Island. Here, large pillows, most of which contain a strong S_1 foliation, are folded.

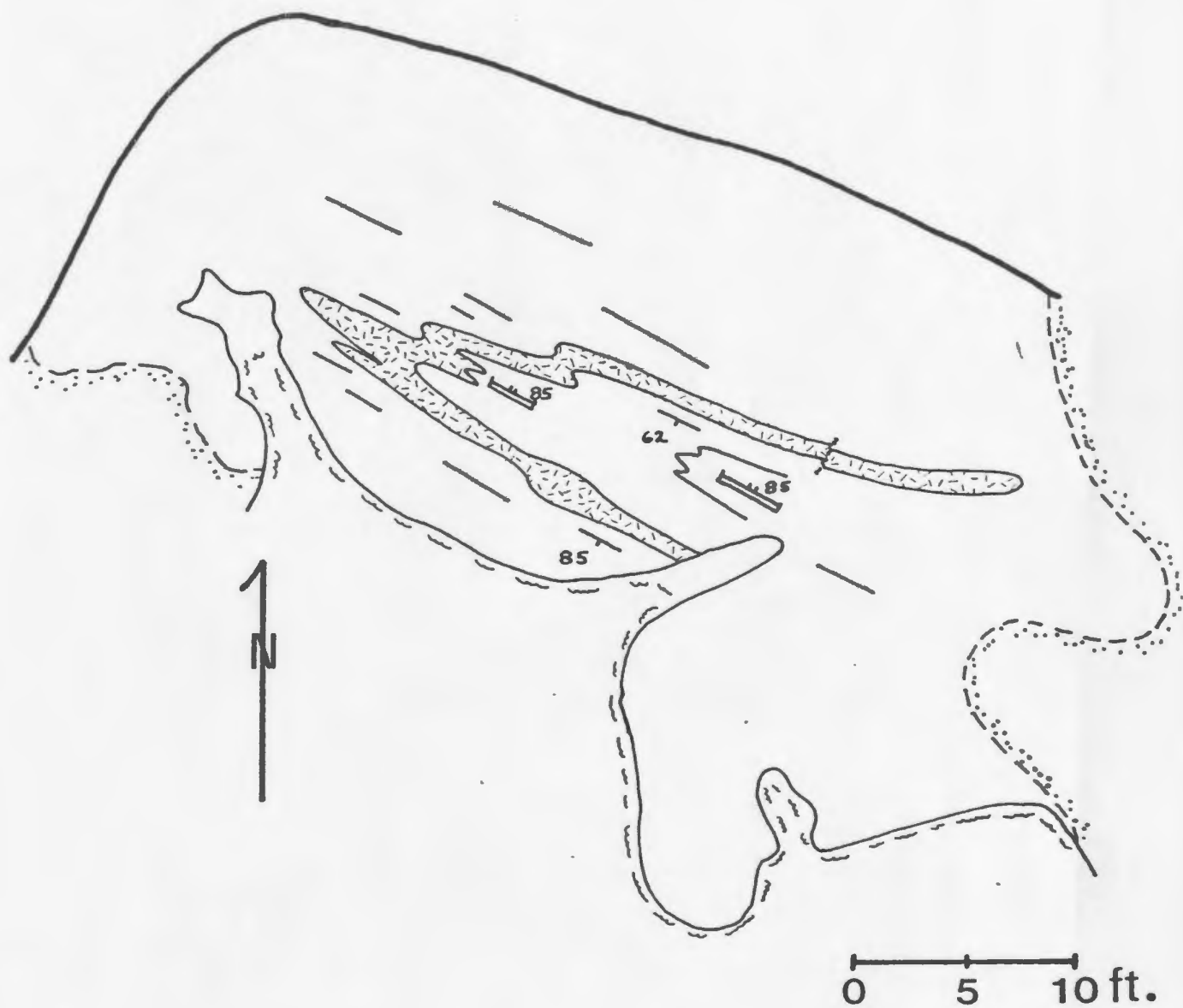


Figure 38: Sketch map of the $F_2(?)$ fold at Jenkins Cove, Twillingate. The fold itself is defined by a folded quartz porphyry dyke. Symbols used in this and the following diagram are defined in plate 1.

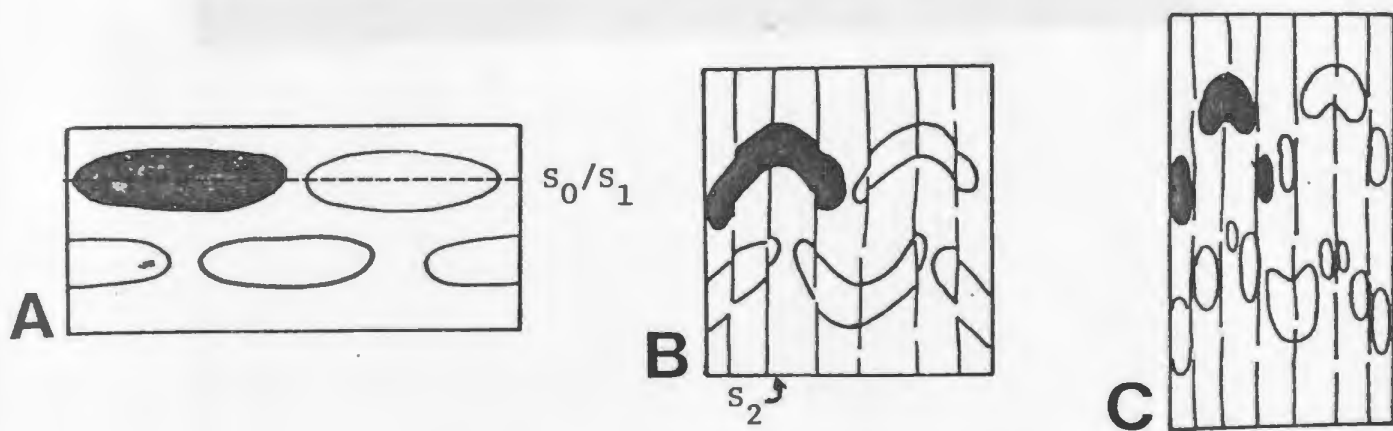


Figure 40: Development of the tectonic pillow breccia on North Trump Island. The shape of the box in each case gives some idea of the finite strain the pillows have suffered. Note especially the presence of preserved fold hinges in diagram 40c.

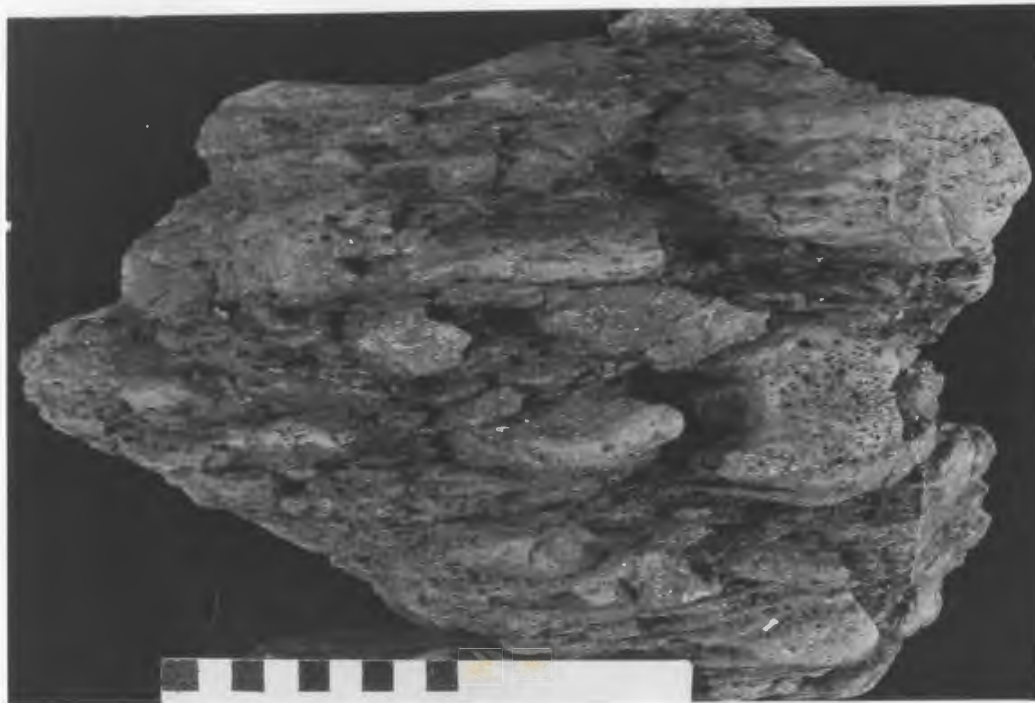


Figure 41: Hand specimen of the tectonic breccia on North Trump Island. Again, as with 40c, note the presence of the F_2 fold hinge in the right central part of the photograph. Scale: 1 box = 1 cm.²



Figure 42: S_2 on Salt Harbour Island. In this region, S_2 (diagonal striping) is often defined by a biotite foliation. Thick, horizontal layering is bedding. Scale: 1 block= 1cm.

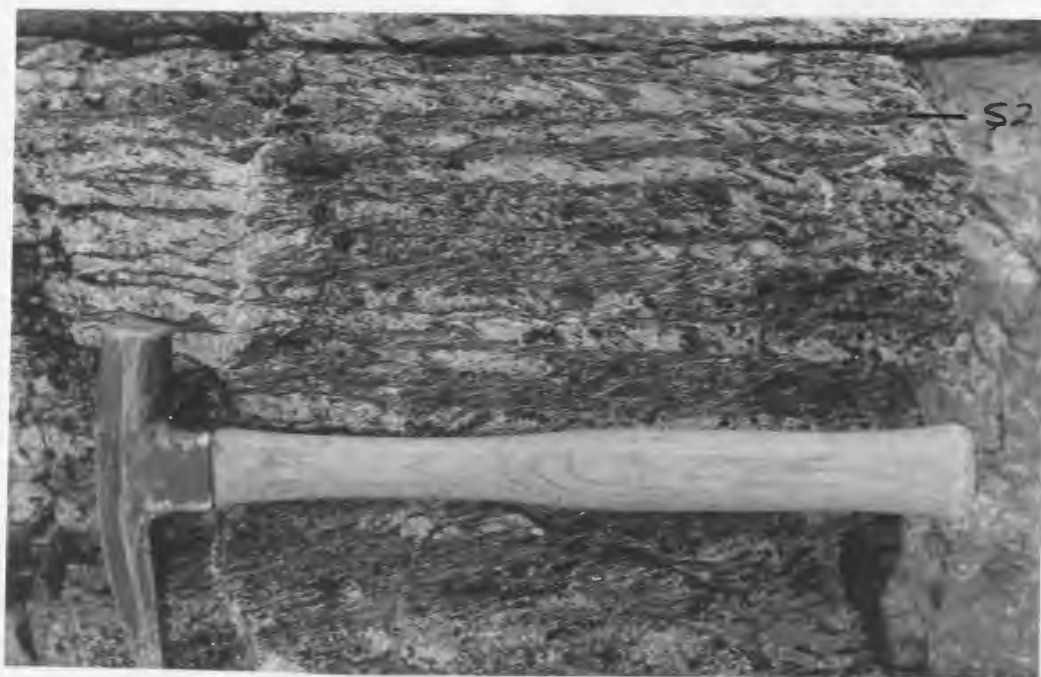
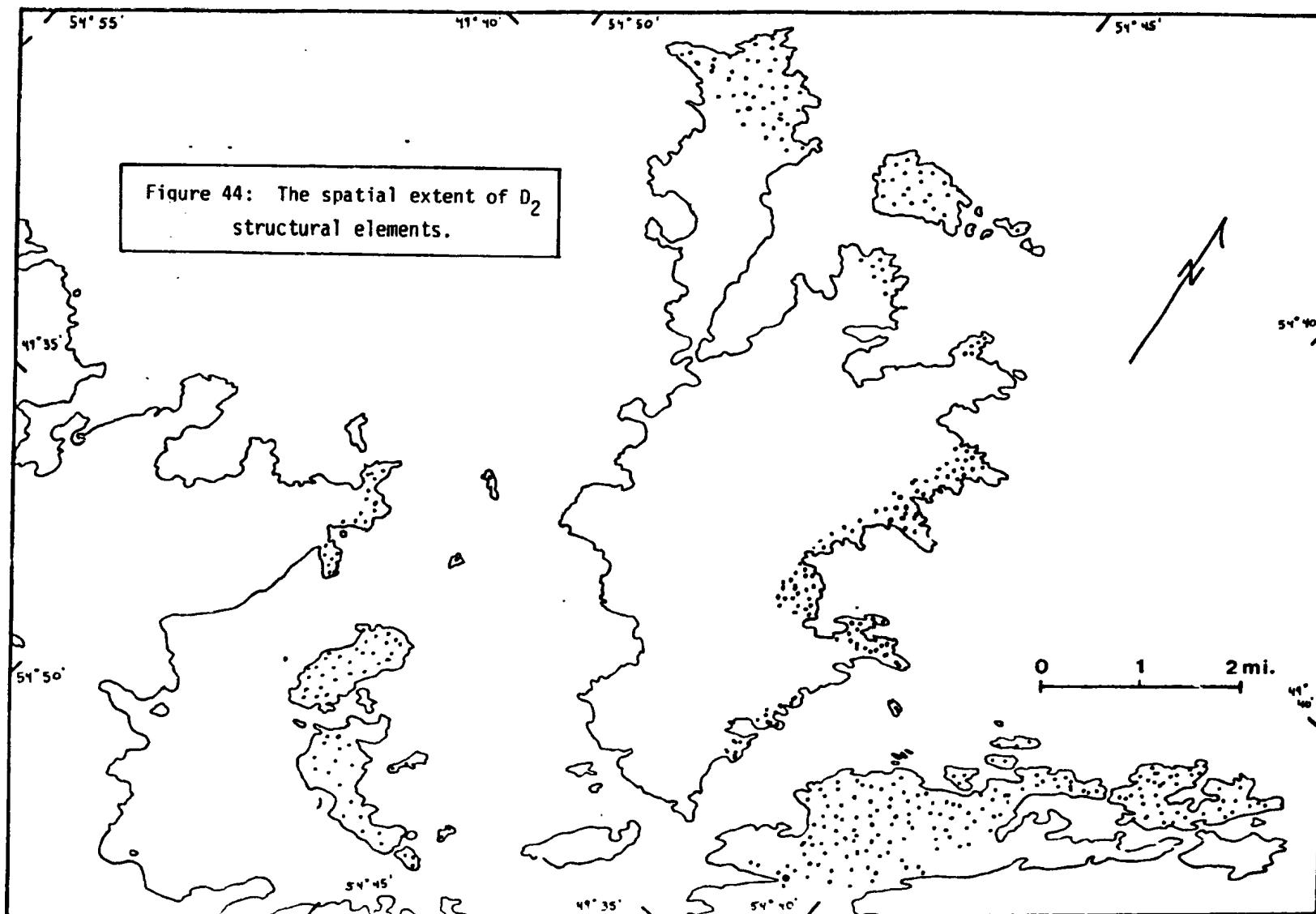


Figure 43: S_2 on North Trump Island. Here, S_2 is defined by a coarse crenulation cleavage produced by the local folding of S_1 .

III.C.3.b. The Spatial Extent of D_2 Structural Elements.

Although the effects of D_2 have been observed throughout the eastern subregion and in parts of the western subregion, the amount of strain suffered by the region as a whole was by no means constant. In the eastern subregion, granite outcrops containing extremely oblate quartz grains and feldspar blebs (S_2) tend to lie just west of a hypothetical triangle which extends from Crow Head to Black Island and has its apex at Codjack Cove. D_2 strain within this triangle was minor to nonexistent, with granite outcrops exhibiting a near equigranular texture. In the western subregion, the effects of D_2 are centered around the BBB zone and decrease rapidly westward (see fig 44).



Note: The dotted portions of this map denote regions affected by D_2 .

III.C.4. The D₃ Deformation-General Characteristics

D₃ was the last major deformation episode to affect the Twillingate study area. Its effect on the region was limited to outcrops adjacent to and within the BBB zone. It is characterized by broad, open F₃ folds and a fine scale crenulation cleavage which is locally developed in the hinge regions of the F₃ structures.

III.C.4.a. Structural Elements

F₃ folds occur on various scales and are primarily found in the Sleepy Cove Group just east of the BBB zone on North and South Twillingate Island. At Grassy Point, they are open, upright folds, often concentric in style, whose axial planes strike northwest-southeast and plunge moderately to the northwest. Variations in plunge are probably the result of the D₃ overprinting of F₂ structures (see figure 27, page 55).

Large scale F₃ structures have been recognized on North and South Twillingate Island, where nearly undeformed pillows have been reorientated into open, southwest plunging anticlines and synclines (Plate 1; X Section). Similarly, the BBB zone itself may have been folded during this event into an extremely large F₃ synform which plunges to the south. By comparing the divergent axes of these folds, an axial plane has been defined which dips 75° towards N 25 E and trends nearly parallel to the F₃ fold axes at Grassy Point (Fig. 45).

Both S_3 and L_3 are spatially restricted to the hinge regions of F_3 folds, and are defined by a fine scale crenulation cleavage and crenulation lineation respectively. S_3 and L_3 are best developed in exposures along the trail connecting Davy Buttons Cove to Crow Head on North Twillingate Island and have also been observed as far south as Bluff Head, where S_3 locally overprints the S_1 foliation.

Where present, S_3 strikes northwest-southeast and dips steeply to the southwest, while L_3 plunges to the northwest and parallels the axis of small scale F_3 folds (fig. 45d).

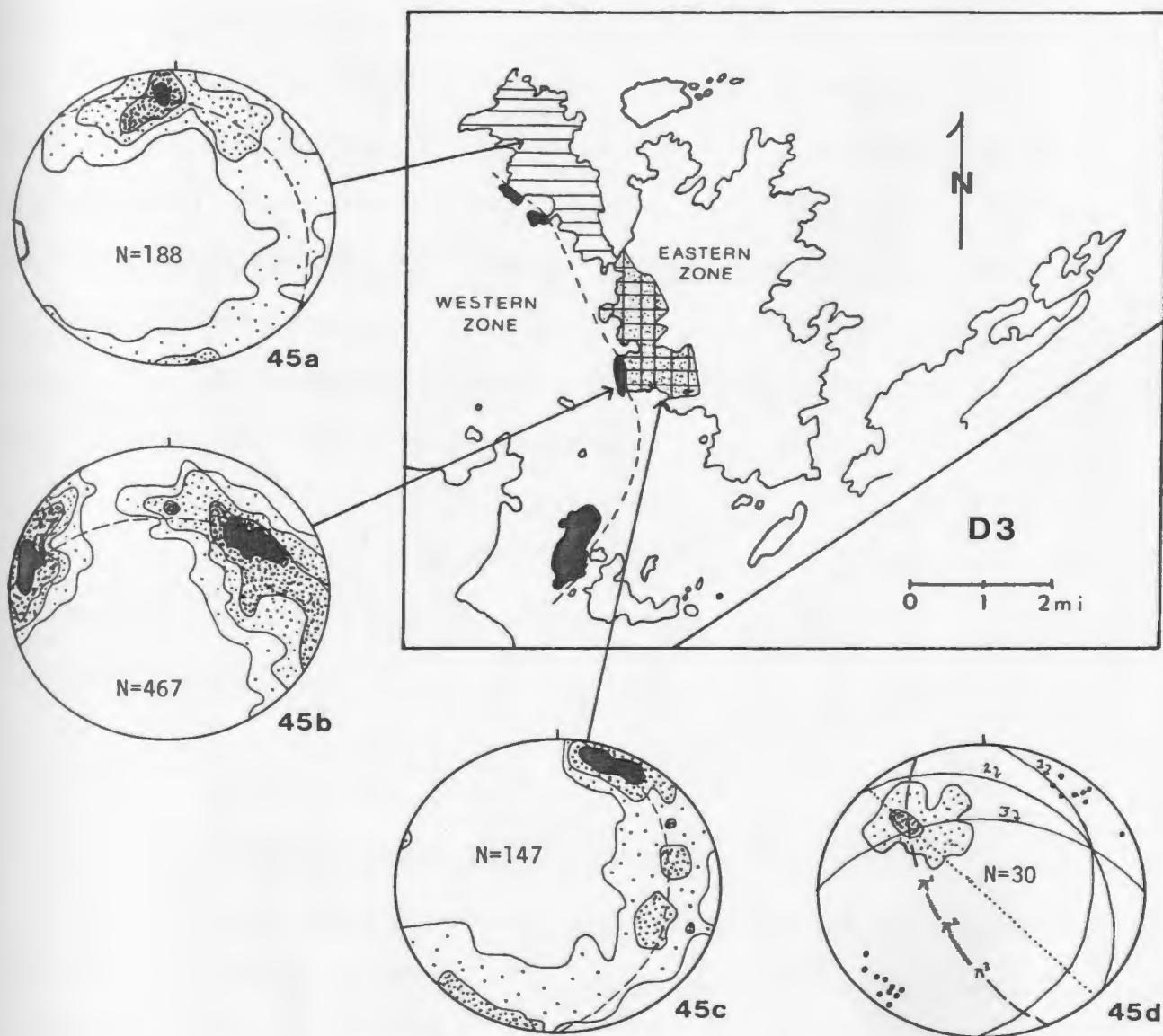


Figure 45a: Poles to S_0/S_2 on North Twillingate Island. Contour interval equals $>0, 5, 10$, and 20% per 1% area.

Figure 45b: Poles to S_1 in the BBB shear zone region. Contour interval is the same as for figure 45a

Figure 45c: Poles to S_0/S_2 on South Twillingate Island. Contour interval is the same as for figure 45a

Figure 45d: Composite diagram for the D_3 deformation. Solid line great circles give the phi girdles from diagrams 46.1-46.3. Dashed great circle defines the constructed axial plane for F_3 . The dots give the orientation of the F_3 axial planes measured at Grassy Point and the dotted great circle defines the average F_3 axial plane orientation. The contoured region contains the orientation of F_3 fold axes (contour interval $= >0$ and 3% per 1% area).

III.C.5. The D₄ Deformation

III.C.5.a. Kinking

Kinks are observed to crosscut all structural features in the Twillingate region (apart from faults), and are therefore assigned to D₄. They are probably the most common features to be found within the study area, and are best developed in regions where strong foliations are developed. On Batrux Island and Back Harbour Head, for example, kinks of different asymmetries are so prevalent that it is difficult to establish the original orientation of S₁. In this region, as elsewhere, the overprinting of one kink generation by another commonly occurs, making it extremely difficult to analyse orientation data.

III.C.5.b. Faults-General Characteristics

Faults are the youngest tectonic features to develop in the Twillingate region. They cut all exposed structures and lithologies, including late Jurassic lamprophyre dykes (Payne, 1974). Most faults are characterized in the field by steep-sided valleys and cliffs separating regions of differing finite strain or structural style. On North Twillingate Island, for example, the Sleepy Cove Fault (Payne, 1974 - see Plate 1) parallels the Long Point escarpment and juxtaposes pristine vesicular pillow lavas against their flattened and sheared equivalents. A major

fault north of Crow Head also separates deformed and undeformed terrains and may be traced onto South Twillingate Island by using this strain contrast as a marker (see Fig. 26, page 52).

Most faults occur as simple, clean fracture surfaces, although some are associated with localized, small scale shear zones. These latter faults may have preferentially nucleated within zones of weakness created by ductile shearing.

III.C.5.b.1. Orientation, Distribution, and Fault Movement

Faults are most extensively developed in the vicinity of New World Island and decrease in abundance to the north. They occur in three principal orientations, with most trending NE-SW and dipping steeply to the northwest (fig. 46). This orientation coincides with the attitude of the Lukes Arm Fault, and suggests that many of the large and small scale faults in the region share a common origin.

Two less common fault orientations were also noted in the field and appear to have developed sequentially. The earlier faults trend NW-SE and are mainly found within the BBB zone, where they are associated with local shear zones (see above). It is likely that these faults either formed during the shear zone episode or much later by nucleation within the sheared region.

East-west trending faults are pervasively developed and crosscut all other faults in the area. They are long,

continuous structures which have been traced throughout the region and locally affect the BBB zone. One of these faults extends from Codjack Cove to Old House Cove and may be responsible for truncating the strong magnetic anomaly pattern noted just offshore of Moretons Harbour (see figure 5, page 19).

Although dykes are extensively developed throughout the region, it was never possible to trace any set of cross cutting dykes across a given fault zone. Consequently, it was also impossible to accurately determine the net slip vector of any of the faults. However, in general, it was noted that vertical dykes on horizontal surfaces were rarely offset to any great degree, while horizontal dykes cut by fault zones rarely reappeared on the other side of the fault. Thus, it is postulated that movement along the faults was principally dip slip, with an unknown, but probably small strike slip component. Slickensides, where observed, support this hypothesis.



Figure 46: 87 poles to fault planes in the Twillingate region. Countour interval= >0 , and 5% per 1% area. The large black dot in the northwest-southeast quadrant gives the orientation of the Lukes Arm Fault according to Dean and Strong (1977). Equal area, lower hemisphere projection.

IV. STRUCTURAL GEOLOGY-MICROSTRUCTURAL ANALYSIS

This chapter, and the one which follows, are concerned with the microscopic analysis of deformation in the Twillingate region. By combining the data contained in these chapters with that presented in the previous chapter, it should be possible to construct a comprehensive and well founded structural history for the whole Twillingate region.

IV.A. General Aspects of Microstructural Development

The interpretation of microstructures in naturally deformed rocks has been the subject of extensive investigation for over 100 years (see references in Sander, 1970). As a discipline, it attempts to qualify the physical processes operative during a deformational episode by defining the changes in grain structure and morphology acquired during that event. These changes are mainly stress-induced, although temperature, strain rate, strain path and impurity content collectively determine the microstructural end product.

The way in which a rock deforms under deviatoric stress is grossly defined by its environment of deformation and grain size. At grain sizes larger than 0.5 mm. and upper crustal conditions (strain rate $>10^{-13}$ sec $^{-1}$; temp $<600^{\circ}\text{C}$) intra-granular slip (or dislocation creep) is the dominant deformation mechanism in most minerals (White, 1975b); while at smaller grain sizes, higher temperatures, or

slower strain rates, Coble Creep predominates. Other diffusion controlled deformation mechanisms, such as Nabarro Creep and Nabarro-Herring Creep, are also known to exist, but are probably not operative under normal geological conditions (White, 1975b).

The conditions required for the operation of any one deformation mechanism may be defined by a set of constitutive equations known as the flow laws (White, 1975b). These laws are based on experimental data obtained at low stresses and high strain rates, and allow the extrapolation of this data set to more reasonable geologic conditions. The flow laws can only be treated as first approximations, however, since many of the variables which influence deformation (ie. the fluid content of the aggregate, its strain path, and impurity geometry) are not directly considered in their derivation.

In the present study, the flow laws are presented as a series of charts or "deformation" maps (White, 1976)(fig. 47). These maps show that deformation in a coarse grained hypabyssal intrusion, such as the Twillingate Granite, should be dominated by dislocation creep processes, although diffusive processes could also be locally important (see, for example, Bouchez, 1977). In dislocation creep, the principal agent of deformation is the dislocation. Dislocations are linear zones of high strain energy developed when an elastically deformed lattice ruptures and produces an interstitial half plane of atoms (Fig. 48). Strain relaxation then occurs by the expulsion of these defects from

the atomic structure.

The geometry assumed by dislocations trapped within a crystal is largely a function of the temperature of deformation. For example, dislocation pile-ups and tangles resulting from the interaction of dislocations with sessile obstructions and other defects are commonly developed at low temperatures, and produce a microstructure known as undulatory extinction (McQueen and Jonas, 1975). At higher temperatures, vacancy diffusion processes (such as dislocation climb) become active and allow the dislocations to climb over obstructions and escape from the atomic structure. This produces deformed crystals with low bound dislocation densities (Sellars, 1978; White, 1976) and large, well defined subgrains.

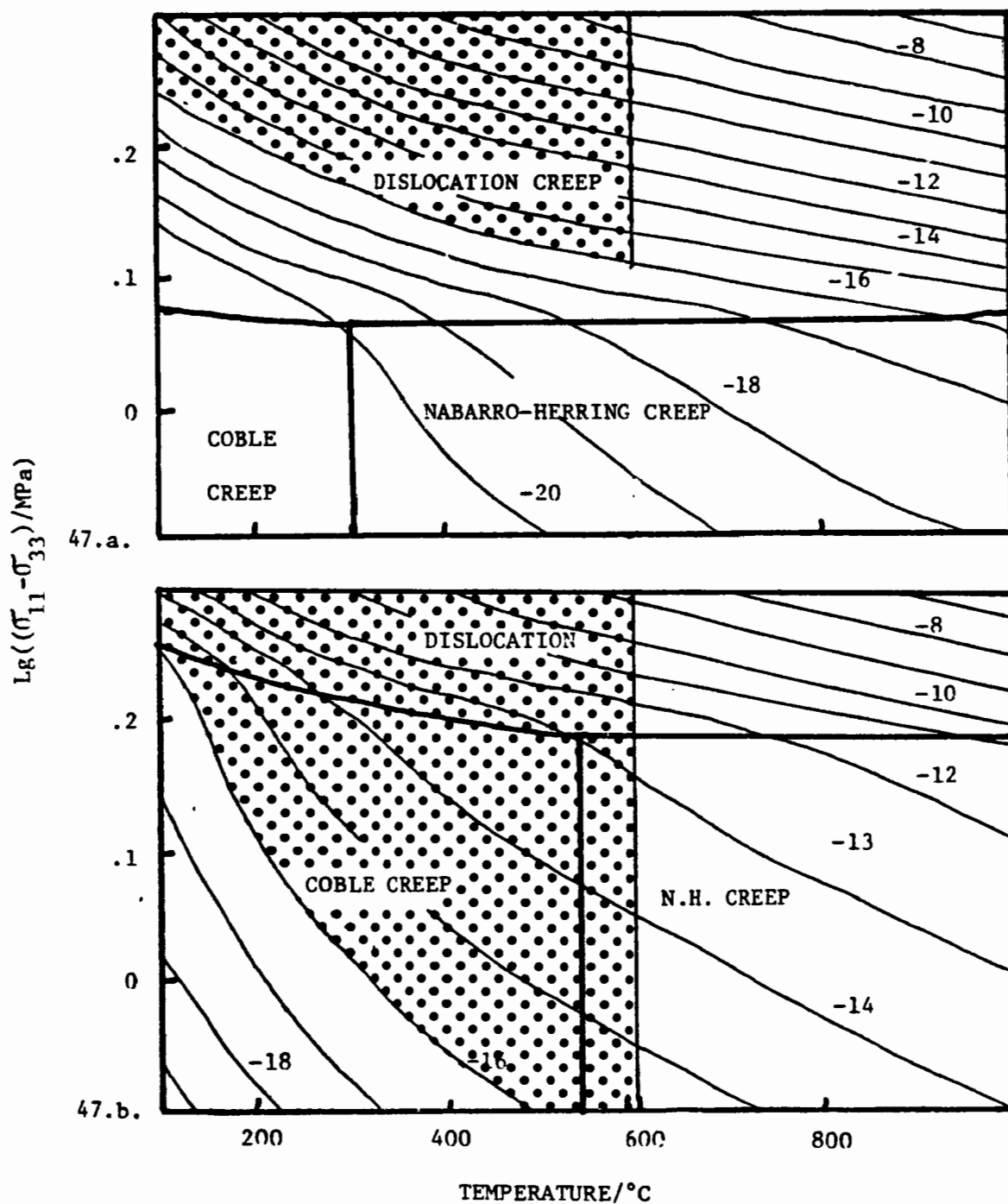


Figure 47: Deformation mechanism maps for quartz grains of 1mm. (47a) and 10 μm . (47b). The dotted region in each diagram gives the most likely temperature/strain rate field for the Twillingate Granite.

After White, 1976, p.81.

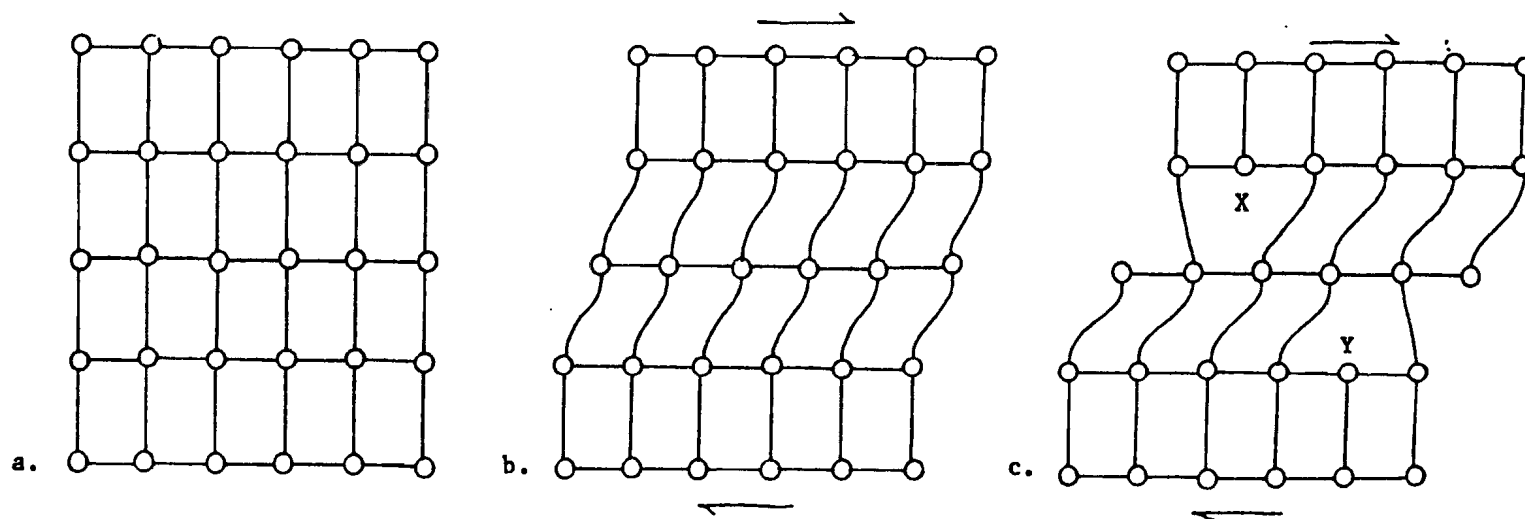


Figure 48: Development of dislocations in a stressed crystal. The dislocations occur at points X and Y in diagram 48c.

IV.B. Microstructures in the Twillingate Granite

Four distinct microstructural types are present in the Twillingate region.

- The TYPE 0 MICROSTRUCTURE: This microstructure is found in those parts of the Twillingate Granite which apparently escaped the effects of deformation. It consists of a hypidiomorphic equigranular aggregate of large anhedral feldspar grains enclosed in a quartz- hornblende-chlorite matrix.

- THE TYPE 1 MICROSTRUCTURE: The type 1 microstructure is found in regions predominantly affected by D_1 and is therefore correlated with that event. It consists of recrystallized feldspar and quartz grain aggregates which define a strong, albeit local L-S fabric in which $L > S$. Feldspar porphyroclasts are rare in thin section, and are usually surrounded by a thick zone of recrystallized feldspar grains.

- THE TYPE 2 MICROSTRUCTURE: This microstructure is restricted to regions predominantly affected by D_2 and is characterized by the presence of serrated grain boundaries and undulose extinction in the quartz grains. Feldspar grains are usually undeformed, and display no evidence of the recrystallization noted in the type 1 microstructure.

- THE TYPE 3 MICROSTRUCTURE has been noted in those sections of the granite which were strongly affected by both D_1 and D_2 . This microstructure consists of flattened and often kinked quartz grains surrounded by recrystallized feldspar grains.

At present, there is no evidence to suggest that D_3 or D_4 produced any major microstructural changes in the granite pluton.

IV.B.1. The Type 0 (Initial) Microstructure.

The type 0 microstructure is a hypidiomorphic equigranular aggregate of large (5mm.-10mm.) anhedral quartz and subhedral feldspar grains with minor amounts of hornblende, chlorite, epidote, and opaques. Boundaries between phases are clean, unserrated, and are usually curvilinear. None of the crystals exhibit any major effects of intragranular strain, although it is possible that some twinning in the feldspar grains may have been deformationally induced. In order of crystallization, feldspar and hornblende were first to form while quartz, epidote, and the opaques fill the interstices between grains. Chlorite is a late metamorphic phase developed at the expense of hornblende.

IV.B.2. The Type 1 Microstructure

IV.B.2.a. Introduction

The type 1 microstructure is well developed in rocks deformed within the SHTI zone and is less commonly observed in the BBB zone, due perhaps to a lower temperature of deformation in the latter region (see Fig. 24, page 45). It is characterized by coarsely recrystallized quartz and feldspar grains, and is easily recognized even after overprinting by later deformational episodes (Fig. 49 and 50).

The type 1 microstructure is not equally well developed throughout the SHTI zone, but gradually diminishes in its intensity of development eastward. Quartz recrystallization, for example, is not apparent east of Merritts Harbour, although there is still some evidence of feldspar recrystallization. This suggests that the SHTI zone either dies out to the east or turns slightly northwards around Merritts Harbour so that its effect on New World Island is lessened.

IV.B.2.b. Morphology of the Type 1 Microstructures

In regions affected predominantly by D_1 , quartz grains in the granite are commonly recrystallized into equigranular aggregates of large new grains. Grain orientations in these aggregates commonly vary in optic axis orientation by as much

as 40-50 degrees (Fig. 51). While no portion of the original grain remains, it is likely that the preferred optic orientation of most of the new grains cluster around the original orientation of the host.

The recrystallized new grains range in size from 100 μm to 1000 μm , although most are larger than 800 μm . They are nearly unstrained, although some appear to exhibit incipient subgrain development. They usually exhibit straight to curvilinear boundaries with their neighbours. Triple junctures between quartz grains commonly meet at 120 degree angles, as do quartz and feldspar boundaries, suggesting that the new grains have developed a microstructure in near equilibrium with respect to surface energy criteria (see Vernon, 1976).

The plagioclase component of the granite also recrystallized during D_1 and forms recrystallized aggregates of equiaxed, unstrained new grains. Crystallographic misorientations across adjacent grain boundaries are small (1-4 degrees) and show a systematic deviation in orientation from a central region, reminiscent of the core and mantle geometry described by White (1975a). This suggests that these grains developed as a result of subgrain rotation from a deforming host. The average diameter of the recrystallized grains ranges from 100 to 200 μm , with larger grains attaining sizes up to 400 μm .

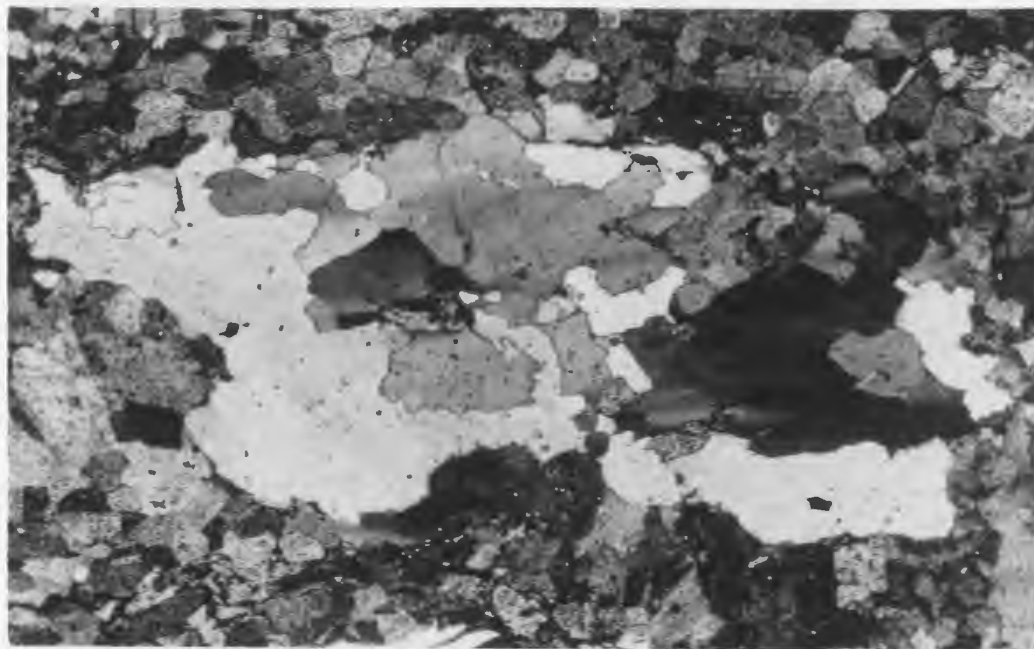


Figure 49: ES-202a. X polars. Recrystallized quartz grain from the southernmost tip of South Twillingate Island. Note the surrounding recrystallized feldspar grains. Scale: 1cm=.25mm.

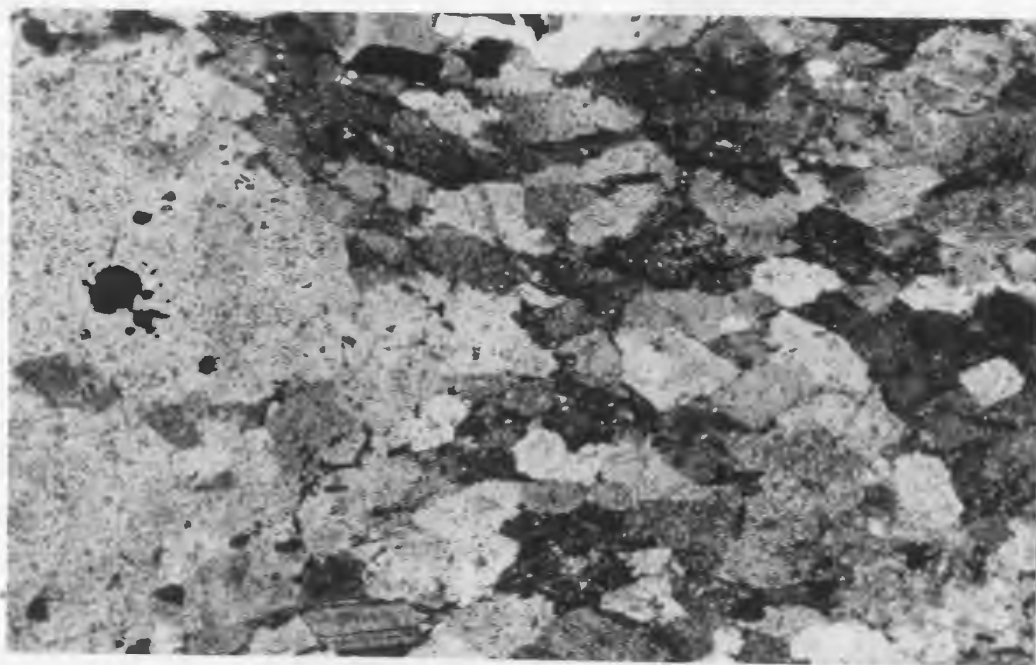


Figure 50: ES-1130. X polars. Recrystallized feldspar grains developing from a host plagioclase phenocrysts. Scale 1cm=.25mm.

Figure 51: AVA diagram of one recrystallized quartz grain.

In this diagram, the arrows denote the plunge of the C-axis in each new grain.

Scale: 1cm.=.12mm.



IV.B.3. The Type 2 Microstructure

IV.B.3.a. Introduction

The type 2 microstructure is well developed throughout much of the granite pluton and overprints the type 1 microstructure at Purcells Harbour, South Trump Island, and New World Island. It is only found in regions which were affected by D_2 , and is therefore correlated with that event.

IV.B.3.b. Morphology of the Type 2 Microstructure

The type 2 microstructure is defined on the basis of quartz morphology as none of the other minerals appear to have been greatly affected by D_2 . Feldspar and epidote, for example, are morphologically similar in both the deformed and undeformed granite, while chlorite is only deformed in regions of medium to high finite strain. Other minerals, such as hornblende and the opaques, occur too rarely to be used as deformation markers and, where present, exhibit few effects of deformation apart from minor fracturing and kinking.

Since most phases in the granite were not noticeably affected by D_2 , most of the ductile strain associated with deformation must have been accommodated by the quartz grains. This strain led to the activation of at least three known dislocation-related deformation mechanisms, each of which

became operative at different strain intensities. They will be described below in their order of development.

Within the least deformed parts of the pluton, flattening of the quartz grains was principally accommodated by intragranular slip. This led to the development of several dislocation-related features, such as undulatory extinction, elongate subgrains, and slip lamellae, which may (Christie et al., 1964) or may not (White, 1973, 1976; Lister et al., 1978) define the actual slip planes.

Undulatory extinction in the quartz grains is an extremely common feature found in all but the least deformed parts of the pluton. Variations in optic axis orientation are usually small, and average 10-20 degrees over the width of the crystal.

Subgrains locally occur in the mildly deformed parts of the pluton, although they are rarely well developed. As can be seen from Figures 52 and 53, subgrains are elongate, evenly spaced, and commonly extend from one margin of the host to the other. They average 100 μm across and rarely vary in orientation by more than 1-2° degrees from each other.

Slip lamellae are common features in the quartz fraction of the Twillingate Granite and always lie parallel to $(000\bar{1})$. This suggests that basal slip was an operative deformation mechanism during D_2 (see figure 52).

In the more strongly foliated parts of the pluton, intracrystalline strain in the quartz grains becomes

Partially accommodated by grain boundary migration and recrystallization. In this region, grain boundary convolutions develop in which local extensions of one grain protrude into the adjacent grains (Fig. 54). These protrusions are often thin ($<10\text{ }\mu\text{m}$) and may extend up to $50\text{ }\mu\text{m}$ into the neighbouring grain. They develop as a result of strain differences between like phases and have been described by Cahn (1970) and McQueen and Jonas (1975), amongst others.

Equiaxed new grains commonly nucleate within the protrusions and rarely exhibit more than a 2-4 degree difference in orientation with their host (bulge nucleation - see Fig. 55). They average $10\text{ }\mu\text{m}$ in diameter and are frequently internally strained, suggesting that they developed during deformation.

In regions of stronger foliation development, grain boundary convolutions increase in frequency to the point where the boundary develops a serrated texture. This boundary zone increases in width as a function of strain intensity and, in some regions, may entirely consume the host grain. This end stage is best developed at Merritts Harbour and Salt Harbour Island, while intermediate states occur at Gunning Head and Durrels Arm (Fig.56).

Within the most strongly foliated regions, the quartz grains were apparently unable to deform entirely by ductile means and suffered some brittle deformation as well (Fig.57). Intragranular fractures are found throughout the quartz

grains and may in part parallel the $(10\bar{1}1)$ rhombohedral cleavage reputed to be present in quartz (Fron­del, 1972). These fractures are pervasively developed in the vicinity of Salt Harbour Island, and have been reported in metals which have less than 5 independent slip systems (quartz has three; see Lister *et al.*, 1978; Cahn, 1970).

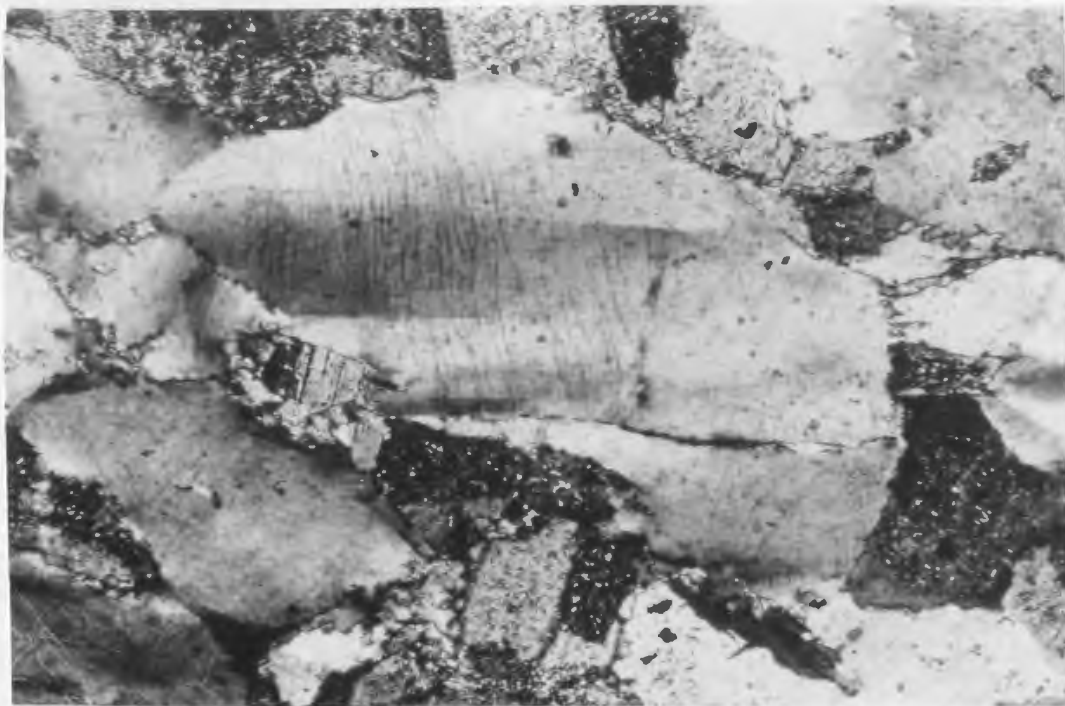


Figure 52: ES-184. Undulose extinction, subgrain boundaries, and basal slip lamellae in a quartz grain from Durrels Arm.

Crossed polarizers. Bar= .25 mm.

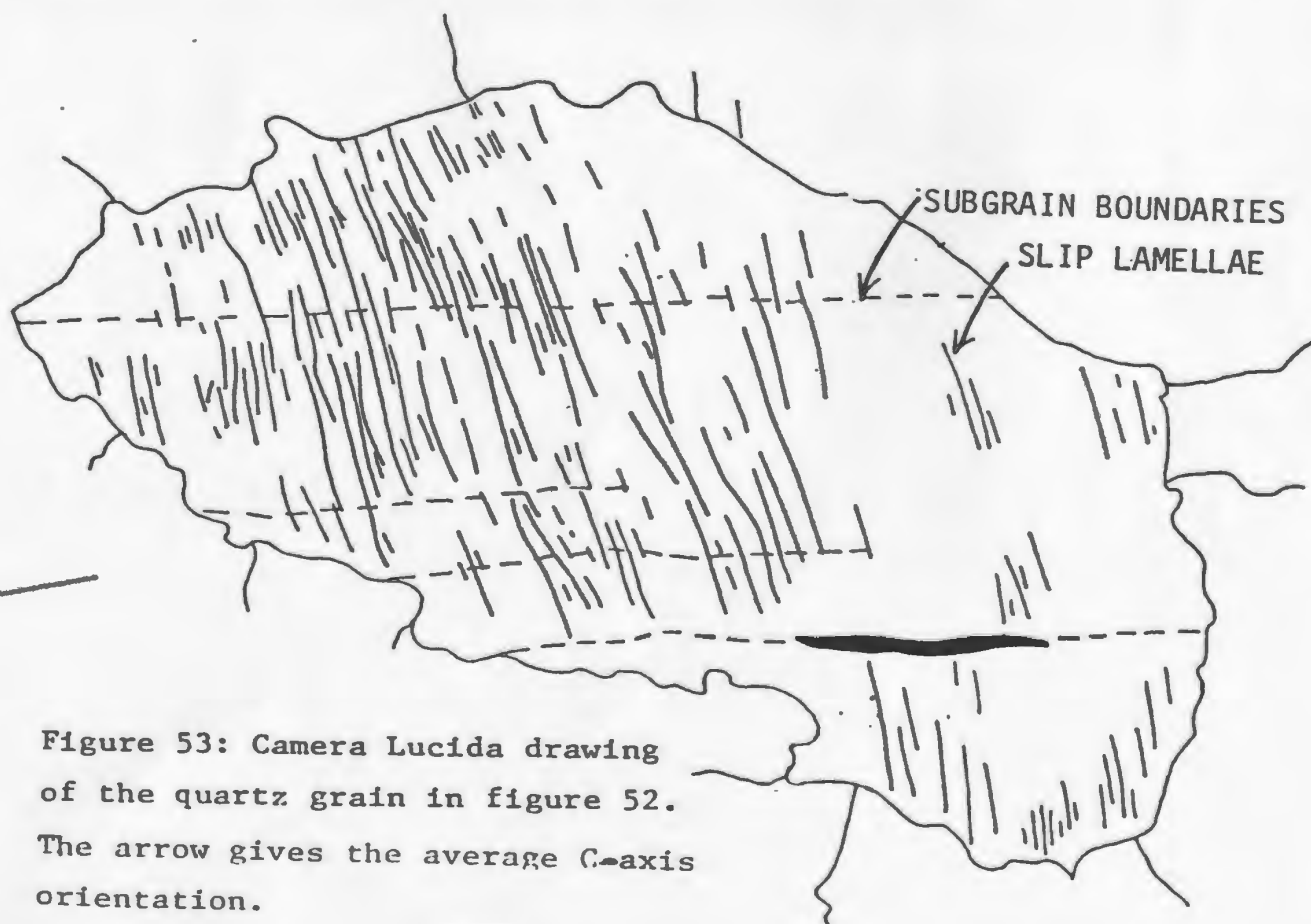


Figure 53: Camera Lucida drawing of the quartz grain in figure 52.

The arrow gives the average C-axis orientation.

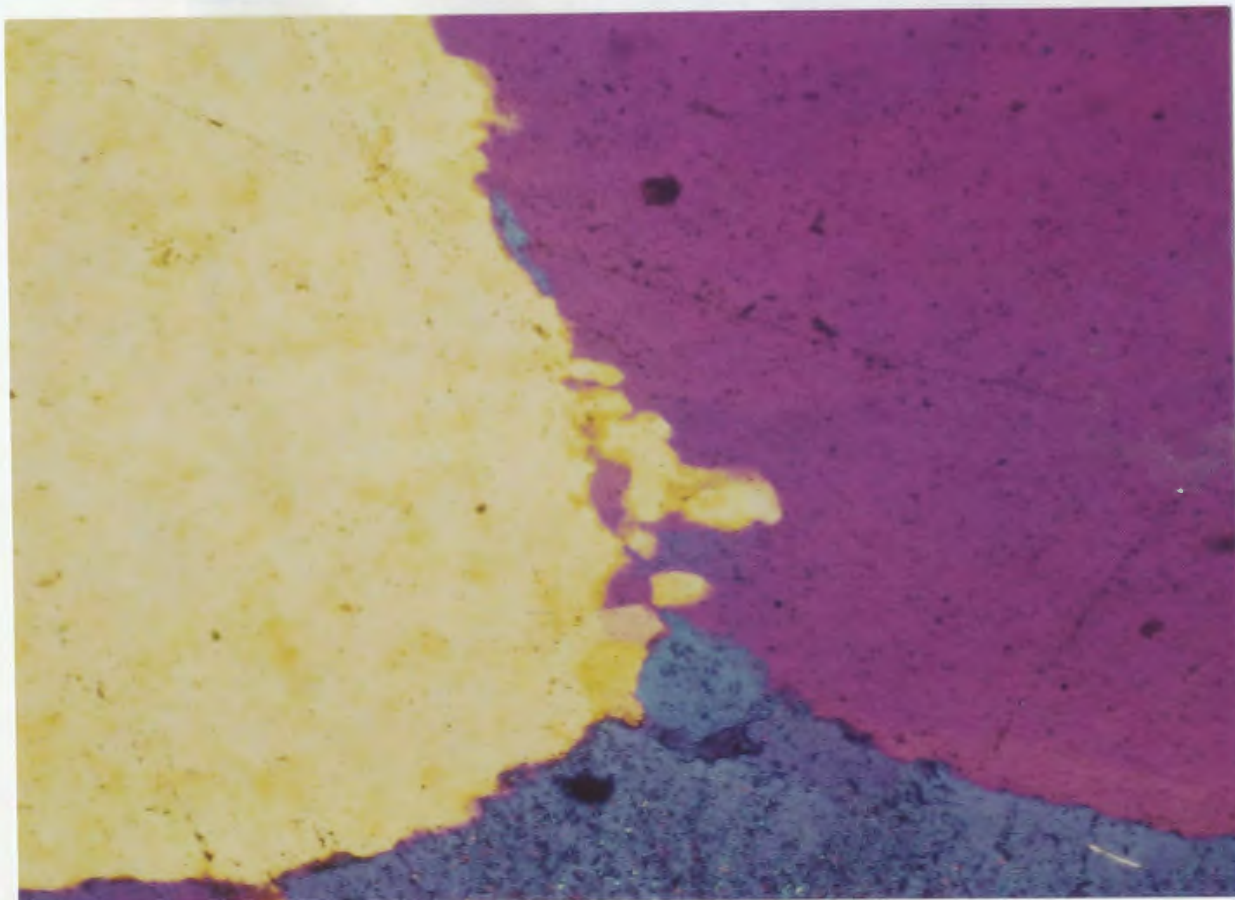


Figure 54. ES-206. Bulge nucleation in quartz grains as noted in a sample collected at Durrels Arm. X polarizers and sensitive tint plate. Scale- 1 cm. = .25 mm.

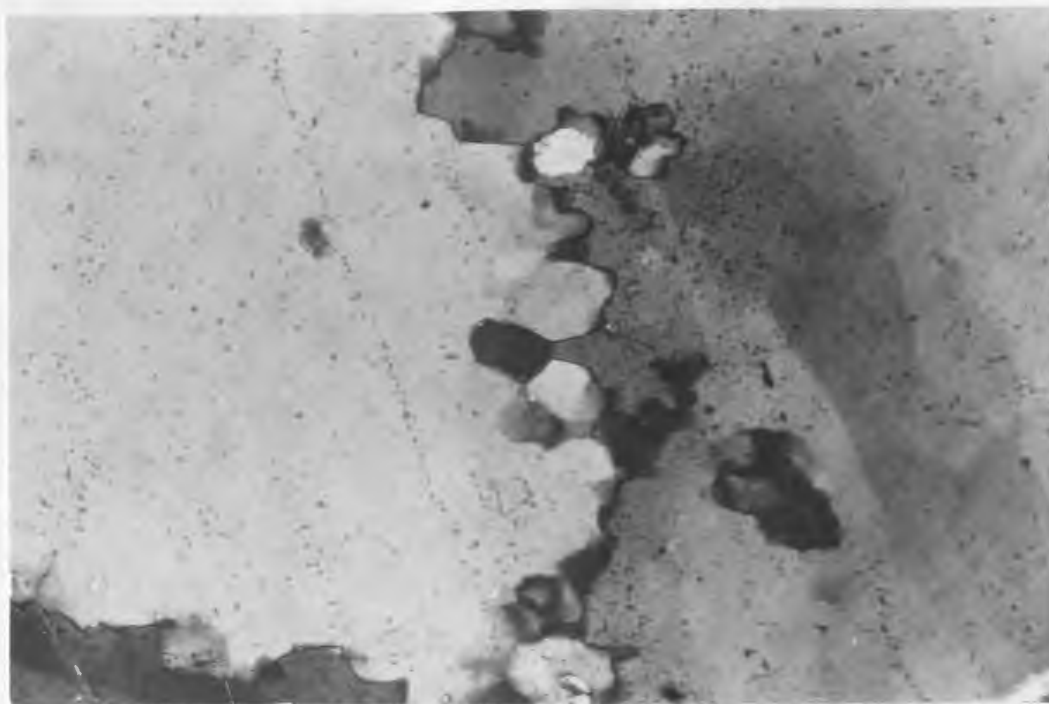


Figure 55: ES-206. X polars. Development of new grains in protrusions. These developed as a result of bulge nucleation. From a sample collected at Durrels Arm. Scale: 1cm=.05mm.

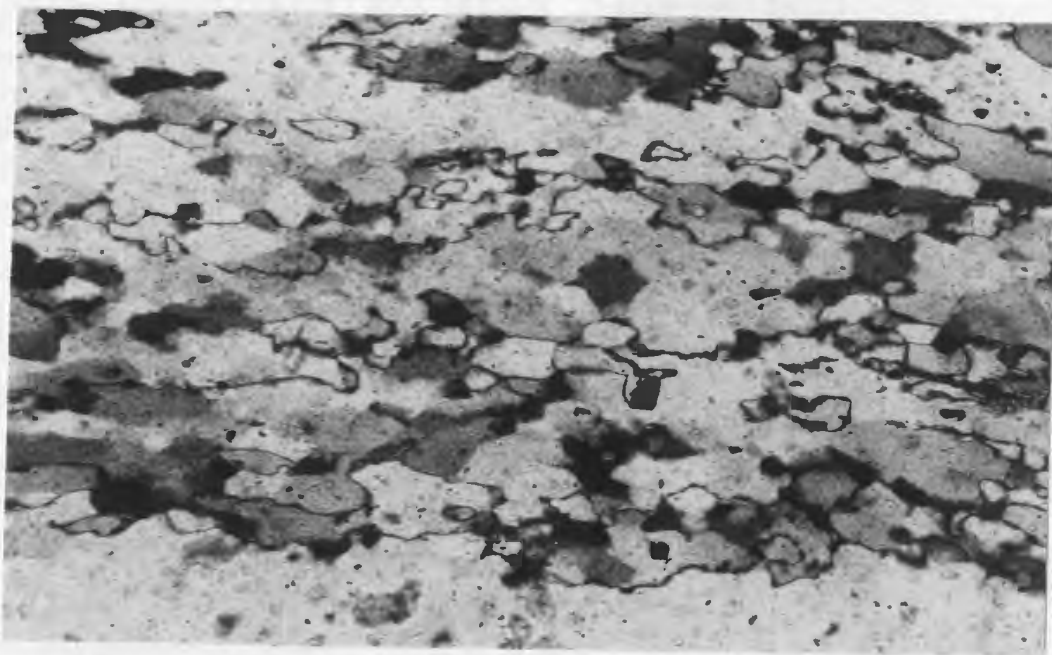


Figure 56: ES-1005. X polars. Serrated grain boundary developed as a result of bulge nucleation. The host grain lies at the bottom of the photograph. From Salt Harbour. Scale: 1cm=.15mm.

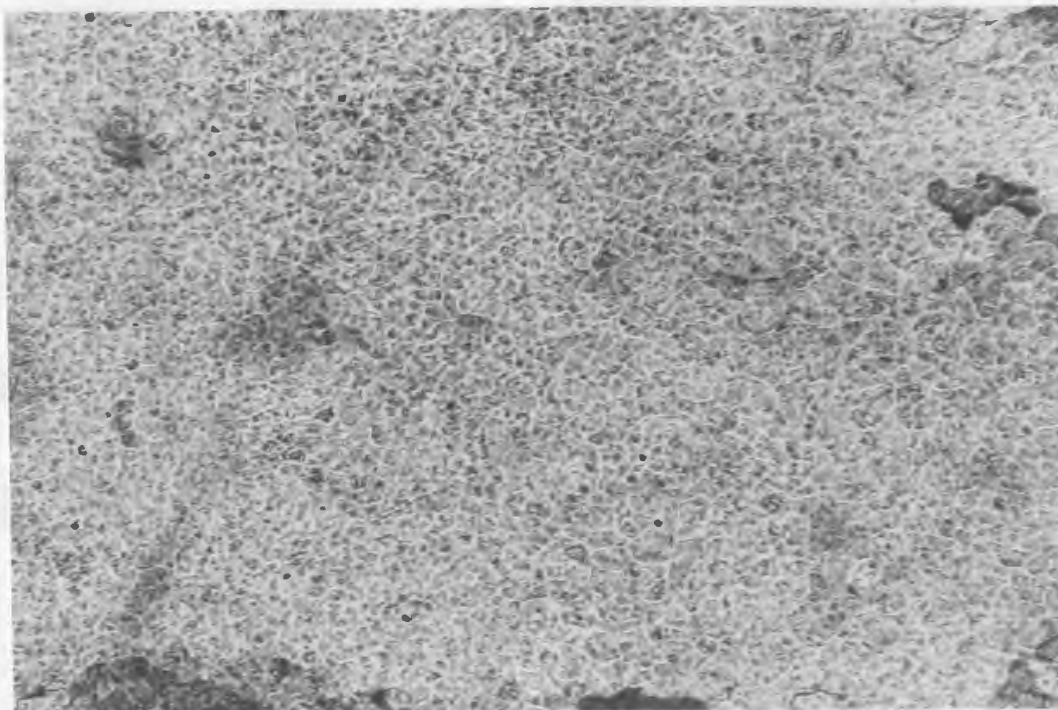


Figure 57: Microcracks (?) in quartz grains at Merritts Harbour. Plane light. Scale: 1cm = .05mm.

IV.B.4. The Type 3 Microstructures

Since the type 1 and type 2 microstructures are morphologically distinct, it has been possible to recognize both microstructures in spite of overprinting. On the bluff southeast of Purcells Harbour, for example, large recrystallized quartz grains characteristic of the type 1 microstructure exhibit the undulatory extinction and serrated grain boundaries identified with the type 2 microstructure. Similar examples may be found throughout the two shear zones, with local exceptions occurring in regions which were relatively unaffected by the D_2 deformation (such as at Lobster Cove).

The type 3 microstructure is only found in rocks which display features of both the type 1 and type 2 microstructures and is characterized by mechanically kinked quartz grains (fig. 59). Kink zones in these grains usually form elongate, parallel regions whose average C-axis orientation differs widely from that noted outside of the zone. According to Bouchez (1977), it is this strong C-axis misorientation which differentiates kink bands from the more commonly observed subgrain boundaries (see fig. 52, page 95).

In some cases, the preferred recrystallization of one kink limb has occurred. This produces 'ribbon grains' of quartz which have a much higher aspect ratio than the original host grains (fig. 59). As a result, it is difficult

to qualitatively determine the finite strain suffered by these rocks from a study of quartz grain morphology.

In the Twillingate region, kinked quartz grains are best developed in the vicinity of Merritts Harbour, where the entire quartz population of several thin sections was observed to be intensely kinked and locally recrystallized along the kink band boundaries. The average dimension of these kink bands varies with the size of the host grain, although their length to width ratio is nearly constant at around 10:1. The boundaries themselves parallel the long axis of the grains and are usually sharply defined with only minor evidence of the grain boundary migration characteristic of the type 2 microstructure.

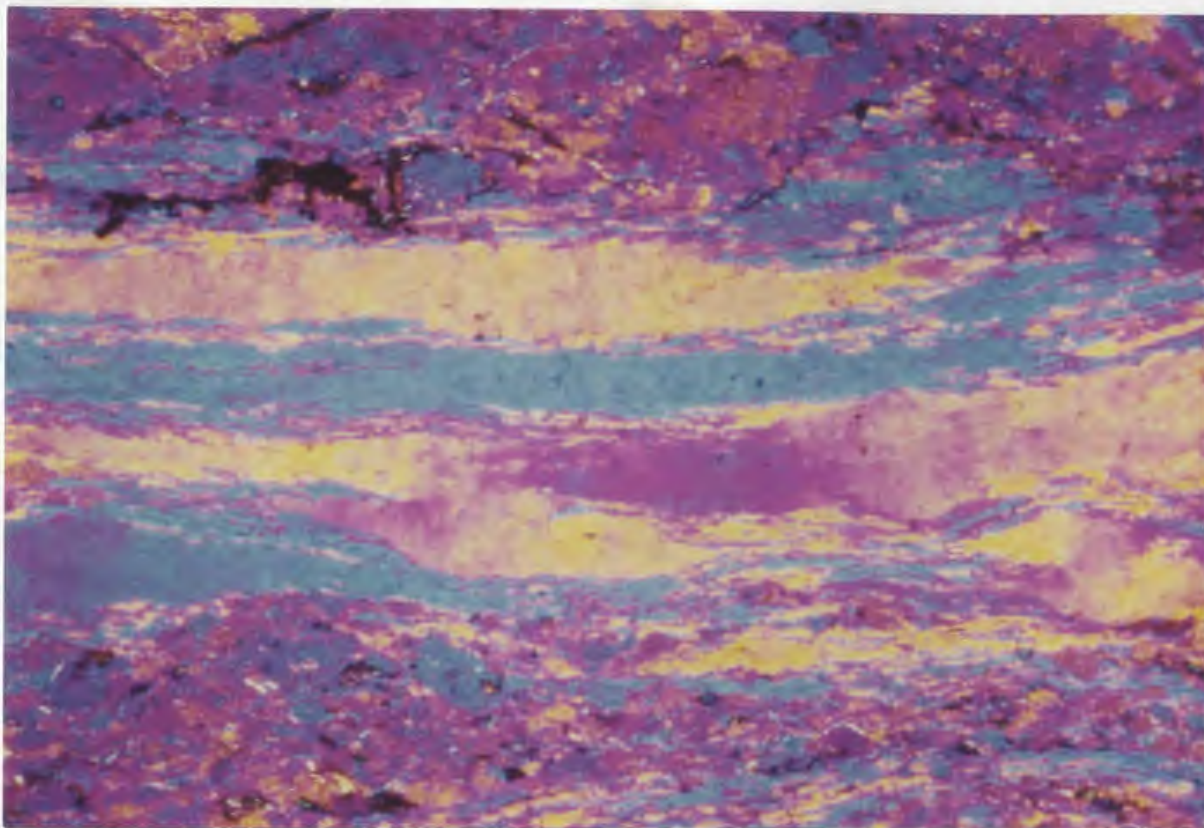


Figure 58 : ES-1055. X polars + sensitive tint plate. 'Kinks' in a quartz grain from Merritts Harbour. Deviations in C-axis orientation in this case average around 60° . Scale: 1cm=.25mm.



Figure 59: ES-1055. X polars. Kinked grain in which one limb has recrystallized. Merritts Harbour. Scale: 1cm=.15mm.

V. STRUCTURAL GEOLOGY - PETROFABRIC ANALYSIS

V.A. Petrofabrics in the Twillingate Granite

V.A.1. Introduction

In the previous chapters, the geometry and age relationships of D_1 through D_4 were defined by macroscopic analysis, and the effects of D_1 and D_2 on the Twillingate Granite were determined by microstructural analysis. In this chapter, quartz petrofabric data are given which support the analyses presented in the previous chapters.

V.A.2. Methods

The first step in analysing the petrofabrics of the Twillingate region lay in choosing the correct specimens for study. These specimens were chosen in the following manner:

1. All specimens were required to contain a significant number of measurable quartz grains. This criterion was deemed necessary for two reasons. First, samples containing less than 20 measurable grains per thin section are difficult to analyse statistically; and secondly, recent studies of quartz petrofabrics have shown that the modal percentage of quartz can seriously affect the strength of the C-axis fabric developed (Starkey and Cutforth, in press). In the 13 samples analysed, the percentage of quartz per section was, in all cases, greater than 40%.

2. All specimens were required to exhibit a well defined and characteristic microstructure (see chapter IV). This parameter made it possible to relate fabric development directly to microstructural development and thus gain insight into the generation of both.

3. All four microstructural types and their variations had to be represented in the samples analysed. This criterion made it possible to compare fabric patterns in samples which suffered contrasting deformation histories at various temperatures.

While it is not implied that the thirteen fabrics described here represent all of the crystallographic fabric geometries present in the study area, it is hoped that they include most of the characteristic fabric types to be found in the region.

Once the 13 samples were chosen, two mutually perpendicular thin sections were taken from each. One of these sections was cut perpendicular to any foliation or lineation present in the rock, while the other was cut perpendicular to the foliation but parallel to the lineation. In measuring the quartz orientations present in these rocks, both sections were utilized to insure that certain, hard to measure C-axis orientations were not underrepresented in the final fabric.

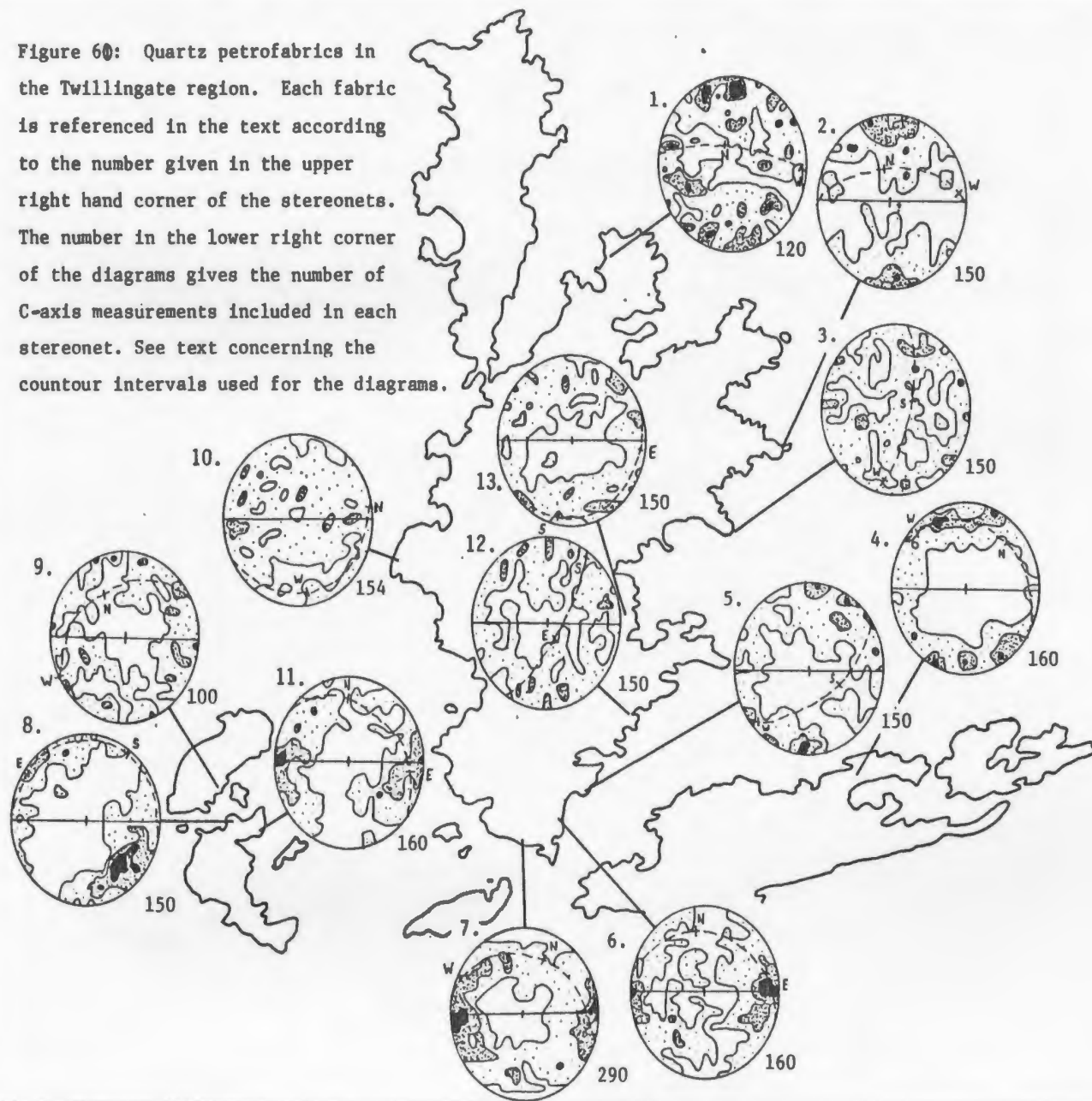
Once all thin sections were cut, 75 to 150 unrecrystallized and type 1 recrystallized quartz grains were measured in each using the standard universal stage techniques described in Emmons (1943). The C-axis orientations of these grains were then plotted onto a Lambert equal area stereonet and rotated into a standard orientation in which the foliation lay east-west and the lineation plunged vertically. The resulting fabrics were then contoured in intervals of 1,3, and 5% per 1% area and drafted together to produce figure 60.

In order to facilitate the comparison of these fabrics with respect to structures noted in the field, each fabric on figure 60 is provided with a dotted great circle giving the orientation of the fabric in terms of True North.

V.A.3. Fabric Classification

Several authors (including Turner and Weiss, 1963, and Lister, 1974) have suggested that fabric geometry is a function of three independent parameters: initial orientation, temperature, and deformation path. While the first two parameters may be determined in most cases from the fabric geometry itself, the third requires a working knowledge of the micro- and macro-structural history the rock has undergone. Thus, in order to classify a suite of quartz C-axis fabrics, each should be analyzed in terms of both fabric geometry and tectonic history.

Figure 60: Quartz petrofabrics in the Twillingate region. Each fabric is referenced in the text according to the number given in the upper right hand corner of the stereonet. The number in the lower right corner of the diagrams gives the number of C-axis measurements included in each stereonet. See text concerning the countour intervals used for the diagrams.



In the present study, the 13 fabrics were classified with respect to these two requirements. The diagrams were first separated into four groups according to their inferred deformational/microstructural history, and were then further subdivided on the basis of fabric geometry.

VI.A.3.a. Group 0 Fabrics

This group includes samples 1 and 3, both of which exhibit the type 0 microstructure in thin section and do not display a definable foliation or lineation in hand specimen.

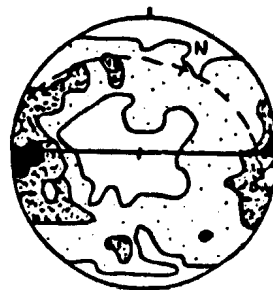
FABRIC SUBGROUP 0: This is a random C-axis fabric characterized by small, pole free areas, low maximum concentrations, and a lack of discernable symmetry elements. Both samples 1 and 3 belong to this subgroup.



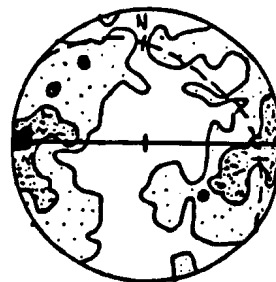
VI.A.3.b. Group 1 Fabrics

Rocks belonging to this group usually exhibit a strong L-S fabric ($L > S$) in hand specimen, and are characterized by type 1 (+ minor type 2) microstructures in thin section. Samples 6, 7, 8, and 11 all belong to this group and fall into three subgroups:

FABRIC SUBGROUP 1a: This subgroup is characterized by two crossed girdles which are equally inclined to the foliation and intersect at a point maximum normal to the lineation. The opening angle between the two girdles is approximately 70 degrees. Specimen 7 belongs to this subgroup.



FABRIC SUBGROUP 1b: Fabric 1b is similar to 1a except that the crossed girdles are incomplete and are absent along a plane passing through the lineation and lying perpendicular to the foliation. In these fabrics, the incomplete girdle may be caused by undersampling of the quartz population. This fabric subtype has been recognized in samples 6 and 11.



FABRIC SUBGROUP 1c: This is a 'tailed maximum pattern' defined by a point maximum which tails off into a partial great circle lying normal to both the foliation and lineation. The C- axis maximum lies at an angle of about 40 degrees to the foliation and is elongate normal to the foliation plane. This is



the only fabric pattern observed which shows monoclinic symmetry. Sample 8 is the only specimen known to contain this fabric.

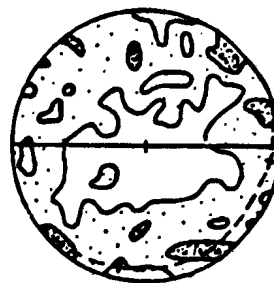
VI.A.3.c. Group 2 Fabrics

Rocks belonging to this group are strongly foliated and are characterized by the presence of the type 2 and the absence of type 1 and 3 microstructures. In hand specimen, the two samples belonging to this group differ in that sample 2 does not contain a well developed lineation, while sample 13 is characterized by a strong L-S fabric ($L=S$). This seemingly minor difference in deformation path has led to the development of two distinct fabric types, both of which are described below:

FABRIC SUBGROUP 2a: This fabric subgroup consists of a strong C- axis maximum (or small circle girdle?) which lies normal to the foliation. It is symmetrically orientated with respect to the foliation and lineation, and displays well developed orthorhombic symmetry. To date, it has only been recognized in sample 2.



FABRIC SUBGROUP 2b: This subgroup could easily be mistaken for a type 1a crossed girdle fabric if not for two distinguishing features. First is the lack of a C-axis maximum in the foliation plane, and second is the presence of the type 2 microstructure. It has only been observed in sample 13 and will be further discussed in the next chapter.

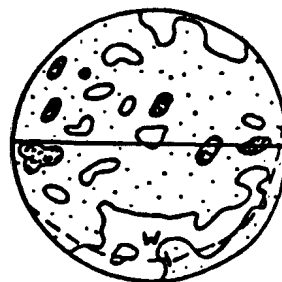


VI.A.3.d. Group 3 Fabrics

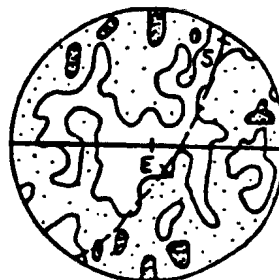
Group 3 fabrics are only found in rocks which exhibit both the type 1 and type 2 microstructures. They are found in the southern part of the region and include samples 4, 5, 9, 10, and 12. Samples 4 and 5 are extremely well foliated and exhibit the type 3 microstructure, while sample 12 is less strained and exhibits only minor effects of the D_2 deformation. Samples 9 and 10 were both collected from quartz porphyry dykes and display a strong L-S fabric in which $S \gg L$.

The group 3 fabrics are subdivided into three subgroups:

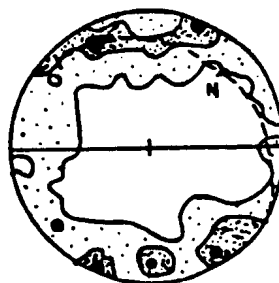
FABRIC SUBGROUP 3a: This fabric subgroup is unique in that it is a random fabric developed in a highly foliated specimen. As with the type 0 fabric patterns, it is characterized by low maximum concentrations, small pole free areas, and a total lack of symmetry elements. Fabric 10 is the only fabric pattern assigned to this group.



FABRIC SUBGROUP 3b: Fabric 3b is directly comparable to subgroup 2b and consists of a weak girdle lying normal to the foliation and lineation. Two samples, 9 and 12, belong to this group. Sample 9 may have been undersampled.



FABRIC SUBGROUP 3c: This subgroup displays elements of both 3b and 2a fabrics and consists of a cleft (or small circle) girdle which lies normal to S_2 and crosses the foliation in a great circle lying 90 degrees from the lineation. Samples 4 and 5 are the only samples containing this fabric, and are also the only two analyzed samples which display the type 3 microstructure.



V.A.4. Fabric Summary

Four main fabric groups are present in the Twillingate region. Group 0 fabrics are only found in the undeformed core of the Twillingate Granite and consist of random C-axis patterns. Group 1 fabrics occur in regions that suffered the D_1 ($\pm D_2$) deformation and exhibit the Type 1 microstructure. In most cases, Group 1 fabrics consists of two symmetrically arranged crossed girdles which intersect the foliation at a point maximum (types 1a and 1b). However, in sample 8 (type 1c), the fabric consists of an asymmetric 'tailed maximum pattern' in which the C-axis point maximum lies 40° from the foliation and tails off towards $S_{1/2}$.

Group 2 fabrics occur in regions which only suffered the D_2 deformation, and therefore exhibit the Type 2 microstructure. These fabrics either consist of a C-axis point maximum oriented perpendicular to S_2 (type 2a), or a near random pattern which lacks C-axis orientations in the direction of L_2 (type 2b).

Group 3 Fabrics are only found in rocks which strongly suffered both D_1 and D_2 and exhibit the Type 3 kinked microstructure. In one case (type 3a), it consists of a random pattern which lacks C-axis orientations parallel to L_2 . In all other cases, it consists of a weak girdle fabric which may (type 3c) or may not (type 3b) display a strong C-axis point maximum perpendicular to $S_{1/2}$. In most respects it closely resembles fabric type 2b described above.

VI. ANALYSIS AND SYNTHESIS

VI.A. Stratigraphic Analysis

The Central Mobile Belt (Williams, 1964) is considered by most workers to contain the last vestige of the Iapetus Ocean, a major geographic feature thought to have existed between 800 and 460 million years ago (Williams, 1979). Isotopic dates on the Twillingate Granite (510 ± 17 ma) and the late diabase dykes (473 ± 9 ma) (Williams *et al.*, 1976), suggest that all units in the region formed within this oceanic environment.

The calc-alkaline nature, and thickness (>8 km.) of the Moretons Harbour Group leaves little doubt that it represents either an island arc or intraplate volcanic pile (Strong and Payne, 1973; Fryer, pers. comm.). However, the same degree of certainty does not extend to the origin of either the Sleepy Cove Group or the Twillingate Granite.

In the past, the Sleepy Cove Group has been modelled as 1) the basal unit of an island arc sequence (Strong and Payne, 1973), 2) a deformed early remnant arc (Williams and Payne, 1975), and 3) the upper layer of an ophiolite suite underlying the island arc terrain (Dean, 1978). The present author favors the third model for the following reasons:

First, the Sleepy Cove/Moretons Harbour Group boundary may be defined on lithological, geochemical, structural, and geophysical grounds. These four parameters together provide a reasonable argument against the continuous volcanic

sequence envisioned by Strong and Payne (1973).

Secondly, the "strong structural contrast" noted at Sam Jeans Cove and Tizzards Harbour by Williams and Payne (1975) appears to have resulted from the fault juxtaposition of deformed and metamorphosed volcanics against undeformed diabase dykes (page 47). Furthermore, the presence of undeformed hornblende-plagioclase pillow lavas at Webber Bight and deformed hornblende-plagioclase feeder dykes at Sam Jeans Cove (page 27) suggests that the Webber Bight pillows were present prior to D_1 .

Finally, there is little evidence to suggest that the Sleepy Cove Group exhibits features characteristic of island arc terrains. Indeed, the group as defined here appears to be a relatively thin (1 to 2 km.) tholeiitic volcanic pile probably underlain by sheeted dykes, gabbros and ultramafics (as hypothesized from diatreme analysis, page 42). The exposed sequence is compatible with that found in the ophiolite occurrences at Betts Cove (Upadhyay, 1973) and the Bay of Islands (Williams *et. al.*, 1972) and argues in favor of a similar mode of development for the Sleepy Cove Group. The only problem with this model lies in the presence of silicic tuffs and agglomerates at Salt Harbour Island, Jenkins Cove, and Back Harbour. These tuffs and agglomerates occupy less than 1% of the total Sleepy Cove area and are presently enigmatic.

The origin of the Twillingate Granite has also been the subject of numerous studies. In the past, the pluton has

been thought to have developed as a result of diapirism within a subduction zone (Payne, 1974) or by partial melting at the roots of an island arc (Payne and Strong, 1979).

While the origin of the granite is mainly a geochemical problem, this study has detailed certain aspects of its geology which should be considered in any model proposed for the petrogenesis of the body. These include:

1) The timing of emplacement- While the Sleepy Cove Group acted as host for the Twillingate pluton, apophyses of the granite are observed to cross the inferred Sleepy Cove/Moretons Harbour Group contact and intrude rocks of the Moretons Harbour Group at North Trump Island and Mouse Island. This requires that the Moretons Harbour "island arc" terrain was present prior to intrusion of the granite.

2) The duration of intrusion = The presence of post-tectonic stocks of trondhjemite within the Twillingate pluton suggests that either the intrusion of the granite was a long lived phenomenon, or a second magma source (melted Twillingate granite?) developed shortly after deformation ceased. At present, both of these possibilities are viable and cannot be discounted without further detailed geochemical work.

The only model being actively considered for the genesis of the Twillingate Granite is that of Payne and Strong

(1979). They hypothesize that the trondhjemitic melt developed by the in-situ partial melting of amphibolite at the base of an active island arc. However, before this model can be considered viable, several points require clarification.

First, what is the geochemistry of trondhjemitic melts developed in such an environment? Preliminary work by Fryer and Strong (pers. comm.) suggests that the trondhjemitic melts occurring as pods and veins at Sam Jeans Cove share few geochemical characteristics with the Twillingate pluton. While the Twillingate Granite exhibits flat rare earth element patterns, the trondhjemitic pods are strongly enriched in light rare earth elements. Similar contrasts are also present in the major and trace element concentrations of the two occurrences making it unlikely that both formed in the same manner.

Secondly, how much amphibolite is required to produce a body the size of the Twillingate pluton? If a 10% partial melt is needed to produce trondhjemites (Payne and Strong, 1979), and the pluton is only 1/2 km. thick, the source amphibolite would have to be a block 140 square kilometers across, and 5 km. thick. This block increases the total thickness of the Moretons Harbour Group to 17 km.. Given a geothermal gradient of 60°C/km. (Payne and Strong, 1979), this places the bottom of the pile well beyond the upper stability limit of amphibole. It is thus unlikely that a homogeneous intrusive body, such as the Twillingate Granite,

could form by such a mechanism.

In the author's opinion, the subduction model of Payne (1974) comes closest to predicting the relationships found in the Twillingate region. This model eliminates the need for a thick pre-existing amphibolite block at the base of the arc by allowing for a continuously replenishing slab of basaltic material. Similarly, the temporal and spatial relationship of the Moretons Harbour Group to the emplacement of the Twillingate Granite argues in favor of a subduction-, rather than a spreading center- related, magmatic source.

While the origin of the Twillingate granite still remains a geochemical problem, it is hoped that the stratigraphic relationships described in this chapter will help set constraints on future models for the body.

VI-B. Structural Analysis

VI.B.1. Structural Summary

Three major and one minor phase of deformation have been recognized in the Twillingate region. Each of these is characterized by its unique macrostructure and microstructure.

The earliest deformation event, D_1 , was responsible for producing two non-parallel shear zones. Of these, the SHTI zone lies adjacent to the Lukes Arm Fault and extends northwards to include Purcells Harbour, Black Island, and the southernmost parts of the Duck Islands and South Trump Island. Associated with this zone is a strong downdip stretching lineation (L_1) which parallels the axis of possible F_1 folds on South Trump Island. These folds share a common axial plane and exhibit curvilinear axes whose vergence suggests that rocks north of the zone moved upwards with respect to those to the south (fig. 29.6, page 56).

In thin section, D_1 related microstructures and petrofabrics display features characteristic of a high-temperature deformation episode. The initially large plagioclase laths found in the undeformed portions of the pluton develop the 'core and mantle' geometry characteristic of feldspars deformed in amphibolite and granulite terrains. Similarly, quartz grains exhibit the effects of

recrystallization and have been reorientated such that their C-axes lie within the foliation, a feature indicative of high temperature prismatic slip (Lisner and Patterson, 1979). Both of these features become less obvious east of Merritts Harbour, suggesting that the zone changes orientation slightly at this point and may turn towards the north.

A second shear zone, the BBB zone, extends northwards from North Trump Island and follows the west coast of the Twillingate Islands. The temperature of deformation within this zone was less than in the SHTI zone and varies from conditions representative of the epidote-amphibolite facies in the south, to greenschist facies to the north. As this zone was mainly developed in the basaltic terrain, its microstructures and petrofabrics were not analysed during this study. However, the gross parallelism of S_1 with that found in the SHTI zone, and the downdip orientation of L_1 in the BBB zone (fig. 29.9, page 56), suggests that both zones may have shared a common kinematic history. Unfortunately, however, the sense of movement within the BBB zone could not be established from field evidence.

D_2 was a lower temperature event in which S_2 paralleled S_1 in regions of greatest D_1 strain. It affected the rocks of New World Island and the east coast of the Twillingate Islands and is poorly represented elsewhere. Geometrically, the region affected by D_2 can be described as lying east of a triangle whose base lies between Crow Head and South Trump Island and whose apex lies at Codjack Cove.

On Salt Harbour Island, a strong mineral lineation (L_2) parallels the axis of F_2 folds and a biotite foliation defines their axial planes. Elsewhere, L_2 is defined as either a stretching lineation (ie. at Tizzards Harbour) or a crenulation lineation (as on North Trump Island). and S_2 is defined by a coarse crenulation cleavage.

In thin section, D_2 is characterized by microstructures produced during a low temperature episode. In regions which were unaffected by D_1 , plagioclase grains are undeformed and quartz grains exhibit good mortar textures, basal slip lamellae, and undulatory extinction. C-axes in these quartz grains lie perpendicular to S_2 , a feature characteristic of low temperature basal slip (Lister et.al. 1978).

Regions which suffered both D_1 and D_2 exhibit kinked quartz grains whose C-axes define crossed girdle fabrics. These features appear to form when σ_1 lies within the plane of active slip (Bouchez, 1977). If so, then the presence of this microstructure defines a unique geometry in which σ_1 parallels the intersection of the kinked basal planes (fig. 61). Spatially, this means that $\sigma_1(D_2)$ plunged approximately 20° towards S40E, or perpendicular to S_2 .

The kinked quartz microstructure also suggest that D_2 was a coaxial (plane strain) deformation, since kinking would not have occurred if σ_1 was allowed to rotate during D_2 . This hypothesis is supported by the Type 2 petrofabrics, which all exhibit geometries similar to that reported in quartzites deformed in plane strain (Tullis, 1977).

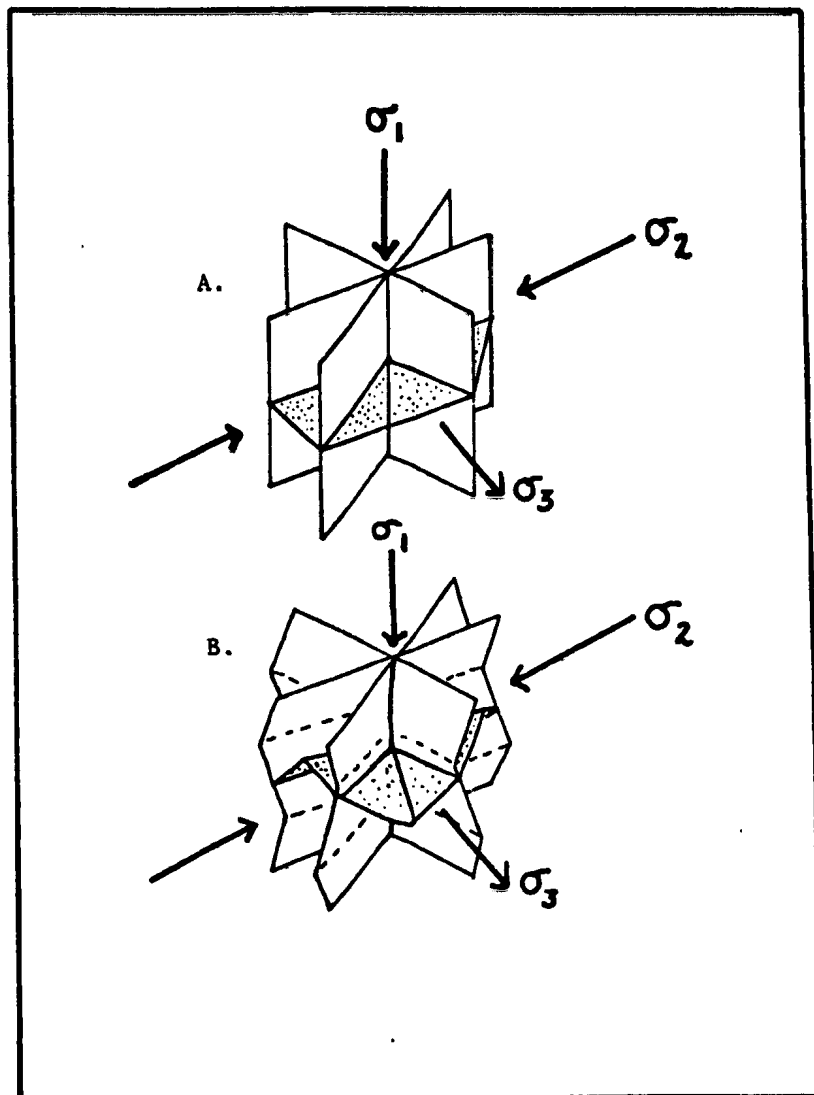


Figure 61: The orientation of basal planes in the kinked quartz grains before (61a) and after (61b) kinking. The stippled plane defines the developing foliation as well as the orientation of the C-axes in the kinked grains.

The D_3 low-temperature episode developed broad, open flexures in the basalts of North Twillingate Island and the BBB zone. S_3 and L_3 are defined by an extremely fine crenulation cleavage and lineation respectively, and were well developed in the cores of the F_3 folds. Since the D_3 episode did not affect the granite terrain to any measurable extent, there are no microstructural or petrofabric data available to define the kinematics of deformation.

The D_4 event was primarily responsible for producing numerous normal faults in the region. Most of these faults parallel the Lukes Arm and Chanceport Faults and juxtapose deformed rocks against their undeformed equivalents.

VI.B.2. Structural Models

In this section, each of the four deformation episodes will be treated separately and, where possible, models will be presented for their development.

VI.B.2.a. The D_1 Deformation

The D_1 deformation is best characterized as being a shear zone episode in which two zones of differing orientation developed under relatively high ambient temperatures.

-The SHTI Zone: Very little is known about the development of the SHTI zone. It is extremely difficult to delineate in the field and is primarily defined on the basis of microstructural evidence; thus its exact boundaries are

unknown. On a broad scale, however, the zone appears to follow the Lukes Arm fault, suggesting that the two structures may have had a co-genetic history. If so, movement on the latter fault was probably updip from the north.

-The BBB Zone: The most important feature of the BBB zone lies in its spatial orientation. For the most part, this zone follows the contact of the Moretons Harbour 'island arc' terrain and the Sleepy Cove 'ophiolite'. This suggests that the shear zone may have nucleated as a result of gravity instabilities developed between the two groups. If so, then movement on the BBB zone was probably downdip to the north.

On the other hand, the close proximity and structural similarity of the BBB zone to the SHTI zone suggests that movement may have been updip to the north. If so, then the BBB and SHTI zones may represent splays of the same thrust system. Unfortunately, neither theory can be further substantiated with the present data set.

VI.B.2. b. The D_2 Deformation

D_2 was a coaxial, plane strain event characterized by large scale variations in finite strain (ie. heterogeneous bulk pure shear). In the Sleepy Cove Group and Twillingate Granite, deformation was most intense along the northern and eastern shorelines of New World Island and the Twillingate

Islands. while the effects of D_2 are virtually non-existent in the Moretons Harbour Group.

There is also good evidence to suggest that finite strain during D_2 was heterogeneous in the vertical direction. This evidence stems from the numerous late high-angle faults which frequently juxtapose undeformed and deformed terrains. Since these faults are considered to have suffered large dip slip displacements, variations in strain intensity which occur between adjacent blocks must reflect strain differences at depth. Thus, in order to model the D_2 deformation, we must first define a situation in which strain varies in both the horizontal and vertical dimension.

One way to develop the required strain geometry is to deform a homogeneous medium about an included rigid object (Savin, 1961). In this situation, an heterogeneous stress field develops about the object such that the magnitude of σ_1 is augmented in the region adjacent to the rigid body and parallel to σ_1 , and is lessened in the matrix lying normal to σ_1 . This stress field has been theoretically modelled by the finite element method (Stromgard, 1973), and is graphically represented in figure 62.

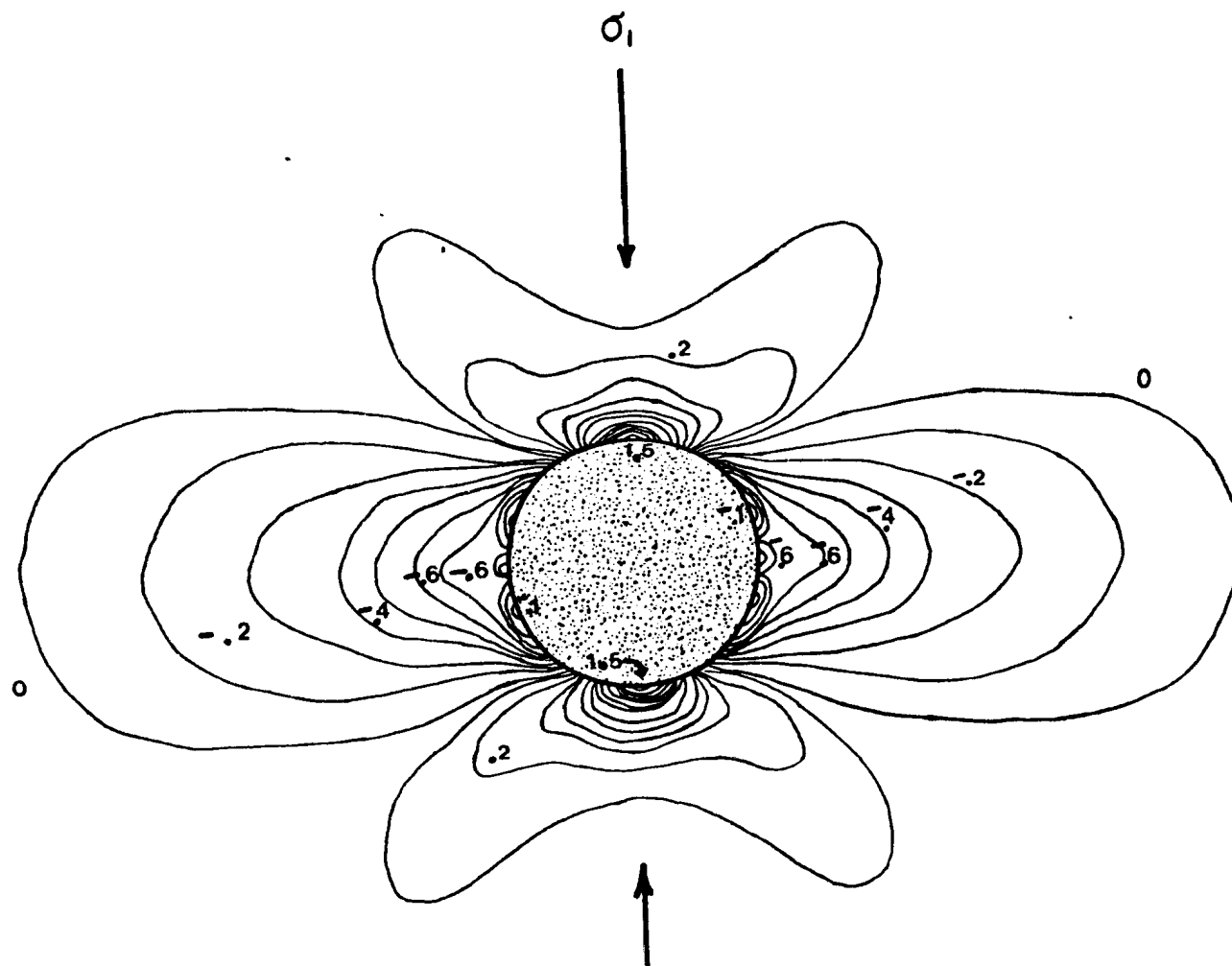


Figure 62; The magnitude of σ_1 as measured around a circular rigid object. σ_1 is tensional when the values given on the diagram are negative. After Stromgard (1973).

As may be seen in this diagram, the domain of least compressive stress forms a cone shaped region which opens towards the more competent body. As one enters this region, σ_1 rapidly decreases in strength and, in the case presented, actually becomes tensional. Since stress and strain are dependant variables, the mean strain should also decrease in this region. This type of stress/strain change would be recognised in the field by a gradational weakening of fabric elements as one approached the 'rigid', undeformed body.

In the Twillingate region, the boundary between the foliated and unfoliated terrains defines a narrow cone shaped region which opens, or widens, towards the west. This suggests that the more competent lithology should lie in this direction if the rigid body model is viable. In the Twillingate region, a likely candidate for the more competent unit would be the massive dyke swarms and basalts of the Moretons Harbour Group. Indeed, the rigid body model may explain why this group has remained relatively undeformed while the nearby Sleepy Cove Group and Twillingate Granite are characterized by their strong D_2 related textures.

In support of this hypothesis, consider the orientation of the strain shadow presented in figure 62. In this diagram, the normal to σ_1 defines a plane which lies perpendicular to the rigid body and bisects the apex of the strain shadow. If the Twillingate 'strain shadow' exhibits a similar geometry, then the rigid body will remain a tenable model to explain the D_2 deformation.

From the geometry of the kinked quartz grains presented above, it can be shown that $\sigma_1(D_2)$ plunges approximately 20 degrees towards S 40 E. If the rigid body model holds true in this region, the Twillingate 'strain shadow' should lie perpendicular to this orientation, or approximately N 60 E.

In Chapter III, the D_2 strain shadow was described as a triangular region whose base lay between Crow Head and Black Island, and whose apex lay at Codjack Cove (fig. 44, page 73). From this geometry, a hypothetical σ_1 direction can be defined and shown to trends approximately S 60 E (fig. 64). Since this orientation is what was expected from the discussion above, it appears that the rigid body model can be applied successfully to the rocks of the Twillingate region.

The origin of stresses operative during D_2 is open to debate, although it is interesting to note that $\sigma_1(D_2)$ was oriented approximately perpendicular to the Lukes Arm Fault. This suggests that rocks south of this lineament may have acted as an indenter to deformation.

VI.B.2. c. The D_3 deformation

Little is known about the D_3 deformation, therefore it is difficult to model. However, since the spatial distribution of D_3 structural elements is similar to that described for D_2 , the rigid body model may hold true for both deformations.

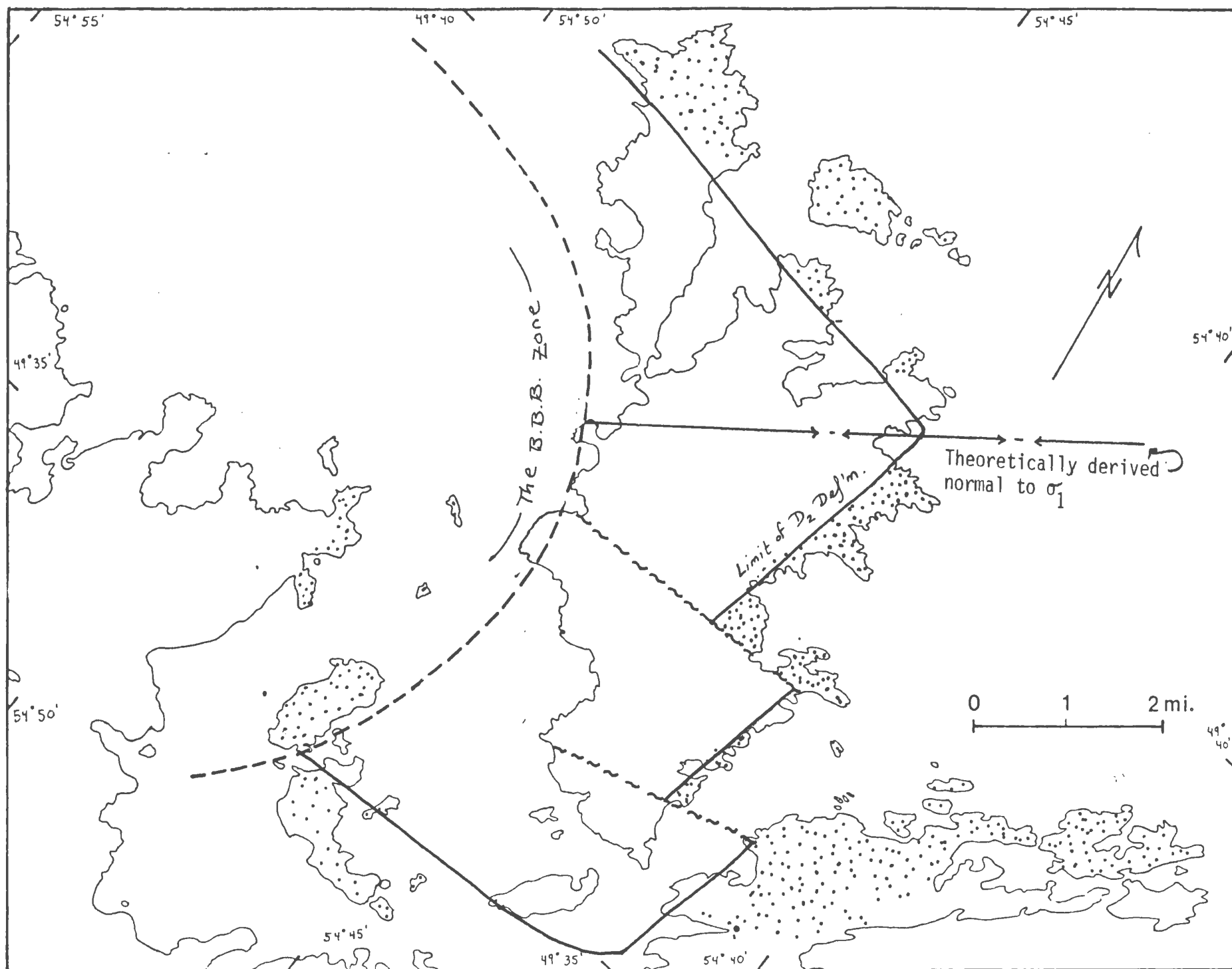


Figure 63: The theoretical orientation of σ_1 as defined by the Moretons Harbour 'strain shadow'.

VI.B.2.d. The D₄ Deformation

Kink bands and faults are the main structural features associated with this event. While little can be said regarding the origin of the kink bands, the spatial relationship of many of the faults to the Luke's Arm Fault merits further consideration.

As mentioned in section III.C.5.b.(page 77), most of the faults in the region are near vertical structures which share a common orientation with the Luke's Arm and Chanceport Faults. As these minor faults also increase in number as one approaches the Luke's Arm fault, it seems logical to assume that the large and small structures are co-genetic. This further suggests that the present expression of the Luke's Arm Fault has developed, for the most part, as a normal fault.

This hypothesis is supported by the regional gravity survey recently published by Miller and Deutch (1978). Their work has shown that a strong gravity contrast lies along the Luke's Arm Fault over its entire length, with the north side exhibiting the higher gravity anomaly. Since this difference in gravity could lead to an isostatic disequilibrium between the two regions, the Luke's Arm Fault, as it exists today, may define the suture between two blocks of rock which are rising at different rates. If so, it is similarly possible that the other faults noted throughout the region may have developed in order to further equilibrate this north-south gravity gradient.

VII. TECTONIC SYNTHESIS AND CONCLUSIONS

VII.A. Tectonic Synthesis

The stratigraphic and structural data presented in this thesis have allowed the development of a detailed tectonic history for the Twillingate region. This history has been summarized in chapter VI, and is presented in outline form below. Where possible, cross references to pertinent sections of the text are provided.

1. The Sleepy Cove group developed during the opening stage of the Iapetus Ocean. The Sleepy Cove Group is most likely ophiolitic in character (page 16), although only the sheeted dyke and pillow lava units are presently exposed. Diatreme evidence suggests that gabbroic and ultramafic units may occur at lower crustal levels in the sequence (page 42).

2. The Sleepy Cove Group was overlain by the Moretons Harbour Group. This massive, nearly undeformed unit is over 8 km thick and is intruded by layered basalt and hornblende-plagioclase porphyritic dykes (pages 23-29). Its calc-alkaline nature suggests that it developed in an island arc environment.

3. The Twillingate granite was emplaced contemporaneously with or slightly later than the formation of the Moreton's

Harbour Group. Intrusion occurred around 510 ma. The Twillingate Granite underlies an insular area of over 150 km². and is trondhjemitic in character. Its size and intrusive relationships with the Moretons Harbour Group (page 41) suggest that it developed in a subduction zone environment.

4. The M₁ metamorphism and D₁ deformation affected both the Twillingate granite and surrounding volcanic terrains. The SHTI shear zone developed parallel to the southern margin of the region and passes close to the more northerly BBB zone at North Trump Island (page 59). This latter zone parallels the contact of the Moretons Harbour and Sleepy Cove Groups and may have developed as a result of density instability tectonics or thrusting of the Moretons Harbour Group over the Sleepy Cove Group/Twillingate Granite Terrain (page 123). Movement on both shear zones appears to have been parallel to the dip of S₁. although the direction of movement is debatable.

5. The low-temperature, coaxial, D₂ event occurred such that $\sigma_1(D_2)$ plunged approximately 20° towards S40E. (page 127). While the origin of this compressive stress is uncertain, the parallelism of deformation to the Luke's Arm fault suggests that rocks south of this lineament may have acted as an

indentor to deformation. The M_2 metamorphic event probably occurred at about this time.

6. A small stock of undeformed granite was emplaced at Gunning Head (page 15). The existence of this body within a region of high D_2 strain suggests that the source for the Twillingate granite may have still been active after D_2 occurred.

7. The D_3 deformation produced local changes in the orientation of existing structural elements in the vicinity of the BBB zone. There is no evidence that this event affected the Twillingate granite to any great extent. Compression during this event was probably horizontal from the northeast-southwest.

8. Diabase dykes were emplaced and provide a U/Pb isochron of 473 ± 9 ma.. This sets a minimum age on D_3 (page 29).

9. The Luke's Arm fault developed along the suture between the Moretons Harbour/Twillingate terrains. and the shales of New World Island. If the inland faults are cogenetic structures with this major lineament. then movement on the fault was downdip. and occurred as late as post Jurassic (as inferred from truncated lamprophyre dykes -page 31). At the same time. however. the parallelism of the SHTI zone to the

Luke's arm fault may indicate a much longer movement history for the latter structure.

VII.B. Conclusions

The following is a list of conclusions reached during the course of this study:

1. The Moretons Harbour and Sleepy Cove Groups are lithologically, geochemically, and structurally distinct units whose boundary parallels the BBB zone over most of its length.
2. Apophyses of the Twillingate granite intrude the Moretons Harbour Group at North Trump Island and at Mouse Island. Thus, the Twillingate granite intruded the volcanic terrain after or during the deposition of the Moretons Harbour Group. The deformed and metamorphosed hornblende-plagioclase dykes noted at Sam Jeans Cove tend to support this conclusion.
3. Both the Twillingate Granite and the Moretons Harbour Group were present in the area prior to D_1 . However, there is some evidence to suggest that the granite body was reintruded by small stocks of similar granite after D_2 .
4. The D_1 deformation produced two high-temperature shear zones in the region. The SHTI zone may have developed during an early movement episode of the Luke's Arm fault, while the

BBB zone may have nucleated as a result of density differences between the Sleepy Cove and Moretons Harbour Groups.

5. Three other deformation episodes also affected the region. The strongest of these was D_2 , a low-temperature, coaxial event which produced a strain shadow in the wake of the Moretons Harbour Group.

6. The BBB zone was rotated into its present orientation during D_3 . There is no evidence to suggest that D_3 has any great effect on the granite pluton.

7. The spatial relationship of the late stage, small-scale faults and the Luke's Arm Fault suggests that the present trace of the latter structure developed as a result of normal displacement.

In conclusion, the Twillingate region has turned out to be a type locality for defining some of the enigmatic lithologic boundaries present in the Notre Dame Bay region of central Newfoundland. Furthermore, the presence of excellent exposure over much of the area has allowed the definition of a well constrained structural history for the study area. It is hoped that the structural and stratigraphic relationships defined herein will aid to future geologists working in this complex part of the Appalachian system.

BIBLIOGRAPHY

- Baird, D.M., 1954. Reconnaissance geology of part of the New World Island - Twillingate area. Geol. Surv. Nfld., Rept. No. 1, 20 p.
- Bird, J.M., and Dewey, J.F., 1970. Lithospheric plate-continental margin tectonics and the evolution of the Appalachian orogen. Bull. Geol. Soc. Am., v. 81, pp. 1031-1060.
- Bouchez, .-L., 1977. Plastic deformation of quartzites at low temperatures in an area of natural strain gradient. Tectonophysics, v. 39, No. 1-3, pp. 25-50.
- Cahn, R.W., 1970. Recovery and recrystallization. In Cahn, R.W. (ed.), Physical Metallurgy. North Holland Publishing Co., pp. 1129-1197.
- Christie, J.M., and Ardell, A.J., 1976. Deformation structures in minerals. In Wenk, H.-R. et. al. (eds.). Electron microscopy in mineralogy. Springer Verlag, Berlin, pp. 374-403.
- Coish, R.A., 1973. Geology and petrochemistry of Trump Island, Notre Dame Bay, Newfoundland. B.Sc. thesis, Mem. Univ. Nfld., 68 p.
- Comeau, R.L., 1972. Transported slices of the coastal complex Bay of Islands - western Newfoundland. Unpub. M.Sc. thesis, Mem. Univ. Nfld., 112 p.
- Dean, P.L., 1978. Stratigraphic and metallogeny of the Notre Dame Bay region, central Newfoundland. Mem. Univ. Nfld. Geol. Rept. No. 7, 204 p.
- Dean, P.L., and Strong, D.F., 1977. Folded thrust faults in Notre Dame Bay, central Newfoundland. Am. J. Sci., v. 277, pp. 97-108.
- Dewey, J.F., 1969. Evolution of the Appalachian-Caledonian Orogen. Nature, v. 222, pp. 124-129.
- Dewey, J.F., and Bird, J.M., 1971. Origin and emplacement of the ophiolite suite: Appalachian ophiolites in Newfoundland. J. Geophys. Res., v. 76, pp. 3174-3266.
- Emmons, R.C., 1943. The universal stage (with five axes of rotation). Mem. Geol. Soc. Am., v. 8, 205 p.
- Fronzel, C., 1962. The System of Mineralogy, v. 3. John Wiley and Sons, Inc., N.Y., 334 p.

- Hansen, E., 1971. Strain facies. Springer Verlag, New York. 207 p.
- Heyl, G.R., 1936. Geology and mineral deposits of the Bay of Exploits area. Geol. Surv. Nfld. Bull. No. 3. 66 p.
- Jukes, J.B., 1842. General report of the Geological Survey of Newfoundland during the years 1889 and 1840. London, Murray (Pub.), 160 p.
- Karig, D.E., 1972. Remnant arcs. Bull. Geol. Soc. Am., v. 83, pp. 1057-1068.
- Lister, G.S., 1974. The theory of deformation fabrics. Ph.D. thesis. Australian National Univ., Canberra, Australia.
- Lister, G.S., and Paterson, M.S., 1979. The simulation of fabric development during plastic deformation and its application to quartzite: fabric transitions. J. Struc. Geol., v. 2. pp. 99-115.
- Lister, G.S., Paterson, M.S., and Hobbs, B.E., 1978. The simulation of fabric development in plastic deformation and its application to quartzite: the model. Tectonophysics, v. 45. pp. 107-158.
- McQueen, H.J., and Jonas, J.J., 1975. Recovery and recrystallization during high temperature deformation. In Arsenault, R.J. (ed.), Treatise on materials science and technology, v. 6. Plastic deformation of materials. Academic Press, San Francisco, California. pp. 393-493.
- Marshall, D.B., and Wilson, C.J.L., 1976. Recrystallization and peristerite formation in albite. Contrib. Mineral. Petrol., v. 57, pp. 55-69.
- Miller, H.G., and Deutch, E.R., 1978. The Bouguer anomaly field of the Notre Dame Bay area, Newfoundland. Dept. Mines, Energy and Res. Canada Grav. Map, Ser. 163. 16 p.
- Murray, A., and Howley, J.P., 1881. Geological Survey of Newfoundland from 1864 to 1880. Geol. Surv. Nfld. Pub., 536 p.
- Payne, J.G., 1974. The Twillingate granite and its relationship to surrounding country rocks. M.Sc. thesis, Mem. Univ. Nfld., 159 p.
- Payne, J.G., and Strong, D.F., 1979. Origin of the Twillingate trondhjemite, north central Newfoundland: partial melting in the roots of an island arc. In Barker, F. (ed.), Trondhjemites, dacites, and related rocks. Elsevier. pp. 490-516.

- Ramsay, J.G., 1967. Folding and fracturing of rocks. McGraw-Hill, New York. 568 p.
- Ramsay, J.G., and Graham, R.H., 1970. Strain variation in shear belts. Can. J. Earth Sci., v. 7. pp. 786-813.
- Sander, B., 1970. An introduction to the study of fabrics of geological bodies. (Translated from German by F.C. Phillips and G. Windsor.) Pergamon, New York. 641 p.
- Savin, G.N., 1961. Stress concentrations around holes. Pergamon Press, Oxford. 430 pp.
- Sellars, C.M., 1978. Recrystallization of metals during hot deformation. Phil. Trans. Roy. Soc. Lond., v. 288. pp. 147-158.
- X Starkey, J., and Cutforth, C., ³⁰ ~~in press~~ ³⁷. A demonstration of the interdependence of the degree of quartz preferred orientation and the quartz content of deformed rocks. Can. Jour. Earth Sci., 15, (pp. 691-697)
- Stromgard, K-E., 1973. Stress distribution during formation of boudinage and pressure shadows. Tectonophysics, v. 16. pp. 215-248.
- Strong, D.F., and Dostal, J., 1980. Dynamic melting of proterozoic upper mantle: evidence from rare earth elements in oceanic crust of eastern Newfoundland. Contrib. Min. Pet., v. 72. pp. 165-173.
- Strong, D.F., and Payne, J.G., 1973. Early Paleozoic Volcanism and Metamorphism of the Moreton's Harbour-Twillingate area, Newfoundland. Can. Jour. Earth Sci., v. 10. pp. 1363-1379.
- Tullis, J., 1977. Preferred orientation of quartz produced by slip during plane strain. Tectonophysics, v. 39. No. 1-3. pp. 87-102.
- Turner, P.J., and Weiss, L.E., 1963. Structural analysis of metamorphic tectonites. McGraw-Hill, New York. 545 p.
- Upadhyay, H.D., 1973. The Betts Cove ophiolite and related rocks of the Snooks Arm Group, Newfoundland. Ph.D. thesis, Mem. Univ. Nfld., 224 p.
- Vernon, R.H. (1976) Metamorphic Processes. George Allen and Unwin Ltd. London. 247 pp.

- White, S., 1973. The dislocation structures responsible for the optical effects in some naturally-deformed quartzes. *J. Material Sci.*, v. 8. pp. 490-499.
- White, S., 1975a. Tectonic deformation and recrystallization of oligoclase. *Contrib. Mineral. Petrol.*, v. 50. pp. 287-304.
- White, S., 1975b. Estimation of strain rates from microstructural features. *Q.J. Geol. Soc. Lond.*, v. 131. pp. 577-583.
- White, S., 1976. The effects of strain on the microstructures, fabrics, and deformation mechanisms in quartzites. *Phil. Trans. R. Soc. Lond. A.*, v. 283. pp. 69-86.
- Williams, H., 1963. Twillingate Map Area. Newfoundland. *Geol. Surv. Can. Paper* 63-36.
- Williams, H., 1964. The Appalachians in northeastern Newfoundland - a two sided symmetrical system. *Am. J. Sci.*, v. 262. pp. 1137-1158.
- Williams, H., 1979. Appalachian Orogen in Canada. *Can. J. Earth Sci.*, v. 16. pp. 792-807.
- Williams, H., Dallmeyer, R.D., and Wanless, R.K., 1976. Geochronology of the Twillingate Granite and Herring Neck Group, Notre Dame Bay, Newfoundland. *Can. J. Earth Sci.*, v. 13. pp. 1591-1601.
- Williams, H., Malpas, J.G., and Comeau, R., 1972. Bay of Islands Map Area (12G). Newfoundland. In *Geol. Surv. Can. Paper* 72-1. pp. 14-17.
- Williams, H., and Payne, J.G., 1975. The Twillingate Granite and nearby volcanic groups: an island arc complex in northeastern Newfoundland. *Can. J. Earth Sci.*, v. 12. pp. 982-995.

THE GEOLOGY OF THE TWILLINGATE REGION

LEGEND

THE DOVE GROUP

UNCONFORMABLE MASSIVE LATE TRIASSIC AND JURASSIC
IN THE DOVE GROUP. THE DOVE GROUP IS A SUBSEQUENT
TO THE TRIASSIC AND JURASSIC. THE DOVE GROUP IS A
SUBSEQUENT TO THE TRIASSIC AND JURASSIC.

THE DOVE GROUP

UNCONFORMABLE MASSIVE LATE TRIASSIC AND JURASSIC
IN THE DOVE GROUP. THE DOVE GROUP IS A SUBSEQUENT
TO THE TRIASSIC AND JURASSIC. THE DOVE GROUP IS A
SUBSEQUENT TO THE TRIASSIC AND JURASSIC.

THE DOVE GROUP

UNCONFORMABLE MASSIVE LATE TRIASSIC AND JURASSIC
IN THE DOVE GROUP. THE DOVE GROUP IS A SUBSEQUENT
TO THE TRIASSIC AND JURASSIC. THE DOVE GROUP IS A
SUBSEQUENT TO THE TRIASSIC AND JURASSIC.

